MONTHLY NOTICES

OF THE

ROYAL ASTRONOMICAL SOCIETY

Vol. 100 No. 8

MEETING OF 1940 JUNE 14

Professor H. C. Plummer, President, in the Chair

The election by the Council of the following Fellows was duly confirmed :—

Ronald Gordon Giovanelli, M.Sc., Rural School, Carlingford, N.S.W., Australia, and National Physical Laboratory, Teddington, Middlesex ;
Richard Francis Turney Granger, Manor Court, Bramcote, Notts ;
Charles Haller, F.R.S.A., F.R.M.S., The White House Cottage, Wimbledon Common, London, S.W. 19 ; and
Gerald James Whitrow, M.A., D.Phil., Christ Church, Oxford, and 37 Cedars Road, Clapham, London, S.W. 4.

Fifty-three presents were announced as having been received since the last meeting, including :—

Gregory (Sir Richard), Religion in Science and Civilization (presented by the author) ;
Walkey (O. R.) and H. Subramania Aiyar, Concise General Astronomy (presented by the authors).

The President announced that during the recess the Library would be opened once a month (on a day yet to be arranged) for the borrowing and return of books.

THE PHYSICS OF WHITE DWARF MATTER

Sir A. S. Eddington, O.M., F.R.S.

1. Five years ago * I concluded that, contrary to the then accepted opinion, the correct relativistic formula for the pressure of completely degenerate matter is the simple formula $P=K\sigma^{\frac{5}{3}}$ given in R. H. Fowler's classical paper.† Having gradually arrived at a clearer view, I shall try in this paper to give the argument a precise and cogent form.

Most of the mathematics of the problem is well known and non-controversial, and will not be repeated here. The crucial step comes earlier, in obtaining a mathematical formulation which correctly embodies the physical conditions of the problem.

Hitherto the theory of white dwarf matter has been concerned almost wholly with the calculation of the pressure ; but in connection with problems of evolution and transmutation of the elements, other points of importance may arise. One such question, which the present theory is able to settle, is considered in § 12.

2. The mechanical characteristics of the material are described by an energy tensor $T_{\alpha\beta}$. The component T_{11} (or T_{22} or T_{33}) is the pressure which we wish to calculate. The procedure in wave mechanics is to consider a unit volume, at rest in the material, and represent its properties by a set of orthogonal wave functions. The contribution to the energy tensor made by an individual wave function, if fully occupied, will be denoted by $\Delta T_{\alpha\beta}$. Owing to the orthogonality of the wave functions their contributions are simply additive.

The operator $(-ih/2\pi)\partial/\partial x_\alpha$ furnishes for each wave function a mechanical vector p_α, whose invariant length $(-p_1{}^2-p_2{}^2-p_3{}^2+p_4{}^2)^{\frac{1}{2}}$ is denoted by m. The difference between the Fowler and the Stoner-Anderson formulæ for the degeneracy pressure arises from the adopted relation between $\Delta T_{\alpha\beta}$ and p_α, namely,

$$\Delta T_{\alpha\beta}=p_\alpha p_\beta/m \quad \text{(Fowler formula)}, \tag{2.1}$$

$$\Delta T_{\alpha\beta}=p_\alpha p_\beta/p_4 \quad \text{(Stoner-Anderson formula)}. \tag{2.2}$$

Since we are interested only in the pressure, the formula (2.1) or (2.2) is at first asserted only for $\alpha, \beta=1, 2, 3$. The possible extension to $\alpha, \beta=4$ is not considered until § 7.

Our programme is firstly to show that (2.1) is the correct formula. This is completed in § 5, and the investigation might have been allowed to terminate at this point. But the rest of the paper goes on to show that the result is

* *M.N.*, 95, 194, 1935.
† *M.N.*, 87, 114, 1926.

not subversive of accepted quantum theory in its ordinary field of application to atomic physics.

3. Consider first the molar aspect of the problem. The deviation of any physical characteristic from perfect uniformity can, by Fourier analysis, be represented by a superposition of simple harmonic waves. There are two such wave systems to be considered—

(*a*) Mechanical waves, *i.e.* sound waves,

(*b*) Electrical waves, *i.e.* changes of electric polarisation with consequent currents and magnetic effects.

To a fairly close approximation the mechanical waves and electrical waves are independent of one another ; but if high enough powers of the amplitudes are retained there are cross-terms which must ultimately bring about an equilibrium distribution of energy between them.

At non-zero temperature there is a field of radiation, determined by Planck's law, which induces waves of system (*b*) in the material ; these in turn maintain waves of system (*a*) by the above-mentioned slow transference of energy. But even at zero temperature the wave systems (*a*) and (*b*) will not entirely vanish, since perfect uniformity is *too improbable*. Accordingly at zero temperature we have waves of both types representing the accidental irregularities or "fluctuations" resulting from the law of chance. It is the pressure and energy of these residual waves that we have to determine.

Turning now to the microscopic aspect, we consider first the electrical waves. The polarisation can be represented as a distribution of a large number of doublets. We denote the (vector) moment of one of the doublets by $e\xi_1$, $e\xi_2$, $e\xi_3$. Considering the n doublets in the unit volume, we count the number of ξ_1, ξ_2, ξ_3 within various ranges and so arrive at a frequency distribution. It is convenient to introduce a single representative doublet —a "statistical doublet"—whose ξ_1, ξ_2, ξ_3 have a probability distribution corresponding to this frequency distribution.

In like manner the sound waves are represented microscopically by displacements x_1, x_2, x_3 of a great number of uncharged particles. These displacements are collected into a probability distribution of displacement x_1, x_2, x_3 of a statistical uncharged particle.

Finally, wave functions are introduced to represent the distribution of the "co-ordinates" ξ_1, ξ_2, ξ_3 and x_1, x_2, x_3 of the statistical doublet and the statistical uncharged particle. The wave functions of each of the two systems of waves afford a means of calculating the total pressure and energy of that system.

4. Returning to the molar aspect, there is an alternative treatment which claims attention. If we think of the material as a superposition of positively charged matter and negatively charged matter, we may consider, instead of (*a*) and (*b*) :

(*a'*) Waves of displacement of the positively charged matter,

(*b'*) Waves of displacement of the negatively charged matter.

This is an equivalent analysis, since electrical waves are given by oscillations (*a'*) and (*b'*) in opposite phase, and mechanical waves by oscillations in the

same phase. But, whereas (a) and (b) are approximately independent, there is very strong interaction between (a') and (b')—so strong that in molar physics it would be considered a waste of time to investigate them separately. The microscopic picture exhibits the mechanism of this interaction. Whenever a proton and electron collide energy is transferred from (a') to (b') or *vice versa*. In a time in which each electron has collided once, an appreciable part of the whole energy has been transferred between one system and the other; so that the time of relaxation is of the order of magnitude of the time between collisions. In white dwarf matter the particles are in continuous collision, and the separate wave systems (a'), (b') can scarcely be said to exist even momentarily.

For white dwarf matter at any rate the eigenstates must be chosen to correspond to the analysis (a), (b), not (a'), (b'). The criterion for the admissibility of a system of eigenstates is well known. If the lifetime of the state is long compared with the period of its eigenfunction, the state is sharp. As the lifetime decreases, the state becomes broadened out of existence. The energy of the system then ceases to correspond to the energy of the states, and passes largely into the perturbing function which causes transitions between the states. When this happens we have to reanalyse into a new set of eigenstates between which transitions are rare, so that the perturbation energy is negligible.

The whole procedure turns on the fact that the energies of eigenstates are easy to calculate, whereas perturbation (interaction) energy is difficult to calculate. For success it is necessary to employ eigenstates between which transitions are known to be rare, so as to ensure that the incalculable perturbation energy is negligible. To employ eigenstates subject to frequent transitions misses the point of the method. This is the initial fallacy of current investigations which yield the Stoner-Anderson formula. They take for eigenfunctions a set of Dirac wave functions which represent electrons moving freely under no forces with constant velocity and constant plane of spin. It would seem difficult to imagine a more unsuitable choice of eigenstates for the problem in hand. Having unnecessarily selected eigenstates between which transitions are exceedingly frequent, the investigator imposes on himself the task of calculating the perturbation energy which must be added to that of the eigenstates. But this is not attempted, and the investigation proves nothing.

If we turn to the other extreme, namely, exceedingly rarefied gas at high temperature, the time between collisions will be long compared with the wave periods chiefly concerned (the occupied states being of high energy owing to the high temperature). The analysis into (a'), (b') then becomes an admissible alternative to (a), (b).

We shall investigate this extreme case—rarefied gas at high temperature—because it can be made to furnish important information by applying the "test of consistency", namely, that the pressure calculated from the wave functions corresponding to (a'), (b') must be the same as the pressure calculated from the wave functions corresponding to (a), (b).

5. To avoid complication we consider hydrogen—ionised into protons

and electrons at the high temperature and low density now contemplated. The "particles" which represent the four molar wave systems, with the notation adopted for their co-ordinates, are

(a) an uncharged particle ; co-ordinates x_1, x_2, x_3,

(b) a doublet ; co-ordinates ξ_1, ξ_2, ξ_3 (representing the separation of charges $+e$ and $-e$),

(a') a positively charged particle, identified with a proton ; co-ordinates x_1, x_2, x_3,

(b') a negatively charged particle, identified with an electron ; co-ordinates x_1', x_2', x_3'.

In each case we consider one statistical particle, with a probability distribution of co-ordinates embodying the actual frequency distribution of co-ordinates of the n particles which it replaces.

The transformation of (a'), (b') into (a), (b) is evidently the transformation of the proton and electron into the external and internal particles of a hydrogen atom—the same as the transformation of the two components of a double star into a star of reduced mass describing the relative orbit together with a mass moving with the centre of gravity. If m, m' are the masses of the proton and electron, the transformation is

$$\mathrm{X}_\alpha = \frac{mx_\alpha + m'x_\alpha'}{m+m'}, \quad \xi_\alpha = x_\alpha' - x_\alpha \quad (\alpha = 1, 2, 3). \tag{5.1}$$

From this we easily derive

$$\frac{1}{m}\frac{\partial^2}{\partial x_\alpha^2} + \frac{1}{m'}\frac{\partial^2}{\partial x_\alpha'^2} = \frac{1}{\mathrm{M}}\frac{\partial^2}{\partial \mathrm{X}_\alpha^2} + \frac{1}{\mu}\frac{\partial^2}{\partial \xi_\alpha^2}, \tag{5.2}$$

where

$$\mathrm{M} = m+m', \quad \mu = mm'/(m+m'). \tag{5.3}$$

Since the mechanical vectors p_α, p_α', P_α, ϖ_α are defined by

$$p_\alpha = (-ih/2\pi)\partial/\partial x_\alpha,$$

etc., (5.2) gives

$$p_\alpha^2/m + p_\alpha'^2/m' = \mathrm{P}_\alpha^2/\mathrm{M} + \varpi_\alpha^2/\mu. \tag{5.4}$$

We find also that the jacobian of the transformation is unity. This secures that statistically there is a one-to-one correspondence between the eigenvalues of the two sides of (5.4), so that the eigenstates in the two methods of analysis are of equal weight.*

If we accept formula (2.1) we have, setting $\alpha = 1$ in (5.4),

$$(\Delta T_{11})_{\text{proton}} + (\Delta T_{11})_{\text{electron}} = (\Delta T_{11})_{\text{external}} + (\Delta T_{11})_{\text{internal}}. \tag{5.5}$$

* The point is that strictly (5·4) has no numerical interpretation, since the two sides do not reduce to eigenvalues simultaneously. But by grouping together a small block of eigenvalues of p^2, p'^2 we get a range of p^2, p'^2 which when expressed as a range of P^2, ϖ^2 includes the *same* number of eigenvalues of P^2, ϖ^2. So that statistically we can arrange the eigenvalues in one-to-one correspondence, although the individual correspondence is not exact. In applying (5·4) the two sides of the equation are understood to refer to this adjusted correspondence, since the small discrepancies introduced by the adjustment cancel one another statistically.

Thus the pressure given by the (a'), (b') analysis is the same as the pressure given by the (a), (b) analysis. We have seen that this is necessary for consistency, since in the extreme case of rarefied hydrogen at high temperature both methods are applicable.

No other formula for ΔT_{11} satisfies this test of consistency, since there is no other relation of the same type as (5.2). In particular (2.2) gives different values of the pressure on the two sides, and must be rejected.

The test of consistency is especially pertinent in the application to white dwarf matter, where the admissible eigenstates correspond to P^2, ϖ^2, and the pressure has to be calculated from P, ϖ. The analogous calculation from p, p' has no independent justification; it will give the right result if the consistency test is fulfilled, and a wrong result if it is not fulfilled. Suppose that for some reason we do not accept the foregoing argument from rarefied hydrogen which provided the consistency test. We are then free to adopt as a hypothesis a formula such as (2.2) which violates the consistency test, remembering that the p, p' calculation will then give a wrong result. But (2.2), when it has been adopted, has always been applied to a p, p' calculation—the calculation which it automatically invalidates!

Besides deciding the formula for ΔT_{11}, which is our main object, we have in (5.3) identified the mass-constants μ, M of the "particles" associated with the electrical and mechanical waves. The remaining steps are familiar. We obtain the Fowler formula $P = K\sigma^{\frac{5}{3}}$, where σ is the electron density and (considering the electrical waves alone)

$$K = \frac{1}{5}\left(\frac{3}{8\pi}\right)^{\frac{2}{3}}\frac{h^2}{\mu}. \tag{5.6}$$

Since

$$\frac{1}{\mu} = \frac{1}{m} + \frac{1}{m'}$$

this is usually regarded as the sum of an electron pressure (denominator m') and a corresponding proton pressure (denominator m).

In addition the mechanical waves will contribute a pressure $P = K_m\sigma^{\frac{5}{3}}$, where

$$K_m = \frac{1}{5}\left(\frac{3}{8\pi}\right)^{\frac{2}{3}}\frac{h^2}{\mathrm{M}}. \tag{5.7}$$

This has not hitherto been recognised. The correction is of no practical importance; but it is interesting to note that (taking (5.6) and (5.7) together) we ought to add to the electron pressure *twice* the proton pressure, since M is very nearly the mass of the proton. This divergence from the usual conclusion is explained by the fact that, in calculating the *minimum* value of P (corresponding to complete degeneracy), the minimising condition ought not to be applied to the electron waves and proton waves separately since they do not exist independently, but it may be applied separately to the internal and external waves since they exist independently.

6. Problems treated in wave mechanics fall into two classes, *separable* and *inseparable* distributions. In the former the eigenstates represent a system

in self-equilibrium ; in the latter they represent a system which is only in equilibrium as part of a larger system. The self-equilibrium of a separable system is not disturbed by giving the system a velocity ; consequently the wave equation which expresses the condition for equilibrium is invariant for a Lorentz transformation of the frame of reference. If an inseparable system is given a velocity it is no longer related to the larger system in the way required to preserve equilibrium ; consequently its wave equation is not invariant for a Lorentz transformation.

A white dwarf star is a separable system ; but it would be impracticable and inappropriate to treat by wave mechanics the molar problem of its internal distribution of density and pressure in gravitational equilibrium. We treat instead a unit cube of white dwarf matter, which is an inseparable system constrained to equilibrium by the rest of the star. To give the cube a velocity would violate the constraints, and the wave equation determining its equilibrium states must therefore be non-invariant for Lorentz transformations. Lorentz invariance is in fact the criterion for physical separability, since it signifies that the surroundings of the system considered can (to the degree of approximation required) be replaced by a purely geometrical frame of reference with no preferential time direction.

The purely negative condition that the wave equations, and therefore the wave functions, of an inseparable system must be non-invariant is not of much help constructively ; and I have therefore not referred to it earlier. But it is the simplest way of disposing of the formula (2.2) which has been so widely employed by astronomers in the form of the Stoner-Anderson theory. All the derivations of it strongly emphasise that the wave functions are Lorentz-invariant. We need no further proof that it is wrong.

7. The pressure system is the three-dimensional part of the energy tensor, and the whole calculation of the degeneracy pressure in §§ 2–5 involves three-dimensional theory only. If the wave functions contain a time factor, we have made no use of it ; nor are we concerned whether the formulæ (2.1) and (5.4) remain true when $\alpha = 4$.

But the more typical parts of quantum theory deal with separable systems which, owing to their Lorentz-invariant property, lead naturally to a four-dimensional theory. Although we have completed our solution of the white dwarf problem, it would perhaps be felt that it had been left rather obscure if we did not show its connection with the more familiar type of quantum problem and explain the reason of the differences which appear. As a first step we shall now recognise a tensor extension of the foregoing theory to four dimensions. This means that we allow the mechanical vector a time component $p_4 = (m^2 + p_1^2 + p_2^2 + p_3^2)^{\frac{1}{2}}$, and introduce a corresponding time factor $e^{2\pi i p_4 t/h}$ in the wave function ; we also allow the suffixes in (2.1) and in § 5 to take the value 4. (Although it does not affect the formal mathematics, the electrical part of the energy, namely, $\varpi_4 = (-ih/2\pi)\partial/\partial\xi_4$, should be re-written as $(h/2\pi)\partial/\partial(i\xi_4)$, because the physically real probability distribution is over the interchange co-ordinate which can be represented as $i\xi_4$.*)

* *Relativity Theory of Protons and Electrons*, pp. 293, 295.

By (2.1) a fully occupied wave function contributes a momentum-density and energy-density $\Delta T_{4\alpha} = p_4 p_\alpha / m$ ($\alpha = 1, 2, 3, 4$). Since our analysis relates to unit volume this is also the total momentum and energy. Thus the momentum-energy vector associated with the wave function (truncated at the boundary of the unit volume) is

$$(p_4/m)p_\alpha. \tag{7.1}$$

This seems to be in conflict with the usual assumption in quantum theory that p_α (here called the "mechanical vector" to avoid confusion) is the momentum-energy vector.

I think this conflict has been the stumbling-block for most physicists who have considered the problem. It was in order to avoid this difference that the denominator was changed to p_4 in the rival formula (2.2). It has not been realised that the difference ought to exist, and is predicted by molar relativity theory. For the separable systems, which form the main theme of quantum theory and provide the stringent experimental tests, p_α is correct. All that we challenge is the current extrapolation to inseparable systems which has been made with insufficient attention to relativity theory.

Before coming to details we may look at the difference from a general point of view. When the mathematician professes to treat a collection of particles constituting a cube of white dwarf matter as a self-contained system without any terms to represent the surrounding matter which is holding it together, a physicist must ask himself how such a conjuring trick is performed. He will not be surprised to find that the mathematician has hidden in each particle an equivalent for the surrounding matter so far as it affects that particle. In discovering the difference $(p_4/m)p_\alpha$ and p_α, we drag to light what the mathematician has hidden.

8. Since $p_4^2 = m^2 + p_1^2 + p_2^2 + p_3^2$, the energy given by (2.1) is

$$p_4^2/m = m + (p_1^2 + p_2^2 + p_3^2)/m = m + 2T \tag{8.1}$$

instead of the commonly adopted value (correct for separable wave functions)

$$p_4 \sim m + (p_1^2 + p_2^2 + p_3^2)/2m = m + T. \tag{8.2}$$

To the classical approximation T is the kinetic energy; and since the different character of the two formulæ is already conspicuous in the classical approximation we need not consider a higher approximation.

The reason for the term $2T$ becomes evident when we include electrostatic energy. If the electrostatic potential is V, the energy of a charged particle includes a Coulomb energy which, both in classical theory and in quantum theory (*e.g.* in Dirac's equation), is taken to be eV. But the total electrostatic energy of a system of particles (*e.g.* the electrostatic energy of the collection of protons and electrons forming the unit volume of neutral matter which we have been analysing) is $E = \frac{1}{2}\Sigma eV$. We may regard the discrepancy in two ways; either

(*a*) The electrostatic energy of a particle is reckoned on double the true scale, or

(*b*) In addition to the energy of the particles there is a field energy $F = -E$ which is not represented by wave functions.

Considering first (*a*) : Since changes of electrostatic energy are balanced by changes of other kinds of energy, we shall not have conservation of energy of the system of particles unless the whole of the variable part of the energy of a particle is reckoned on double the true scale. The formula (8.1) provides for this double-scale reckoning of the true kinetic energy T. There is no need to extend the double reckoning to the *constant* rest-energy m of a particle ; and since this is directly compared with molar masses, the true reckoning is employed for m.

In relativistic theory mechanical energy is connected with an inertial and gravitational field in the same way that electrical energy is connected with an electromagnetic field ; and the double reckoning of kinetic energy in the wave functions, like that of electrostatic energy, appears explicitly.

The point of view (*b*) can be developed more fully. In practice the eigenfunctions for an assembly of charged particles are computed by successive approximation, in order that the eigenfunctions finally adopted may correspond to a "self-consistent field." In calculating the energies (hamiltonians) of the eigenstates this field is treated as *rigid*. Thus the energy H_r of an eigenstate is not the same as the increase of energy of the system produced by the addition of a particle in that eigenstate ; for the addition would involve recalculation of the self-consistent field and of the whole set of eigenfunctions dependent on it. Nominally the energy of the system is

$$H = \Sigma j_r H_r + F, \tag{8.3}$$

where j_r is the probability of occupation of the state H_r, and F is the field energy if any. But this will not agree with the actual energy unless the j_r have the particular values j_r^0 assumed in calculating the self-consistent field from which the H_r are derived. Unless the differences $j_r - j_r^0$ are mostly small it may not even be a tolerable approximation. Nevertheless we have to accept (8.3) as the orthodox quantum formula for the energy.*

We have seen that in the case of electrostatic energy half the electrostatic part of $\Sigma j_r^0 H_r$ is cancelled by the term F. The field energy is therefore

* Quantum theory, unlike relativity theory, is not primarily a rational theory, and therefore its formulæ are generally enunciated without any indication of the conditions in which they are valid. A formula established empirically in certain conditions is extended to conditions in which it has not been verified by a procedure known as "the principle of induction" or less euphemistically as "blind extrapolation." Such extrapolation, though often leading to progress, is fairly sure to break down sooner or later ; but the limits of application are, as it were, an afterthought, and are not derived along with the formula as in a rational theory. The formula (8·3), expressing the energy as the sum of individual contributions from the eigenstates, is primarily an induction of this kind. In the case of electrostatic energy the limitation of its validity is already recognised. But that has not deterred investigators from appealing to it as a recognised quantum formula in the still more extreme conditions of white dwarf matter. It is left to us to find the limits of its validity in these conditions.

equivalent to a negative occupation $-\frac{1}{2}j_r^0$ of the eigenstates. We therefore eliminate the field energy by adopting a modified occupation factor

$$k_r = j_r - \tfrac{1}{2}j_r^0. \tag{8.4}$$

The total energy (8.3) is then

$$H = \Sigma k_r H_r. \tag{8.5}$$

The physical meaning of (8.4) is that a levy is made on the energy of the eigenstates to provide the field assumed in calculating the eigenstates. The particle has a dual aspect, (1) as an entity whose presence coupled with the presence of the field produces an addition to the energy of the system, (2) as an entity required to produce the field whose presence is assumed in calculating the energies of other particles. "Removing" the particle means removing only its aspect (1), since the rigid-field convention implies that there is no removal of the source of the field. To provide for the removal of one aspect without the other we have (effectively) to divide the particle into two halves each associated exclusively with one aspect.

In relativistic theory the same considerations apply to the mechanical energy, which is associated with the inertial-cum-gravitational field $g_{\alpha\beta}$. The $g_{\alpha\beta}$ are also coefficients determining the metric of the co-ordinate system, and in that capacity they must be fixed before the analysis into eigenfunctions begins. Quantum theory always treats the metrical field as rigid; its particles are supposed to be displaceable and to undergo changes of momentum without any consequential changes of $g_{\alpha\beta}$. Just as in the case of electrostatic energy, a nominal energy $H = \Sigma j_r H_r + F$ is assigned to the system, although this will only agree with the true energy when the j_r have the special values j_r^0 representing the state of occupation for which the $g_{\alpha\beta}$ constitute a self-consistent field. As before the two aspects of the particle —as affected by, and as exerting a field,—of which only the former is regarded as removable, are separated by assigning half the standard occupation factor j_r^0 to one aspect and half to the other, so that the effective occupation factor giving the energy in the inertial-cum-gravitational field is (8.4).

The only physical difference from the electrostatic case is that normally the gravitational effects of a particle have a much wider range than its electrostatic effects. The "levy" $\frac{1}{2}j_r^0 H_r$ on its energy is made in order to provide for the metrical field, not only in the unit volume or even throughout the star, but everywhere where metric exists. It is evident even in Newtonian theory that the energy which we attribute to a particle is not a net addition to the energy of the universe, since it will be substantially reduced by the negative gravitational energy of the equivalent mass combined with all other masses throughout the universe. Relativity theory, which recognises that all energy is a mutual energy of pairs of entities, and therefore (on the rigid-field convention) subject to double reckoning, shows that the reduction factor is $\frac{1}{2}$.

But there is also a subjective difference. Quantum theory recognises that the rigid electrostatic field is a fiction, and that the energy (8.5) is only nominal; but it does not recognise that the rigid metric is a fiction, and,

so far as mechanical energy is concerned, (8.5) is accepted as the energy without qualification. We must therefore not expect a general agreement between energies as computed in relativity theory and energies as computed in quantum theory, but only an agreement in the special case when the metric is a self-consistent field of the eigenstates in their actual state of occupation.

9. In the completely degenerate matter, to which our main investigation relates, the states up to a certain level are fully occupied and above that level wholly unoccupied, so that j_r^0 is either 1 or 0. The $g_{\alpha\beta}$ must be a self-consistent field for this state of occupation. By (8.4) the factors k_r for other states of occupation are either $j_r - \frac{1}{2}$ or j_r.

In more advanced theory (second quantisation) the state of occupation is described, not by a numerical probability ranging from 1 to 0, but by a symbolic operator $\mathcal{J}_r$ with eigenvalues 1 and 0, of which j_r is the expectation value. Thus the two forms of occupation or "existence" operator are

$$\mathcal{J}_r - \tfrac{1}{2}, \qquad \mathcal{J}_r, \tag{9.1}$$

where $\mathcal{J}_r$ satisfies $\mathcal{J}_r^2 = \mathcal{J}_r$. The "particles" corresponding to these operators are distinguished as Einstein-Bose and Fermi-Dirac particles respectively.*

Thus, when an eigenstate is fully occupied ($\mathcal{J}_r = 1$) the energy of the particle is for a Fermi-Dirac particle the whole energy of the eigenstate, and for an Einstein-Bose particle half the energy of the eigenstate (the other half having already been taken into account in the $g_{\alpha\beta}$ field). Since the Fermi-Dirac particle is not debited with any contribution to the field, it is to be conceived as a pure addition to the system which determines the rigid metric. If the metric is static (as usually assumed) the standard system is self-equilibrating, and the Fermi-Dirac additions form a separable system with independent conditions of equilibrium. The Einstein-Bose particles, on the other hand, are constituents of the standard system, and are inseparable from it.

It may seem surprising that this discrimination of the two fundamental classes of particles appears naturally in the study of completely degenerate matter, and has little relevance to more ordinary conditions in which the j_r^0 are not limited to the values 1 and 0. The fact is that the development of wave mechanics (rigid-field convention, distinction of E-B and F-D particles, etc.) has taken such a course that it is only adapted to treat completely degenerate matter or conditions approximating thereto. This characteristic of their method has at length forced itself on the attention of the quantum physicists themselves. They have found it necessary to postulate that all the energy levels up to a certain level (which they adopt as zero-level) are with rare exception fully occupied. In the positive energy levels (*i.e.* those above the adopted zero-level) a comparatively small † number

* *Relativity Theory of Protons and Electrons*, § 16·3.

† Instead of limiting the number of particles in positive levels (to avoid over-straining the rigid-field approximation) the current practice is to assume the number in the negative levels infinite, so that any finite number is " comparatively small." This gratuitously re-introduces the difficulties of infinitude which relativity theory encountered and overcame twenty years ago.

of particles may be introduced. This condition, in which the levels up to a certain limit are nearly all occupied and above that limit very sparsely occupied, is that which we study in a white dwarf.

For this reason the white dwarf problem appears to be the best starting-point for the development of relativistic quantum theory. We cannot, of course, pursue the development here; and we must confine attention to the immediate problem of the relation of the formulæ (8.1) and (8.2) each applying in its own sphere.

10. The difference between (8.1) and (8.2) is that the first refers to inseparable (Einstein-Bose) eigenstates and the second to separable (Fermi-Dirac) eigenstates. We have seen that owing to the modified occupation factor, the energy of an Einstein-Bose particle is half that of the eigenstate. The energies of the corresponding *particles* are accordingly

$$\tfrac{1}{2}m+T, \qquad m+T. \tag{10.1}$$

Thus in each case the energy T has its ordinary significance as the variable part of the energy of a particle. In regard to the constant difference $\frac{1}{2}m$, it must be recalled that the term "mass of a particle" is not always used to signify the energy associated with it in a state of rest; for example, the mass μ in (5.3) is not a rest-energy. Commonly the mass is identified with the *mass-constant*, *i.e.* the coefficient m in the expression $(p_1^2+p_2^2+p_3^2)/2m$ for the kinetic energy. Following this usage, both expressions in (10.1) refer to particles of the same mass m. When the term "mass" is intended to mean the rest-energy, it is presumably implied that the system is separable, so that only the second of the expressions in (10.1) is relevant. However, the reader can if he wishes regard the mass of the Einstein-Bose particle as $\frac{1}{2}m$, provided that he revises the dynamical equations so as to distinguish between the mass and the mass-constant.

The factor $\frac{1}{2}$, affecting the energy of an Einstein-Bose particle, should apply to all components of the energy tensor including the pressure. This is in fact true. But since pressure (in the elementary sense of a force exerted by a system on its surroundings) occurs only in inseparable systems, the factor has been absorbed into the definition. The pressure of the particles in the unit cube is their rate of transfer of momentum across the boundary by passing out of the cube. But this is only half the total pressure T_{11}, the other half being contributed by particles from outside entering the cube.

In § 7 we called attention to the trick of the mathematician who professes to treat the unit cube without introducing its physical surroundings. The actual trick is the modified occupation factor k_r, which enables us to represent H as the sum of energies of particles only instead of the sum of energies of particles plus a field energy.

11. The conclusion may be summarised as follows. The investigation in §§ 2–5 determines the pressure but not the energy of degenerate matter. The calculation of the energy is distinct, because there is a preferential time-direction defined independently of the cube of matter under consideration, namely, the time-direction with respect to which the matter surrounding

the cube is at rest. The discussion in §§ 6–10 is, however, primarily intended not to supply the missing calculation of the energy of degenerate matter, but to elucidate a more general question of theory. We notice that, when considered as a special application of a four-dimensional tensor analysis, the wave representation which we have been using is such that a momentum-energy $E_\alpha = p_4 p_\alpha / m$ is represented by a wave function with $(-ih/2\pi)\partial/\partial x_\alpha = p_\alpha$, whereas in more familiar problems it would be represented by a wave function with $(-ih/2\pi)\partial/\partial x_\alpha = E_\alpha$. We point out, firstly, that this difference of representation is occasioned by the fact that in one case we are dealing with an inseparable system and in the other case with separable systems. Secondly, the difference is the starting-point of the currently recognised distinction between Einstein-Bose and Fermi-Dirac wave functions. Consequently it fits naturally into place in current quantum theory ; and the theory is not subversive in tendency, though it corrects (as it was intended to correct) certain unjustified extrapolations which have been too hastily accepted.

It is further shown that, if we do not take account explicitly of the energy of the self-consistent inertial-cum-gravitational field, the particles in inseparable systems must be assigned energies which are half the energies p_4^2/m represented by the eigenfunctions. This makes the kinetic energy of a white dwarf particle $(p_1^2+p_2^2+p_3^2)/2m$, which is the same (to a non-relativistic approximation) as that of a separable particle and not double as at first sight seemed indicated. From this we can calculate the energy-density of white dwarf matter ; it is, as in an ordinary monatomic gas, $\frac{3}{2}$ times the pressure. But since this has not been a principal aim of the investigation, I am not prepared to say whether the result is exact or approximate.

12. In matter which deviates only slightly from the state of a perfect gas the free electrons become somewhat concentrated round the ions (Debye-Hückel effect).* It might be suspected that this concentration would continually increase with the deviation from a perfect gas, and become very intense in the completely degenerate state. It is evidently important to decide this question as a preliminary to any attempt to calculate the absorption coefficient in white dwarf stars. It appears also to be important in connection with theories of transmutation of hydrogen.† It seems to be generally assumed that the concentration does not increase, and that the electrons are fairly uniformly distributed ; but I do not think the question has been seriously investigated.‡ Clearly it is outside the scope of current investigations of white dwarf matter which neglect collisions altogether.

The present investigation answers this question directly, since our co-ordinates ξ_1, ξ_2, ξ_3 represent the position of an electron relative to a proton. Up to distances comparable with the average distance between neighbouring protons, the probability distribution of ξ_1, ξ_2, ξ_3 represents

* *M.N.*, **88**, 352, 1928.

† A roughly uniform distribution of electrons is an essential assumption in an investigation by W. A. Wildhack, *Phys. Rev.*, **57**, 81, 1940.

‡ The question was considered briefly and rather inconclusively in Fowler's original paper.

the probability of finding an electron at any given distance from a specified proton; it will therefore reveal any considerable concentration of the electrons in the neighbourhood of the protons.

The distribution of ξ_1, ξ_2, ξ_3 has been analysed into Fourier components. Its standard deviation will be of the order of magnitude of the mean wavelength of the Fourier components or wave functions; this is of order $(V/n)^{\frac{1}{3}}$, where V is the volume analysed and n the number of electrons or protons. The standard deviation is therefore of the same order as the distances between the protons, showing that there is at any rate no large concentration. The current assumption is therefore justified.

Summary

The theory of the calculation of the pressure of a degenerate gas is reinvestigated, and the author's earlier conclusion that $P = K\sigma^{\frac{5}{3}}$ is the correct relativistic formula is confirmed. It is pointed out that, since the calculation of interaction or perturbation energy is generally impracticable, the success of the method depends on choosing eigenstates for which the perturbation energy is negligible as evidenced by the rarity of transitions. This rules out investigations which employ Dirac wave functions, since they represent states between which transitions are excessively frequent. An analysis is employed which, from molar considerations, is known to satisfy the condition of few transitions. By means of a "consistency test" derived from the consideration of rarefied gas at high temperature, the relation of the pressure to the mechanical vector p_a is uniquely determined. In §§ 6–11 the relation of the white dwarf problem to more typical quantum problems is explained, and apparent contradictions are reconciled. In § 12 it is shown that the electrons are not strongly concentrated in the neighbourhood of the protons or ions.

VARIATION OF FAINT FRAUNHOFER LINES ACROSS THE SOLAR DISC (SECOND PAPER)

M. G. Adam, M.A.

(Communicated by the Director of the University Observatory, Oxford)

Introduction.—The anomalous behaviour of faint Fraunhofer lines towards the limb of the Sun has already been established for the region λ 5100.* From absolute measurements at centre and limb it was shown that the equivalent widths of strong lines decreased to the limb, in agreement with theoretical predictions, but that faint lines showed a marked strengthening which could not be accounted for by the usual theories of line formation. The strengthening of faint lines was finally ascribed to "reduced re-emission" in faint-line frequencies, which was interpreted as interlocking.

The possibility of interlocking does not, however, exist for all faint lines, and this interpretation therefore divides faint lines into two classes according to the reason for their faintness in the solar spectrum. A Fraunhofer line may be faint because it originates from an oscillator of low relative abundance (such lines we henceforth refer to as "rare-element faint lines"), or because it originates from a transition of low probability in an abundant oscillator ("abundant-element faint lines"). Rare-element faint lines will be of high transition probability, and for them there is no possibility of interlocking; it is for the abundant-element faint lines only that we may predict interlocking of the type we have already described.

It is thus easy to test the correctness of the interlocking hypothesis by observations of the centre to limb behaviour of both classes of faint lines. The lines in the region λ 5100 A. are almost wholly abundant-element faint lines, and therefore do not provide the means for making this test. In order to do this, further observations are needed in a region of the spectrum which includes faint lines of both classes. The present paper is an account of the application of this test in a region of the spectrum where faint lines of both classes are to be found. In sections 1 and 2 the choice of a region and the determination of equivalent widths therein is described. The marked strengthening of faint lines is again established, and some evidence for the existence of interlocking is obtained, but since the rare-element faint lines also show limb strengthening, interlocking cannot be the full interpretation. In section 3 a detailed examination of the current theories of line formation is made, and the strengthening of faint lines is finally attributed to an anomalous temperature distribution in the outer layers of the solar atmosphere.

* *M.N.*, **98**, 112, 1938 (Paper I).

Section 1. Observational Procedure

Choice of a Wave-length Region.—Of the two classes of faint lines, we should expect that the rare-element faint lines will be most difficult to find, while with so many possible oscillators it is fairly likely that in any given region of the spectrum we shall find a fair number of abundant-element faint lines. It is not immediately obvious which of the elements, apart from the Rare Earths, we may regard as rare from the point of view of the interlocking theory. Russell has calculated the abundances of elements in the Sun*, but his values are based on unknown atomic transition probabilities and necessarily inaccurate observational data. A more objective procedure from our point of view is to consider, as rare in the Sun, those oscillators none of whose lines has a Rowland Intensity (R.I.) greater than +1. From our general knowledge of the distribution of atomic energy levels we may assume that a faint line will not be interlocked with a strong one if no such strong one occurs within a range of 2500 A. This criterion of rarity gives the elements shown in Table I as rare oscillators for our purpose.

TABLE I

Rare Oscillators in the Solar Spectrum

Element	Max.† R.I.	Log S*	Element	Max. R.I.	Log S	Element	Max. R.I.	Log S
He	0	...	*Cb*?	−2	−0·2	Cs^+	−1	...
Be	−3	1·8	*Mo*	−2	0·5	La^+	1	1·8
C	0	7·4	*Ru*	0	1·0	Ce^+	0	2·4
N	−2	7·6	*Rh*	−2	−0·3	Pr^+	−1	0·6
S?	−1	5·7	*Pd*	0	0·6	Nd^+	0	2·0
K	0	2·8	*Ag*	0	0·0	Sa^+	−1	1·5
Ga	−1	0·2	*Cd*	−1	2·1	Eu^+?	1	1·4
Ge	0	2·5	*Sn*	−2	0·3	Gd^+?	0	1·1
Sr	−1	0·6	*Sb*	−3	0·4	Dy^+	0	1·6
Y	0	0·8	*W*	−2	−0·1	Er^+?	−1	0·1
Zr	−1	0·9	*Tl*?	−2	−0·8	Yb^+?	−1	...
			Pb	−2	0·2	Hf^+	−1	0·4

As a first step in choosing a region, *Rowland's Revision* was examined from λλ 3800–6300, the practical limits of spectroscopy, avoiding the water-vapour lines, for the lines of La^+, Sa^+, Pr^+, *Mo*, Dy^+, *Rh*, *Ru*, Eu^+, *W*, Gd^+, *Zr*, *Y*, *Cb*. This showed that the line density for a variety of rare elements was probably greatest in the region of H_δ (λ 4100) where the lines of the Rare Earths occur. In the region λλ 4105–4160 we find the rare-element faint lines given in Table II, none of which are closer than ·05 A. to any other line, and which, therefore, we should have a fair chance of

* *Ap. J.*, 70, 11, 1929. The abundance is here given in terms of S, the number of atoms per unit area of the Sun's surface.

† *Rowland's Revision*, p. xv.

measuring. It will be seen that, with the possible exception of Ce^+, these are all due to oscillators which Russell also gives as comparatively rare.

TABLE II

Rare-element Faint Lines from $\lambda\lambda$ 4105–4160.

Element	Max. R.I.	Log S	λ	Element	Max. R.I.	Log S	λ
Nd^+	0	2·0	4109·46	Gd^+	0	1·1	4130·45
			4116·82				
			4133·36	Zr	−1	0·9	4135·69
			4135·30				
				Cb	−2	−0·2	4137·12
La^+	1	1·8	4141·66				4139·73
			4141·76				
				Pr^+	−1	0·6	4143·16
Sa^+	−1	1·5	4123·95	Ce^+	0	2·4	4115·38
			4155·20				4119·80
Y	0	0·8	4128·31				4119·92
			4142·85				4120·84
							4123·88
Rh	−2	−0·3	4128·90				4124·79
							4127·38
Eu^+	1	1·4	4129·73				4137·66
							4142·41
Ru	0	1·0	4145·76				4144·52
							4145·01

Comparison with Harrison's recent tables (G. R. Harrison, *Wavelength Tables*, 1939) makes the identification of 4116·82, 4119·80, 4119·92, 4141·66 doubtful. λ 4130·45 is identified as Cr by Miss Moore. *

The representation of the abundant-element faint lines in the same region was determined from Miss Moore's table.* In this table, lines which are faint members of a strong multiplet, or lines of a theoretically faint multiplet, were selected and gave the lines in Table III. Where a line of at least two intensities greater on the Rowland scale occurs in the same multiplet, no further justification is given in column 6 ; where the multiplet as a whole is taken as being interlocked, details of possible interlocking are given in this column. s in column 5 means that the line is a singlet.

For both classes of faint lines the region to the red of H_δ is thus satisfactory, and was therefore selected for an observational test of the interlocking hypothesis.

Solar Spectra.—Solar spectra at λ 4100 were obtained by means of the Oxford solar telescope and 30-foot prism spectroscope.† The spectroscope was used with two 60° prisms and one 30° reflecting prism, which gave a

* C. E. Moore, *A Multiplet Table of Astrophysical Interest*, 1933.

† H. H. Plaskett, *M.N.*, **99**, 289, 1939; *Engineering*, May 10, 1939.

TABLE III

Abundant-element Faint Lines from λλ 4105–4160.

El.	λ	R.I.	Multiplet	Max. R.I. in Mult.	Reason for Possible Interlocking of Multiplet. λ and R.I. of Stronger Lines with same Upper State
Fe	4104·95	1	$z^5F^\circ - 13$	4	
	4105·06	−1	$z^5F^\circ - 2$	*s*	4433·2 (3), 4485·7 (3).
	4116·96	1	$z^5D^\circ - 33$	4	
	4117·74	−2	$z^5P^\circ - 55$	*s*	5859·6 (5), 6420·0 (4).
	4119·67	0	$z^7F^\circ - e^5F$	2	
	4126·86	1	$b^3P - y^3P^\circ$	4	
	4137·98	0	$z^7F^\circ - e^5F$	2	
	4138·86	0	$a^3P - x^5P^\circ$	2	
	4145·20	1	$a^3G - x^5G^\circ$	...	4010·8 (2), 4556·1 (4 blend).
	4156·45	1	$z^5F^\circ - 14$	4	
	4156·67	1	$b^3G - 26^\circ$	*s*	3827·6 (2), 3869·6 (3), etc
Fe^+	4122·67	1	$b^4P - z^4F^\circ$	3	
Cr	4118·43	−2	$a^5P - v^5D^\circ$	*s*	3841·3 (1), 3850·0 (masked).
	4127·28	0	$a^5G - y^5G^\circ$	2	
	4153·06	−1	$a^5G - y^5G^\circ$	2	
Cr^+	4112·57	−1	$b^4D - z^4P^\circ$	...	3382·7 (4), 3422·8 (4), etc.
	4132·41	0	$a^4P - z^4D^\circ$	...	3393·8 (2), 3394·3 (2), etc.
	4146·50	−1	$a^4P - z^4D^\circ$	...	
Zr^+	4110·04	−1	$a^2P - z^2D^\circ$	...	3630·0 (1), 4048·7 (1).
Y^+	4124·92	0	$a^1D - z^3F^\circ$	3	
Ni	4115·99	0	$y^3D^\circ - g^3G$	...	3363·6 (1), 3422·3 (1), 3479·3 (1), 4195·5 (1).
	4148·72	−1	$z^5D^\circ - f^3F$	...	4115·4 (2), 4918·4 (2), 4935·8 (2), etc.
V	4116·48	1	$a^6D - y^6D^\circ$	4	
	4116·71	1	$a^6D - y^6D^\circ$	4	

dispersion of 0·4 A. per mm. in this region. For the solar spectra, a metal diaphragm was placed over the spectroscope slit, which reduced its extent to just less than 1 cm. This diaphragm is crossed by three wires, so that the full 1 cm. was not exposed, and the effect of light scattered in the spectroscope perpendicular to the dispersion thereby reduced. The effect of light scattered parallel to the dispersion was reduced by the use of a Wratten blue filter (F. 39).

After careful focussing tests, the plates were finally exposed between 1938 November 21–27. Exposures were made when the seeing was most favourable and the sky in the vicinity of the Sun free from cloud. The limb spectra

were obtained with the slit radial to the E. and W. limbs, giving a range of cos θ from 0·45 approximately to 0·0, and the solar image was carefully guided throughout the exposure; for the centre spectra no change in the image position could be observed.

Two solar exposures were made on each plate (both centre or both limb), and calibration spectra were then put on in an auxiliary spectroscope with a Zeiss platinum step wedge.* The wedge was illuminated through the filter F. 39 by light from a 6-volt spiral filament lamp diffused off a magnesium carbonate block, and four calibration spectra of different densities (obtained by varying the slit width) were put on each solar plate. A comparison helium spectrum was put on with each wedge spectrum. Seventeen usable calibrated solar plates were finally obtained, of which three centre and three limb plates were selected for measurement; the details for these plates are given in Table IV below. All the plates were stored for 24 hours after the last exposure was made, and then developed in Parkhurst two-solution developer.

TABLE IV

Measured Plates

Plate	Slit	Date G.M.T.	Exposure	Details	Calibration		Emulsion
					Date	Exposure	
	mm.		m s			m s	
A_{52}	·05	Nov. 21·479	4 00	Limbs E. + W.	Nov. 21	4 00	Ilford Sp. Rapid.
A_{53}	·05	21·497	3 00	Centre	21	3 00	,, ,,
A_{54}	·05	21·517	6 00	Limbs E. + W.	22	6 00	,, ,,
A_{57}	·05	22·465	14 00	Limbs E. + W.	23	14 00	Ilford Rap. Pro. Pan.
A_{64}	·05	24·479	3 30	Centre	25	3 30	Ilford Sp. Rapid.
A_{69}	·05	26·455	4 00	Centre	27	4 00	,, ,,

Section 2. Measurement and Reduction of Plates

Characteristic Curves.—Characteristic curves for the solar plates were obtained from the wedge spectra on each plate, by sliding the blackening-log transmission curves they give to form a single smooth curve. The calibration of the wedge, which is an essential preliminary to this procedure, was carried out by the method described by H. H. Plaskett †, in which the light intensity is reduced by a known amount by diaphragming the collimating lens. The illuminating source finally used was a standardised ribbon filament lamp. An image of the filament was focussed on to the slit of the auxiliary spectroscope by means of a wide aperture lens 15 cm. in diameter and approximately 70 cm. focal length. The lamp current (about 16 amps.) was carefully controlled during each exposure, which lasted for 60 secs. The blue filter

* D. S. Evans, *M.N.*, **100**, 157, 1940.

† H. H. Plaskett, *M.N.*, **91**, 878, 1931.

F. 39 was again used, and comparison spectra were put on from an iron arc. Twenty plates in all were obtained, 10 wedge erect and 10 wedge reversed.

The wedge calibration plates were carefully marked on a Hilger micrometer at λ 4144 approximately, and microphotometered at this wavelength. The final transmission values obtained for the wedge at λ 4144 are shown below; each erect and reversed value is the mean of 10 values.*

Wedge Strip	Transmission at λ 4144		Mean	S.D. of a Single Plate
	Erect	Reversed		
O	·829	·838	·833	± ·056
A	·593	·588	·591	± ·031
B	·426	·437	·431	± ·018
C	·316	·312	·314	± ·015
D	·193	·200	·196	± ·007
E	·132	·135	·133	± ·004
O′	·854	·853	·854	± ·053

The four calibration spectra on each solar plate were put on, two with the wedge erect (strip *O* uppermost) and two with the wedge reversed (strip *O′* uppermost), so that in deriving characteristic curves the effect of a linear non-uniformity in the calibrating illumination is eliminated. Even if such a linearity is established, it is preferable to determine the distribution of intensity of illumination along the slit, and correct the wedge-erect and wedge-reversed curves before combining them. Five plates to measure the intensity distribution were taken with the identical set-up used for the solar plates, and gave a linear change of intensity across the slit height of 2·6 per cent. The wedge constants used in deriving the characteristic curves were accordingly corrected for this non-uniformity of illumination.

Instrumental Profile.—The instrumental pattern of the spectroscope is a normalized function operating at each point in the spectrum and therefore does not alter equivalent widths, with which we are primarily concerned. But it determines the resolution of close lines, and since the solar spectrum is so densely populated with lines it determines which of our selected lines will be measurable. The instrumental pattern for the Oxford spectroscope

* The method of wedge calibration described was undertaken after a calibration had been completed by the method described by D. S. Evans (*M.N.*, **100**, 157, 1940), using a set-up similar to that for the plate calibration. This was carried out for λ 4090 and λ 4190, and showed clearly that the difference in transmission over 100 A. was negligible. The difference between wedge-erect and wedge-reversed step transmissions showed, however, that in our case slight differences from Evans' set-up had introduced errors into the wedge calibration (but not into the plate calibration) due to the prismatic form of the wedge. The calibration described was therefore undertaken to eliminate this error, and the good agreement between wedge-erect and wedge-reversed values shows the extent to which this was achieved.

has been determined by D. S. Evans *, and from this determination the pattern $S(x)$ for slit width ·05 mm. at λ 4100 was deduced. A true contour $I(x)$, which after passing through the spectroscope would fit the observed profile $O(x)$ of a line of equivalent width (E.W.) ·032 A. (R.I. between +1 and 0), was deduced. $I(x)$ is such that

$$O(l) = \int_{-\infty}^{+\infty} I(x)S(l-x)dx.$$

The instrumental distortion of two close lines of true shape $I(x)$ was then determined. Two contours $I(x)$ were separated by 0·1 A., and the light $I'(x)$ from the pair incident on the spectroscope slit was deduced from an η, r † curve. The slit pattern $S(x)$ was then applied to $I'(x)$.

This investigation showed that it was impossible to get true contours for two lines of R.I. between +1 and 0 if they are as close as 0·1 A., but that the central intensity is only in error by 3 per cent. approximately and could be corrected and used to read off equivalent widths from an r-E.W. curve.

Measurement of Selected Lines.—The solar spectra were microphotometered parallel to the dispersion with a magnification of 6·9; this meant that the spectra at λ 4120 were examined on the tracing with a dispersion of 18 mm. per A. With the tracings and *Rowland's Revision* a detailed consideration of blending was made for each selected line. In this way the procedure to be adopted in measuring each line was arrived at, and an estimate of the correction to be applied to the result determined. 40 of the 53 lines in Tables II and III proved to be measurable. Wings of strong lines were taken into account by drawing them in on each tracing, and where necessary using this wing as the continuous background. The corrections for blending with faint lines were estimated from the results of the investigation above and are thus only very approximate; as the corrections never exceed 4 per cent. however, this uncertainty is not very serious.

Table V shows the mean corrected ‡ central intensities and mean equivalent widths obtained for the selected lines from three centre and three limb (cos θ ·311) plates. Except as shown, each mean value is obtained from three individual plate values. For the central intensities the average dispersion of the individual plate measures from the uncorrected mean r was ·009 or 1·1 per cent. at the centre, and ·012 or 1·6 per cent. at the limb. The equivalent widths, of which the mean is given in columns 4 and 7 of Table V, were obtained from planimeter measurements of contours. The

* D. S. Evans, *Observatory*, **62**, 231, 1939.

† η in Eddington's notation is the ratio of line-absorption to continuous absorption. r is the residual line intensity. It was assumed that where the lines overlapped, the η's were additive.

‡ The actual blending corrections applied to r_{centre} and r_{limb} are as follows :—

λ 4116·48 r	increased 4 per cent.	λ 4128·31 r	increased 2 per cent.
λ 4123·88 r	,, 2 ,,	λ 4130·45 r	,, 2 ,,
λ 4123·95 r	,, 2 ,,	λ 4142·85 r	,, 3 ,,
λ 4127·38 r	,, 2 ,,		

contours were obtained from each tracing by measuring the line width (or half width if blended on one side) at different r values; the average dispersion from the mean E.W. was 5·5 per cent. at the centre, and 7·9 per cent. at the limb. From the individual plate values of E.W., fig. 1, showing the relation between central intensity and equivalent width, was obtained. We have taken the same r-E.W. relation (the smooth curve shown) for all classes of lines at the centre and at the limb, since the observational material does

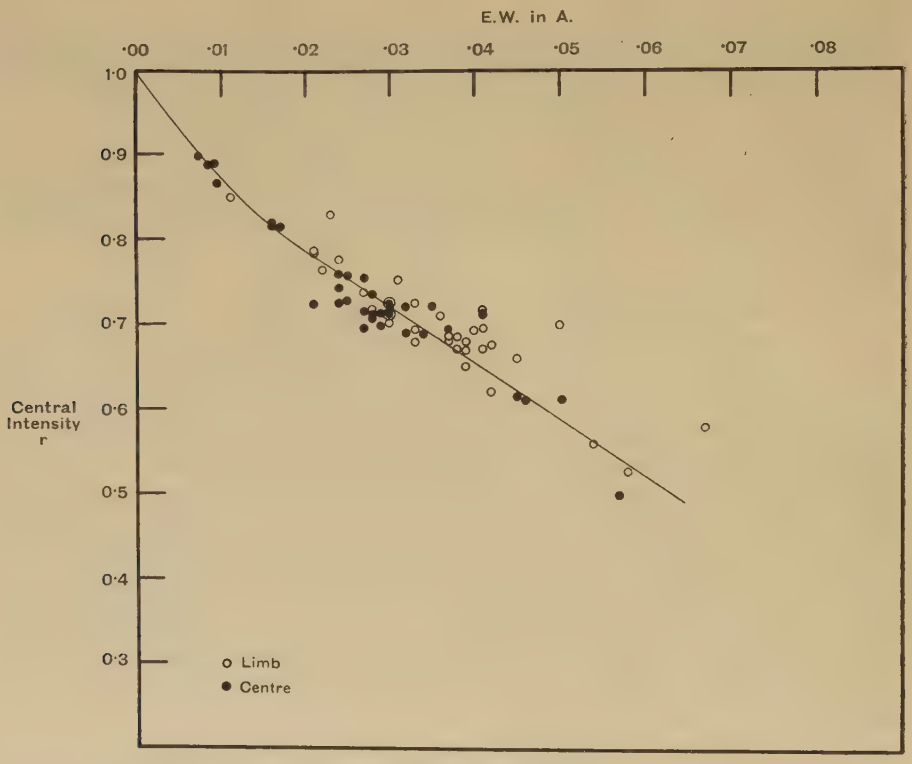

Fig. 1.—*Relation between central intensity and equivalent width.*

not justify any refinement on the procedure: we have only a few lines of any one class, and the wide instrumental pattern tends to disguise any real difference in profile.* Measured equivalent widths are available for only a few lines, while we have the mean central intensity at centre and limb for all lines alike. E.W.s at centre and limb for all 40 lines were therefore

* The measures give some indication that the *Fe* lines lie on a slightly steeper r-E.W. curve, and that for Eu^+ the curve is shallower, and that for all classes of lines the limb curve is slightly shallower than the centre curve, in agreement with the difference between centre and limb already found at λ 5100 (Paper I, p. 119) (*cf.* A. D. Thackeray, *P.A.S.P.*, 48, 119, 1936). We may point out that if such distinctions were confirmed, the limb strengthening would be even more pronounced for the faint lines of R.I. 0 and +1, and the behaviour of the rare-element faint lines and abundant-element faint lines more nearly the same.

obtained from the mean corrected r of Table V and fig. 1. The results are shown in columns 6 and 9 of Table V, which thus contain the final observational data the investigation was planned to provide.

TABLE V

Equivalent Widths at Centre and Limb for Selected Lines

Wavelength	Ident.	R.I.	Centre			Limb ($\cos\theta$ ·31)			L/C
			Mean Measured E.W. in A.	Mean r	C E.W. from Curve in A.	Mean Measured E.W. in A.	Mean r	L E.W. from Curve in A.	
4104·95	*Fe*	1		·619	·0452		·572	·0523	1·157
4109·46	*Nd*$^+$	1	·032	·698	·0332	·042	·674	·0368	1·108
4112·57	*Cr*$^+$	−1		·918	·0062		·891	·0084	1·355
4115·38	*Ce*$^+$	−1		·904	·0072		·890	·0085	1·181
4115·99	*Ni*	0	·030	·722	·0294	·034:	·712	·0311	1·058
†4116·48	*V*	1		·619	·0452		·595	·0490	1·084
4116·71	*V*	1	·027*	·750	·0252	·030*	·706	·0321	1·274
4116·96	*Fe*	0	·030	·718	·0302	·038	·678	·0363	1·202
4119·67	*Fe*	0		·808	·0168		·768	·0225	1·339
4119·80	*Ce*$^+$	0		·785	·0200		·776	·0214	1·070
4119·92	*Ce*$^+$	0		·778	·0210		·750	·0252	1·200
4120·84	*Ce*$^+$	−1	·0094:	·884	·0090	·017:	·849	·0122	1·356
4122·67	*Fe*$^+$	1	·057*	·515	·0611	·060:	·573	·0522	0·854
†4123·88	*Ce*$^+$	−1		·813	·0162		·821	·0152	0·938
†4123·95	*Sa*$^+$	−1		·764	·0231		·778	·0210	0·909
4124·79	*Ce*$^+$	0	·024	·751	·0251	·029:	·752	·0249	0·992
4124·92	*Y*$^+$	0	·016	·815	·0159	·022	·773	·0217	1·365
4126·86	*Fe*	1	·025	·719	·0300	·036	·687	·0350	1·167
4127·28	*Cr*	0		·820	·0153		·807	·0170	1·111
†4127·38	*Ce*$^+$	−1		·849	·0122		·831	·0141	1·156
†4128·31	*Y*	−1		·903	·0073		·887	·0087	1·192
4128·90	*Rh*$^+$	−1		·921:	·0059		·905	·0072	1·220
4129·73	*Eu*$^+$	1	·041:	·710:	·0314	·045:	·707:	·0319	1·016
†4130·45	*Gd*$^+$	0		·917	·0063		·897:	·0080	1·270
4133·36	*Nd*$^+$	1		·920	·0060		·895	·0081	1·350
4135·30	*Nd*$^+$	0		·882	·0092		·849	·0122	1·326
4137·66	*Ce*$^+$	1	·032	·703	·0324	·036	·685	·0352	1·086
4137·98	*Fe*	0		·783	·0202		·737	·0273	1·351
4138·86	*Fe*	0		·843	·0128	·021*	·796	·0185	1·445
4139·73	*Cb*	−1		·945	·0041		·926	·0055	1·341
4141·66	*La*$^+$	0		·855	·0116		·813	·0162	1·397
†4142·85	*Y*	−1		·935	·0048		·936	·0047	0·979
4144·52	*Ce*$^+$	0		·930	·0052		·937	·0046	0·885
4145·01	*Ce*$^+$	0	·0079:	·896	·0081		·920	·0060	0·741
4145·20	*Fe*	1	·027	·705	·0322	·030	·701	·0327	1·016
4145·76	*Ru*	1	·047	·609	·0467	·041	·647	·0410	0·878
4146·50	*Cr*$^+$	−1		·926	·0055		·937	·0046	0·836
4153·06	*Cr*	−1		·898	·0078		·870	·0102	1·308
4155·20	*Sa*$^+$	−1		·949	·0037		·959	·0029	0·784
4156·45	*Fe*	1		·585*	·0504	·058*	·539	·0573	1·137

: Mean of two values. * One value only. † Mean central intensity corrected for blending.

For comparison with the present equivalent widths we have those of Woolley * and Allen.† Woolley's measurements were made with a liquid in glass prism and have been found by several observers to be systematically too small. Mulders ‡ finds E.W.s 50 per cent. (for lines of R.I. +1) greater than Woolley's, in good agreement with second measurements by Woolley with a glass prism. Thackeray § agrees with Mulders' higher

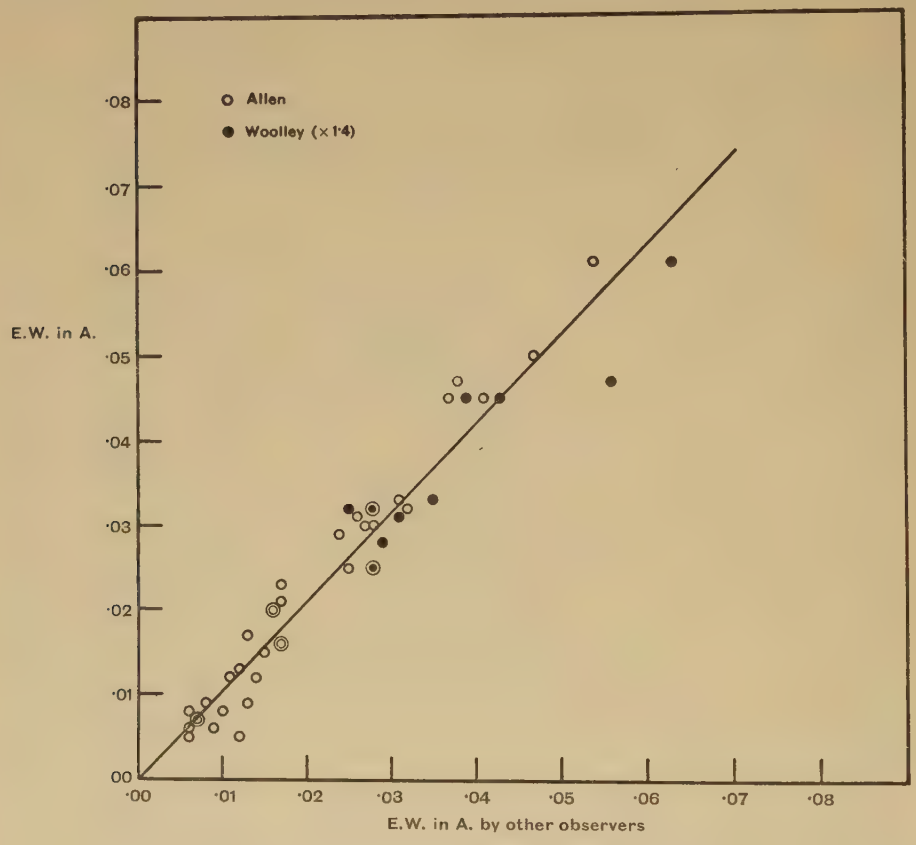

FIG. 2.—*Comparison of equivalent widths with those obtained by other observers.*

value, and Allen † multiplies Woolley's E.W.s by 130 per cent. to bring them into agreement with his own. Allen has measured 35 of the 40 lines in Table V; the average value of the ratio of the present determination to Allen's E.W. for the same line is 1·046. The agreement between the two determinations is shown graphically in fig. 2, together with Woolley's measurements multiplied by 140 per cent. While there is considerable scatter about the mean ratio of 1·046, this is not surprising for these faint and often blended lines.

* R. v. d. R. Woolley, *Annals of the Sol. Phys. Obs. Camb.*, Vol. III, Part II.
† C. W. Allen, *Mem. Sol. Commonwealth Obs.*, **6**, 1938.
‡ G. F. W. Mulders, *Zeit. für. Ast.*, **10**, 309, 1935.
§ A. D. Thackeray, *A.J.*, **84**, 405, 1936.

There are two obvious possibilities for the 5 per cent. increase in E.W.s now obtained, one is the more complete elimination of scattered light in the present instance *, and the other that the discrepancy may be introduced by the r-E.W. relation used in the two investigations. Allen's procedure for obtaining this relation was less objective than that here described, in that he employed blended (with empirical corrections) as well as unblended lines, but it has the advantage of being obtained from a very much greater number of lines (more than 200). If, however, the r-E.W. relation is a function of wave-length, then the use of a large number of lines extending over a long wave-length range is not desirable.

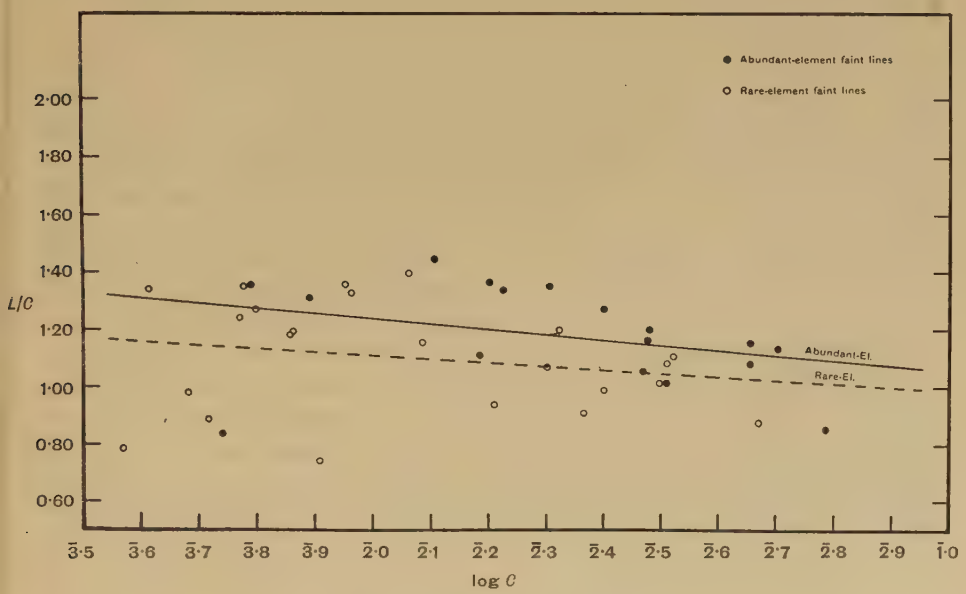

FIG. 3.—*Ratio L/C against log C.*

Change of Equivalent Width from Centre to Limb.—In column 10 of Table V is given the ratio of the E.W.s at centre and limb (L/C) for each of the observed lines, and in fig. 3 the relation between L/C and log C is shown graphically. It is first of all obvious that the marked strengthening of faint lines to the limb, found earlier, is confirmed; further, there is some tendency for the rare-element faint lines to show a smaller value of L/C than the abundant-element faint lines. In order to check the truth of the last statement a least squares solution was made for the linear relation between L/C and log C. Taking log C as the independent variable, accurately known, we find the following values and probable errors for the constants m and k in the equation

$$L/C = m\,(\log C + 3) + k.$$

* D. S. Evans (*M.N.*, **100**, 168, 1940) estimates that the scattered light is less than 1 per cent. in the Oxford spectroscope.

	No.	m	k
Abundant-element faint lines	17	$-\cdot178 \pm \cdot137$	$1\cdot416 \pm \cdot187$
Rare-element faint lines	23	$-\cdot118 \pm \cdot125$	$1\cdot229 \pm \cdot139$

These straight lines are shown on fig. 3. If we omit from the rare-element faint lines the ones whose identification was considered earlier to be doubtful (see note to Table II), the difference between the two groups of lines is still more pronounced.*

Section 3. Theoretical Discussion

Our two investigations of faint-line behaviour, based on observations made at different times, with different equipments, different methods of plate calibration, and in different regions of the solar spectrum, establish beyond doubt the existence of a marked limb strengthening for all faint lines. The present investigation shows that this behaviour cannot entirely be interpreted by the obvious theory of interlocking, although evidence is at the same time obtained for the existence of interlocking in some cases. We therefore now examine the existing theories of absorption-line formation, to see how far they account for the strengthening of all faint lines to the limb of the Sun, and for the increased strengthening of interlocked lines.

There are two types of atmospheric models to examine, the Schuster pure scattering atmosphere with a bounded photosphere, from which the continuous intensity arises and above which the absorbing material lies, and an Eddington model, in which the continuous spectrum is formed all the way up in the atmosphere.

A Pure Scattering Atmosphere.—$r(\theta)$ on this model is given, in terms of σ_1, the total optical depth in the line frequency by †

$$r(\theta) = \frac{1}{2} \cdot \frac{1-(1/3)u_1}{1-u_1+u_1\cos\theta} \left[\frac{1+(3/2)\cos\theta}{1-(1/3)u_1} + e^{-\sigma_1 \sec\theta} \left\{ \frac{2(1-u_1+u_1\cos\theta)}{1-(1/3)u_1} - \frac{1+(3/2)\sigma_1+(3/2)\cos\theta}{1+\phi(\sigma_1)} \right\} \right] \quad (1)$$

This expression is completely exact, except that the observed darkening to the limb has been represented as a linear change

$$I(\sigma_1, \theta) = I(\sigma_1, 0)(1-u_1+u_1\cos\theta).$$

It is easy to remove this approximation by replacing $(1-u_1+u_1\cos\theta)$ where

* See note on p. 602 on the effect of the r-E.W. relation.

† H. H. Plaskett, *M.N.*, **91**, 909, 1931.

it occurs by the observed $\frac{I(\sigma_1, \theta)}{I(\sigma_1, 0)}$, and performing mechanically the integration $\int I(\sigma_1, \theta) \cos\theta \sin\theta \, d\theta$.*

The ratio $r(\theta)/r(0)$ on this model is controlled by the coefficient of darkening u_1, which of course increases towards the violet end of the spectrum. u_1 at λ 5100 was determined from the observations of Moll, Burger and Van der Bilt †, which give $u_1 = 0{\cdot}68$ for $\cos\theta{\cdot}3$. Unfortunately their observations do not extend beyond the region λ 4500 A. Abbot's values ‡ extend down to λ 3700, and the limb darkening $\frac{I(\sigma_1, \theta)}{I(\sigma_1, 0)}$ at λ 4100 A. for $\cos\theta{\cdot}3$ was determined from a combination of both sets of observations as 45·2 per cent., giving $u_1 = 0{\cdot}78$. At λ 5100 we have already shown that equation (1) gives limb § strengthening for values of $r(0) > 76$ per cent.; at λ 4100, with the increased limb darkening, no limb strengthening is predicted. Since no further modification of this model is possible, we must therefore reject it, since at λ 4100 it does not account for the strengthening of non-interlocked lines.

An Eddington Model Atmosphere.—The Eddington model has much more flexibility than the pure scattering atmosphere. In the equation of transfer ||, with the usual Eddington notation,

$$\cos\theta \frac{d\mathcal{J}_v'(\theta)}{d\tau} = (1+\eta)\mathcal{J}_v'(\theta) - (1-\epsilon)\eta\mathcal{J}_v' - \epsilon\eta\mathcal{J}_T - \mathcal{J}_T, \qquad (2)$$

η and ϵ as well as $\mathcal{J}_T$ may vary with optical depth. We have already investigated the case η constant, ϵ constant, and $\mathcal{J}_T$ a linear function of depth ¶ at λ 5100. It was found that no limb strengthening was predicted for any ϵ value, but that $\epsilon = 0$ gives the best fit with the stronger lines. At λ 5100 the ratio $\frac{b}{a}$ in $\mathcal{J}_T = a + b\tau$ is 2·11; at λ 4100 the observed surface brightness ratio $\frac{I(0,\theta)}{I(0,0)} = 45{\cdot}2$ per cent. gives $\frac{b}{a} = 3{\cdot}61$; this value of b/a gives even more pronounced weakening for faint lines to the limb.

We now investigate two further modifications of the Eddington model, (*a*) η an arbitrary function of depth, (*b*) $\mathcal{J}_T$ a non-linear function of depth.

(*a*) η *varies with Depth.*—The solution of (2) now becomes a much more difficult problem; it is only for very special forms of η variation that we can derive an explicit expression for $\mathcal{J}_v'$. If $\mathcal{J}_v'$ is obtained, equation (2) may still not be soluble, but provided we can get an integrating factor

* Abbot's curve for λ 4100 approximately gave a negligible effect,

$$\int I(\sigma_1, \theta) \cos\theta \sin\theta d\theta = {\cdot}365 \text{ and } \frac{1-(1/3)u_1}{2} = {\cdot}364.$$

† Paper I, p. 125.

‡ C. G. Abbot, *Smithson Ann.*, 4, 221, 1922.

§ All numerical results for the limb in this section refer to $\cos\theta{\cdot}3$, $r(l) = r(\cos^{-1}{\cdot}3)$.

|| A. S. Eddington, *M.N.*, 89, 624, 1929.

¶ Paper I, p. 127.

we may resort to mechanical integration. We distinguish three methods by which the problem of variable η may be attacked: (1) η is a continuous function of depth such that we can derive an exact expression for $\mathcal{J}_\nu'$; (2) η varies continuously with depth and we derive an approximate expression for $\mathcal{J}_\nu'$; (3) the atmosphere is divided into discontinuous layers within each of which η has a different constant value.

Method (1) * has been considered by several writers; it is cumbersome and the form of η variation limited.† We have here adopted methods (2) and (3). In method (2) we follow Minnaert.‡ For small η we neglect η in $\mathcal{J}_\nu'$, and substitute for $\mathcal{J}_\nu'$ in (2) the continuous spectrum value

$$\mathcal{J} = a + b\tau + \frac{(2/3)b - a}{1 + 2/\sqrt{3}} e^{-\sqrt{3}\tau}.$$

(2) then becomes ($\epsilon = 0$)

$$d\mathcal{J}_\nu'(\theta) e^{-\int (1+\eta)\sec\theta d\tau} = -(\eta\mathcal{J} + \mathcal{J}_T) e^{-\int (1+\eta)\sec\theta d\tau} \sec\theta d\tau,$$

i.e.

$$\mathcal{J}_\nu'(\theta)_{\tau=0} = \int_0^\infty (\eta\mathcal{J} + \mathcal{J}_T) e^{-(\tau+\tau_\nu)\sec\theta} \sec\theta d\tau,$$

where $\tau_\nu = \int \eta d\tau$ is the optical depth in the line frequency. For any given η distribution we may integrate this mechanically. We have investigated $r(\theta)$ for (*a*) η increases with depth, (*b*) η decreases with depth:

	τ	0·0	0·2	0·4	0·6	0·8	1·0	2·0	3·0	4·0
(*a*)	η	0·00	0·05	0·10	0·15	0·20	0·25	0·50	0·75	1·00
(*b*)	η	0·30	0·20	0·10	0·00	0·00	0·00	0·00	0·00	0·00

(*a*) At λ 4100 gives $r(0)$ ·92 → $r(l)$ ·96, *i.e.* weakening.
(*b*) ,, λ 4100 ,, $r(0)$ ·95 → $r(l)$ ·94, *i.e.* strengthening?
(*b*) ,, λ 5100 ,, $r(0)$ ·98 → $r(l)$ ·96, *i.e.* strengthening.

Method (3) is due to Eddington.§ We may hope to get some clue to the way in which η varies with depth by considering a layer of constant η at different depths in the solar atmosphere. For any layer in which η is constant we have

$$\left.\begin{aligned} \mathcal{J}_\nu' &= a + b\tau + De^{-q\tau} + Ee^{+q\tau} \\ H_\nu' &= \frac{1}{3(1+\eta)}[b - qDe^{-q\tau} + qEe^{+q\tau}] \end{aligned}\right\} \quad q^2 = 3(1+\eta)(1+\epsilon\eta).$$

The constants D and E are different for each layer, but from the continuity of $\mathcal{J}_\nu'$ and H_ν' at the internal boundaries, and the fact that at $\tau = 0$ $\mathcal{J}_\nu' = 2H_\nu'$, these constants are determinable for each layer. We then calculate $\mathcal{J}_\nu'$ throughout the atmosphere, and substitute the calculated $\mathcal{J}_\nu'$ in equation (2).

* A. S. Eddington, *M.N.*, **89**, 624, 1929. † L. Spitzer, *Ap. J.*, **87**, 1, 1938.
‡ M. Minnaert, *Zeit. für. Ast.*, **12**, 313, 1936. § *Loc. cit.*

In solving numerically we have kept $\eta = 0$ except in one layer; the resulting $r(\theta)$ values for different positions of this layer are given below ($\epsilon = 0$):

Layer	η	Extent τ to τ	$r(0)$	$r(l)$	Effect at Limb	λ in A.
Deep	0·76	0·5 2·0	·823	·935	Weakening	4100
Higher	0·76	0·3 0·8	·849	·907	,,	4100
Surface	0·76	0·0 0·5	·813	·856	,,	4100
Thin surface	0·76	0·0 0·2	·933	·927	Strengthening?	4100
,,	0·76	0·0 0·2	·936	·902	Strengthening	5100
,,	2·0	0·0 0·2	·76	·89	Weakening	4100
,,	2·0	0·0 0·2	·79	·80	Weakening?	5100

So that a thin surface layer of $\eta \neq 0$ will give the required limb strengthening at λ 5100 and much less at λ 4100, and for smaller r values gives weakening.

Methods (2) and (3) agree in showing that only a layer of absorbing material concentrated close to the surface above an optical depth of $\tau = 0{\cdot}6$ gives even qualitative agreement with the observations. This cannot be regarded as satisfactory; apart from the difficulty of justifying theoretically such an early decrease in η, the strengthening predicted at λ 5100 is so much greater than for λ 4100, whereas the observed effects are approximately equal.

(*b*) $\mathcal{J}_T$ *has a Non-linear Variation with Depth.*—The existence of a non-radiative temperature distribution in the outer layers of the solar atmosphere has already been deduced from the observations of limb darkening.* We now attempt to evaluate what effect such a temperature distribution will have on absorption line intensities. From (2) we have

$$d\mathcal{J}_\nu'(\theta)e^{-(1+\eta)\tau\sec\theta} = -[(1-\epsilon)\eta\mathcal{J}_\nu' + (1+\epsilon\eta)\mathcal{J}_T]e^{-(1+\eta)\tau\sec\theta}\sec\theta d\tau.$$

For constant η we may integrate the L.H.S. from $\tau = \infty$ to $\tau = 0$ and obtain $\mathcal{J}_\nu'(\theta)_{\tau=0}$. On the R.H.S. we introduce a variation of $\mathcal{J}_T$ with depth, which is always linear, $\mathcal{J}_T = a + b\tau$, but in which the constants a and b vary from layer to layer. The R.H.S. is then evaluated by integrating in a series of steps from $\tau = \infty$ to $\tau = 0$, over each of which a and b are constant. The contribution to $\mathcal{J}_\nu'(\theta)_{\tau=0}$ from a layer extending from τ_2 to τ_1 is given by

$$\left(a + \frac{b\cos\theta}{1+\eta}\right)(e^{-(1+\eta)\tau_2\sec\theta} - e^{-(1+\eta)\tau_1\sec\theta}) + b(\tau_2 e^{-(1+\eta)\tau_2\sec\theta} - \tau_1 e^{-(1+\eta)\tau_1\sec\theta})$$
$$+ \frac{X}{q\cos\theta + 1 + \eta}(e^{-(q+(1+\eta)\sec\theta)\tau_2} - e^{-(q+(1+\eta)\sec\theta)\tau_1}), \qquad (3)$$

where

$$X = (1-\epsilon)\eta \cdot \frac{(2/3)b - a}{1 + \eta + (2/3)q}.$$

In order to find $\mathcal{J}_\nu'(\theta)_{\tau=0}$ we add a number of such contributions equal to the

* H. H. Plaskett, *M.N.*, 96, 402, 1936.

number of layers postulated for $\mathcal{J}_T$; $r(\theta)$ is then given by dividing $\mathcal{J}_\nu'(\theta)_{\tau=0}$ by such a summation for $\eta=0$ in expression (3).

As a guide to the form of $\mathcal{J}_T$ distribution with τ which we should expect, we consider that already deduced from limb darkening. For any one wavelength $\mathcal{J}_T = \text{const.} \left(e^{\frac{hc}{k\lambda T}} - 1\right)^{-1}$. From the temperatures given by H. H. Plaskett, $\left(e^{\frac{hc}{k\lambda T}} - 1\right)^{-1}$ was calculated at each optical depth, and multiplied by a numerical factor to make the resulting $\mathcal{J}_T/a$ distribution agree with the linear form $\mathcal{J}_T/a = 1 + b/a\,\tau$ for the deeper layers. The resulting $\mathcal{J}_T/a$ distributions for λ 4100 and λ 5100 are shown in fig. 4. It will be seen that the "hump" reaches higher $\mathcal{J}_T/a$ values as λ decreases.

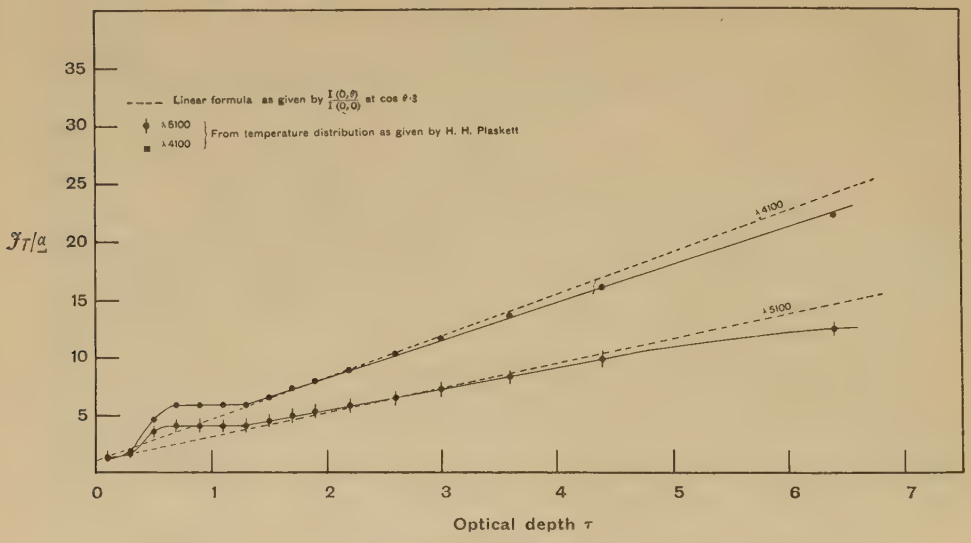

FIG. 4.—*$\mathcal{J}_T/a$ from temperature distribution as given by H. H. Plaskett.*

The first requisite of any $\mathcal{J}_T$ distribution is that the observed limb darkening $\dfrac{I(0,\theta)}{I(0,0)}$ should be fitted for all θ. After a great many trials for a $\mathcal{J}_T$ distribution which would fit the observed darkening and at the same time predict limb strengthening for faint lines, the following distribution was found to be successful: —

$\mathcal{J}_T/a$		Extent	
λ 4100	λ 5100	τ_1	τ_2
1	1	0·0	0·4
5	4	0·4	1·8
$1+3{\cdot}61\tau$	$1+2{\cdot}11\tau$	1·8	∞

Fig. 5 shows that such a distribution, considering the artificial simplicity of its form, gives sufficiently good agreement with the observed limb darkening. At λ 4100 A. we have aimed at reproducing the curvature of the $\frac{I(0,\theta)}{I(0,0)}$ curve, characteristic of Moll, Burger and Van der Bilt's observations

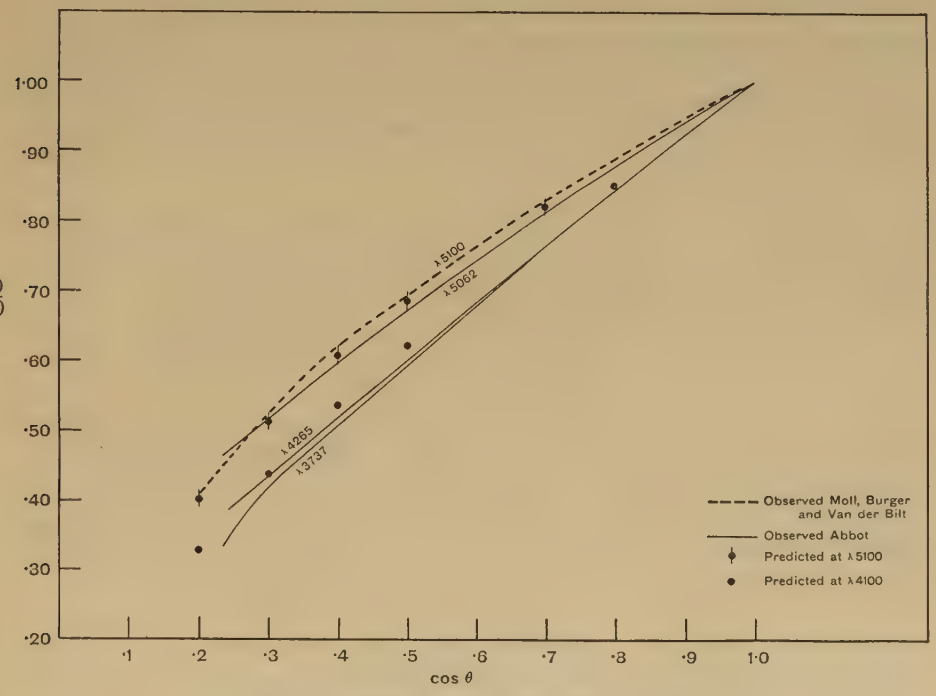

FIG. 5.—*Observed and predicted limb darkening.*

and the systematic increase they find above Abbot's values.* The $r(\theta)$ values predicted by these distributions are given below :

		$\epsilon=0$		$\epsilon=1$		$\epsilon=0{\cdot}5$	
	η	$r(0)$	$r(l)$	$r(0)$	$r(l)$	$r(0)$	$r(l)$
λ 4100	0·2	·862	·843	·876	·878	·867	·860
	0·4	·763	·723	·787	·783	·776	·756
	1·0	·576	·511	·622	·618	·606	·573
	2·0	·418	·367	·474	·520	·458	·472
	3·0	·321	·266	·386	·496	·366	·427
λ 5100	0·2	·888	·857	·902	·893	·893	·874
	0·4	·802	·746	·830	·813	·817	·782
	2·0	·477	·412	·575	·584	·527	·524
	3·0	·376	·303	·459	·565	·435	·488

* H. Raudenbusch, *A.N.*, **266**, 301, 1938.

It will be seen that we have now a powerful mechanism for strengthening lines to the limb, and that the introduction of $\epsilon \neq 0$ predicts strengthening for small η and weakening for large η.

It therefore remains only to investigate the effect of reduced re-emission in this atmospheric model. The effect of reduced re-emission is to modify the coefficient of $\mathcal{J}_\nu'$ in the equation of transfer (2). Adopting D. S. Evans' notation*, this coefficient becomes $(1-\epsilon-\delta)\eta$, where $\frac{1-\epsilon-\delta}{1-\epsilon} = \beta$ of Paper I. For the contribution to $\mathcal{J}_\nu'(\theta)_{\tau=0}$ from a layer between τ_2 and τ_1 we now have expression (3) in which the first two terms are multiplied by the factor q^2/s^2, and the last term becomes

$$\frac{q^2}{s^2}(1-\epsilon-\delta)\eta \cdot \frac{(2/3)b - a(1+\eta)}{1+\eta+(2/3)s}\left(e^{-(s+(1+\eta)\sec\theta)\tau_2} - e^{-(s+(1+\eta)\sec\theta)\tau_1}\right)$$

where $s^2 = 3(1+\eta)(1+\epsilon\eta+\delta\eta)$.

The substitution of $\delta = 0{\cdot}1$, $\epsilon = 0{\cdot}5$, $\eta = 0{\cdot}2$ gives at λ 4100 A.

$$r(0)\ {\cdot}854 \rightarrow r(l)\ {\cdot}852,$$

i.e. very little change from the non-interlocked case. We have already pointed out † that the extreme case of $\beta = 0$ produces no change in the $r(l)/r(0)$ ratio. Interlocking must, however, be a process that occurs in the outer layers of the solar atmosphere after the strong lines are effectively formed. If we assume $\delta \neq 0$ only for the outer layer ($\mathcal{J}_T/a = 1$) of our model, the modified expression (3) now leads to increased strengthening

$$r(0)\ {\cdot}867 \rightarrow r(l)\ {\cdot}857,$$

since the limb line has a higher level of formation than the centre line.

The representation of $\mathcal{J}_T$ which we have assumed in order to simplify the calculations is admittedly extremely artificial, but it nevertheless indicates the form of $r(\theta)$ variation we should obtain from a more elaborate representation of $\mathcal{J}_T$. By use of it we are able to account simultaneously for the weakening of strong lines and the strengthening of weak lines, and the increased strengthening of interlocked weak lines towards the limb of the Sun. We therefore conclude that the anomalous behaviour of faint lines indicates definite departures from the radiative equilibrium value of the temperature distribution in the outer layers of the solar atmosphere, of the general form we have suggested.

Summary

1. In order to test the interlocking hypothesis already proposed to account for the limb strengthening of faint lines, equivalent widths at centre and limb of the Sun are obtained for 17 "abundant-element faint lines" and 23 "rare-element faint lines" in the region λ 4100.

2. A marked increase in equivalent width at the limb for both classes

* D. S. Evans, *M.N.*, **100**, 156, 1940.

† Paper I, p. 131.

of faint lines is established. The "abundant-element faint lines" show a slightly greater increase than the "rare-element faint lines."

3. Current theories of line formation are examined, and the strengthening of faint lines is finally attributed to an anomalous temperature distribution in the outer layers of the solar atmosphere.

4. A form for the variation of $\mathcal{J}_T$ (black-body radiation) with depth is found which fits the observed limb darkening in the continuous spectrum, and predicts limb strengthening for faint lines and weakening for strong lines. The introduction of "reduced re-emission" into the model also accounts for the increased strengthening of the "abundant-element faint lines."

My grateful acknowledgment is due to Professor H. H. Plaskett for his constant help and advice throughout this investigation. I should also like to thank Mr. D. S. Evans for many helpful discussions.

University Observatory, Oxford :
1940 *June* 12.

CONVECTIVE EQUILIBRIUM AND SOLAR LIMB DARKENING

A. D. Thackeray, M.A., Ph.D.

Observations of the darkening to the Sun's limb in integrated light and in different frequencies, and of the distribution of energy in the continuous spectrum, have lent support in the past to the conception that the Sun's atmosphere is in radiative equilibrium.* Judged by modern standards the agreement between observation and refined theory cannot be regarded as altogether satisfactory. Moreover, Unsöld's † work has revived interest in the possibility of convection controlling the equilibrium, at least locally, in the Sun's atmosphere. Schwarzschild showed many years ago that the observed darkening is not that to be expected if the atmosphere were in convective equilibrium; the proof of this, however, depends on the assumption that k is constant, independent of *depth*. Recent calculations of the absorption coefficient as a function of temperature and pressure in atmospheres composed of a "Russell mixture" indicate that k is roughly proportional to total pressure p and independent of temperature in the conditions existing in the solar photosphere and reversing layer.‡ This result, which is shown in the following analysis to have an important effect on the predicted limb darkening, does not seem to be essentially altered by taking into consideration the effect of negative hydrogen ions. §

We proceed to examine here the darkening in convective equilibrium when k varies with depth, with special reference to the case

$$k \propto p,$$

and a value of the ratio of specific heats

$$\gamma = 4/3.$$

In these circumstances it is found that the darkening bears a close resemblance to that in radiative equilibrium.

A gas expanding adiabatically obeys the law

$$p \propto \rho^{\gamma}. \tag{1}$$

The equation of hydrostatic equilibrium and that for a perfect gas give

$$\frac{dp}{dx} = g\rho, \tag{2}$$

$$p = \frac{R\rho T}{m}. \tag{3}$$

---

* Milne, *Hand. d. Astrophysik*, III/1.

† *Sternatmosphären*, p..380 *et seq.*

‡ See, for example, Pannekoek, *Publ. Ast. Inst. Amsterdam*, **4**, 46, 1935.

§ Wildt, *Ap. J.*, **90**, 611, 1939.

We require to find the variation of T with optical depth τ defined in the usual way,

$$d\tau = k\rho \,.\, dx, \tag{4}$$

k here is the mass-absorption coefficient. To consider the general case let

$$k \propto p^a T^b. \tag{5}$$

Combining these equations (1) to (5), and assuming g constant, we find

$$\tau \propto T^{b+\frac{\gamma}{\gamma-1}(a+1)}.$$

In the particular case, applicable to the solar atmosphere, we have $a=1$, $b=0$; and if we further assume that $\gamma=\frac{4}{3}$, the temperature gradient is

$$T \propto \tau^{\frac{1}{8}}.$$

This leads to a law of darkening for integrated radiation

$$\frac{I(\theta)}{I(0)} = (\cos\theta)^{\frac{1}{4}}. \tag{6}$$

Schwarzschild's case, when k is assumed independent of depth, leads to a law of darkening $I(\theta) = \cos\theta \,.\, I(0)$ which is at variance with observation.* The law of eqn. (6), however, which is plotted in fig. 1*a*, fits closely both observation and the radiative law ($u=\cdot 56$, taking account of the blanketing effect), at least as far as $\sin\theta=\cdot 85$. It should be remembered that the region from $\sin\theta=\cdot 9$ to 1·0, where the two theoretical curves deviate appreciably, refers only to small effective optical depth, where the variation of k with depth may differ from that at the centre of the disk ; moreover, it is just in this region that observational difficulties due to scattered light are greatest. Recent observations by Wesselink † at the 1936 eclipse have shown that the darkening in the last 5 per cent. near the limb is even slower than that predicted by radiative equilibrium ; further, there is the peculiar circumstance that the colour remains constant as the limb is approached. Until the behaviour in this region is explained it would seem to be premature to claim that the observed limb-darkening in integrated light can distinguish between radiative equilibrium and convective equilibrium with our two assumptions.

The Law of Darkening as a Function of Wave-length.—The emergent radiation at angle θ is given by the usual equation,

$$I_\lambda(0,\theta) = 2hc^2\lambda^{-5}\int_0^\infty \frac{e^{-\tau}d\tau}{e^{hc/\lambda RT(\tau\cos\theta)}-1}. \tag{7}$$

With the assumption of convective equilibrium, $k \propto p$, and $\gamma=\frac{4}{3}$, put

$$T = f \,.\, \tau^{1/8}, \tag{8}$$

---

* Milne, *Hand. d. Astrophysik*, III/1.

† *B.A.N.*, **328**, 81, 1940.

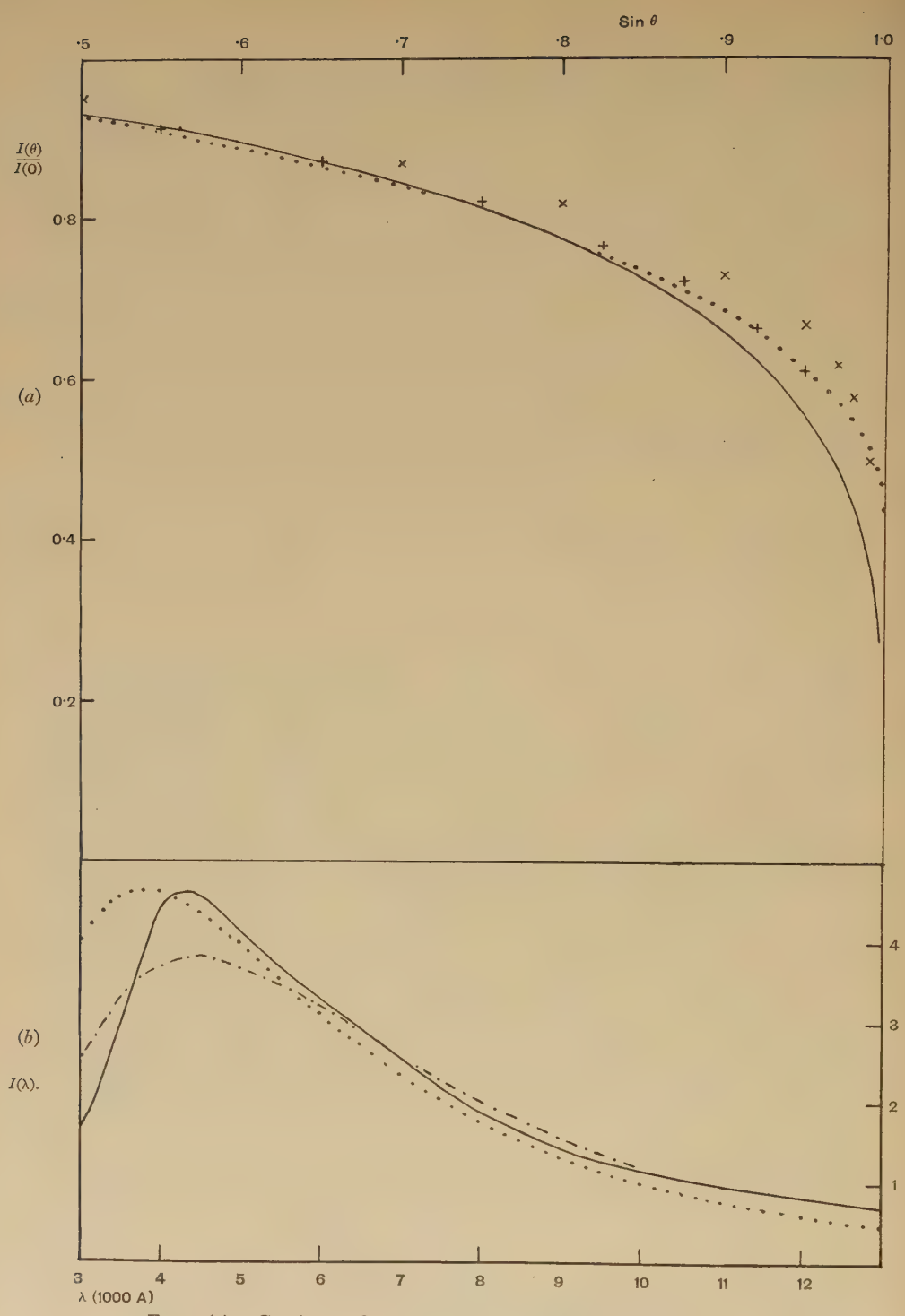

FIG. 1 (*a*).—*Continuous Curve: Convective Equilibrium* ($k \propto p$, $\gamma = \frac{4}{3}$).
Dotted Curve: Radiative Equilibrium ($u = \cdot 56$).
\+ *Observed* (*Abbot, Fowle, Aldrich*).
× *Pettit* (*Mt. Wilson Annual Report*, 1939).

FIG. 1 (*b*).—*Intensity Distribution in the Solar Spectrum.*
Continuous Curve: Observed (*Mulders*).
Dotted Curve: Convective Equilibrium ($k \propto p$, $\gamma = \frac{4}{3}$).
•−·−•−: *Radiative Equilibrium* (*with blanketing effect*).
The ordinate of intensity is on an arbitrary scale.

where f is a constant with regard to τ, and let

$$\alpha = hc/\lambda Rf(\cos\theta)^{1/8}. \tag{9}$$

Then

$$I(0, \theta) = 2hc^2\lambda^{-5}\int_0^\infty \frac{e^{-\tau}d\tau}{e^{\alpha\tau^{-1/8}} - 1}. \tag{10}$$

The corresponding integral for radiative equilibrium, which has been evaluated by Milne, involves two disposable parameters (functions of λ, θ and T_0); in the case under consideration the three variables λ, θ and T appear together in one disposable parameter α. The integral has been evaluated numerically for a set of values of α between 1·0 and 10 as shown in Table I. In the range $\alpha = 2{\cdot}5$ to 10 the integral can be closely represented by the formula

$$\log_{10} I = -q\alpha,$$

where the coefficient q varies slowly between 4·3 and 4·4. In the range $\alpha = 1$ to 2·5 the variation of q is more rapid, but with the results of Table I it was found possible to interpolate with the required accuracy.

In order to calculate the darkening at a given wave-length it is first necessary to evaluate the coefficient f of eqn. (8) which gives α corresponding to any wave-length λ, according to (9). This is achieved by considering the effective temperature T_θ corresponding to the integrated radiation at any part of the disk.

We have

$$T_\theta^4 = \int_0^\infty f^4(\tau\cos\theta)^{\frac{1}{2}}e^{-\tau}d\tau$$
$$= f^4(\cos\theta)^{\frac{1}{2}} \cdot \Gamma(1{\cdot}5).$$

Integrating now over the whole disk, the effective temperature is given by

$$T_e^4 = \tfrac{2}{5}f^4\Gamma(1{\cdot}5).$$

With $T_e = 5740°$, we find

$$f = 7439.$$

Thus we have, for instance, a value $\alpha_0 = 3{\cdot}21$ at the centre of the disk corresponding to $\lambda = 6000$ A. The darkening to the limb at any wave-length is now calculated by taking the appropriate α_0 at the centre, and at any other part of the disk

$$\alpha = \alpha_0(\cos\theta)^{-\frac{1}{8}},$$

and finding the corresponding values of the integral (10) from Table I. Values of $I(\theta)$ calculated in this way are given in Table II, and compared with the observations of Moll, Burger and van der Bilt as quoted by Hertzsprung *, and with Milne's predictions from radiative equilibrium.

* *B.A.N.*, **296**, 140, 1937. The figures quoted by Hertzsprung for λ 3220 apparently refer to Abbot's observations; the extreme limit observed by Moll, Burger and van der Bilt was 4500 A.

TABLE I

The Integral $I=\int_0^\infty \frac{e^{-\tau}d\tau}{e^{\alpha\tau^{-1/8}}-1}$

(Values in brackets interpolated)

a	$-\log_{10} I$	a	$-\log_{10} I$
1·0	0·273	(5·0	2·228)
1·5	0·586	(6·0	2·656)
2·0	0·856	(7·0	3·077)
2·5	1·104	8·0	3·492
3·0	1·340	(9·0	3·905)
4·0	1·791	10·0	4·312

TABLE II

Limb-Darkening at Different Wave-lengths

λ	3,220			4,500			6,000			8,500			15,000		
	I_o	I_c	I_R	I_o	I_c	I_R	I_o	I_c	I_R	I_o	I_c	I_R	I_o	I_c	I_R
Sin θ															
0	1·0	1·0	1·0	1·0	1·0	1·0	1·0	1·0	1·0	1·0	1·0	1·0	1·0	1·0	1·0
0·7	·72	·78	·70	·82	·83	·76	·86	·86	·84	·90	·89	·88	·95	·93	·92
0·85	·56	·62	·52	·68	·68	·65	·76	·75	·74	·81	·80	·79	·90	·86	·85
0·95	·38	·40	·36	·49	·51	·50	·61	·58	·61	·70	·66	·68	·82	·76	·78
0·98	·29	·27		·35	·38		·47	·40		·57	·56		·69	·67	
0·99				·24	·30								·50	·62	

I_o ; Observed by Moll, Burger and van der Bilt.
I_c ; Convective equilibrium ($k \propto p$; $\gamma=4/3$).
I_R ; Radiative equilibrium ($u=0{\cdot}56$, from Milne, *Phil. Trans.*, A, **223**, 209).

Again convective and radiative equilibrium give much the same results, and there is little to choose between them in the comparison with observation. At λ 4500 the agreement is rather better for convective equilibrium, at λ 3220 radiative equilibrium gives a closer representation of the observations.

The Continuous Spectrum at the Centre of the Disk.—The variation of emergent radiation $I(0, \theta)$ with wave-length is very simply calculated by means of eqn. (10). The result is shown in fig. 1*b* and compared with Mulders' * reduction of Abbot's observations and also with the predictions of radiative equilibrium † taking into account the blanketing effect of absorption lines. Both theoretical curves assume k independent of λ. The agreement of the convective curve is actually rather better on the red side of 4000 A., and it is distinctly interesting to find that the wave-length of maximum intensity in this curve is shifted so far to the violet of that predicted by the simple Wien law. Both theoretical curves, however, fail to reproduce the observed distribution in the ultraviolet. In this region

* *Zs. f. Ap.*, **11**, 132, 1935.

† The curve was taken from Unsöld, *Sternatmosphären*, fig. 47, p. 108.

absorption by numerous lines is known to introduce serious observational difficulties, and it is possible that these have still received inadequate attention.

It may be pointed out that the difference between the energy curves given by convective and radiative equilibrium may lead to interesting conclusions in the interpretation of stellar colour temperatures. Since the difference becomes marked only on the violet side of the maximum it is not likely to have a serious bearing on the question of colours of early type stars. But part of the colour differences of G- or K-type giants and dwarfs (normally ascribed to differences in ionisation temperature) might be due to dwarf atmospheres being controlled by convective equilibrium to a greater extent than giants. Alternatively, if convective equilibrium plays a greater rôle in giant atmospheres, the difference in ionisation temperature must be greater than heretofore supposed. This question should also be considered in the analysis of colour-changes of variable stars. Cepheids have been known to show greater changes in colour-temperature than their magnitude variation demanded, and this would arise if convection played a greater rôle at light maximum than at minimum.

TABLE III

Angle-variation of the ratio Spot/Disk

λ	4100		6600	
	S_c/D_c	S_c/D_R	S_c/D_c	S_c/D_R
Sin θ				
0·0	·220	·221	·361	·336
0·70	·200	·214	·348	·333
0·85	·189	·209	·338	·327
0·95	·171	·183	·310	·298

The Equilibrium of Sunspots.—Sunspots have often been considered to be regions of the solar surface cooled to a temperature about 1500° to 2000° lower than the photosphere by adiabatic expansion of gases rising from below. Milne * has proposed a model of an adiabatic column balancing a radiative column outside, which yields a pressure difference and an Evershed outflow in good numerical agreement with observation. In an important paper Minnaert and Wanders † applied two tests of the adiabatic hypothesis, namely, the variation of the ratio Spot/Disk from centre to limb ("angle-variation") and in different wave-lengths ("wavelength-variation"). They came to the conclusion that neither of these tests was satisfied by the assumption of convective equilibrium in spots, while both were satisfied by assuming radiative equilibrium. Observations by Richardson ‡ have confirmed their conclusions concerning the angle-variation.

* *M.N.*, **90**, 487, 1930.
† *Zs. f. Ap.*, **5**, 297, 1932.
‡ *Ap. J.*, **90**, 230, 1939.

Minnaert and Wanders, however, assumed k to vary according to

$$k \propto p/T^{3/2}.$$

Calculations of the angle- and wavelength-variations have been carried out for the two hypotheses:

(1) Both disk and spot in convective equilibrium.
(2) Spot in convective, disk in radiative equilibrium.

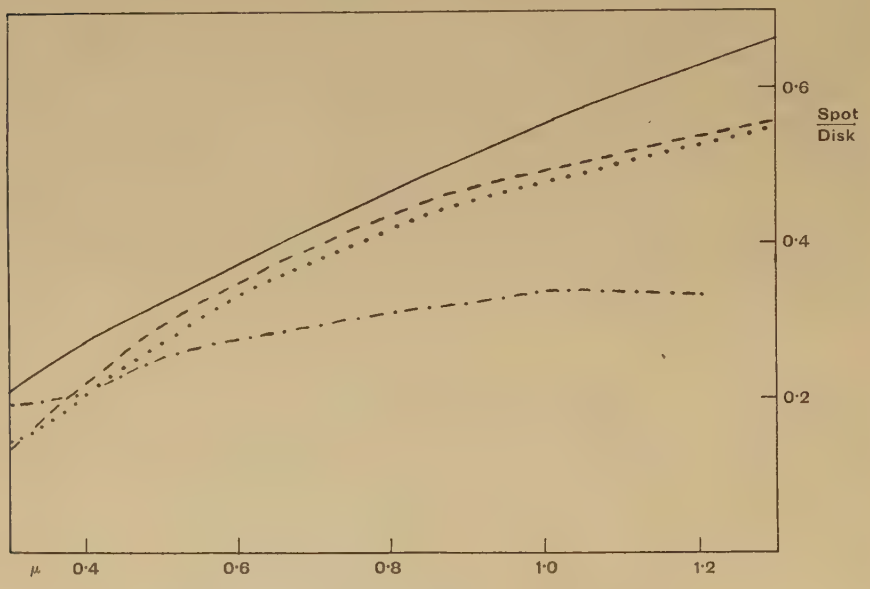

FIG. 2.—*Wave-length variation of Ratio* $\frac{Spot}{Disk}$.

——— *Mean Observed (Pettit and Nicholson).*
. . . . . *Both convective.*
– – – – – *Both radiative.*
– . – . – . *Spot (convective) : Disk (radiative).*

In both cases the results for convective equilibrium are based on the assumptions $k \propto p$, $\gamma = 4/3$. The angle-variation is given in Table III for Richardson's extreme wave-lengths $\lambda\lambda$ 4100 and 6600; columns headed S_c/D_c and S_R/D_R correspond to hypotheses (1) and (2) respectively. A temperature of 4300° has been assumed for the spot. Comparison with Richardson's observations shows that one cannot distinguish between hypotheses (1) or (2) or the third (3) that both spot and disk are in radiative equilibrium.

The wavelength-variations yielded by the hypotheses are shown in fig. 2 and compared with Pettit and Nicholson's * observations. Here we find the interesting result that although hypotheses (1) and (3) give practically identical results in fair agreement with observation, the assumption that the

* *Ap. J.*, **71**, 153, 1930.

spot is in convective and disk in radiative equilibrium seems to be definitely ruled out.*

In conclusion, the observed darkening to the limb and distribution of energy in the spectra of disk and spot can on the whole be equally well represented by the assumption of either radiative equilibrium or convective equilibrium, provided in the latter case that $k \propto p$ and $\gamma = 4/3$. It must not be forgotten that although these conditions may be realised at a certain level of the reversing layer or photosphere they may not be true for the higher layers which affect the limb observations. No particular reason can be assigned for the choice of $4/3$ for the value of γ, and it would be interesting to repeat the calculations for other values ; it is known that this represents a lower limit for a whole star, as a smaller value would produce instability, but Unsöld † has shown that locally convective zones may occur owing to the ionisation of hydrogen. It may be further remarked that the formation of molecules in sunspots may also help materially to diminish γ in these regions.

It should be remembered that a necessary condition for convective equilibrium is the inequality

$$\left(\frac{d \log T}{d \log P}\right)_{\text{conv}} < \left(\frac{d \log T}{d \log P}\right)_{\text{rad}}$$

and Unsöld's model shows that this occurs in the range of optical depth $\tau = 1{\cdot}6$ to ~ 170. The condition cannot hold at the extreme boundary where radiative equilibrium must predominate. With our assumptions, $\left(\frac{d \log T}{d \log P}\right)_{\text{conv}} = 0{\cdot}25$ and radiative equilibrium begins to take control at ‡ $\tau = 2/3$, *i.e.* considerably nearer the boundary than in Unsöld's model.

It is of interest to recall that Plaskett's § analysis of Moll, Burger and van der Bilt's observations at λ 5500 indicates an isothermal layer at almost precisely this level. But the fact that radiative and convective equilibrium can yield such very similar laws of darkening stresses the observational accuracy that will be required before such a temperature gradient as Plaskett finds can be regarded as established with certainty.

Reference should be made to a paper by Keenan ‖ who has carried out a detailed solution of the limb darkening of the disk, using a model of convective equilibrium bounded above τ_1 by a surface layer in radiative equilibrium ; the fact that Keenan found a value of $\tau_1 = 2/3$ gave good agreement with observation suggests that the predicted darkening is much the same whether the surface layer is in convective or radiative equilibrium. Thus the simplified treatment, applied here, which assumes convective equilibrium throughout, is not seriously invalidated.

* The hypothesis of a radiative spot and convective disk is also ruled out by the wavelength-variation ; in the range 4000 to 12,000 A. the ratio S_R/D_c increases by a factor 10 as opposed to the observed factor of about 3.

† *Sternatmosphären*, p. 380 *et seq.*

‡ Pointed out to the author by Sir Arthur Eddington.

§ *M.N.*, **96**, 422, 1936. ‖ *Ap. J.*, **87**, 45, 1938.

Summary

1. The consequences of assuming convective equilibrium with $k \propto p$ and $\gamma = 4/3$ in the solar atmosphere are studied. The darkening to the limb in integrated light and in different wave-lengths, and the distribution of energy in the continuous spectrum are very similar to the results predicted by radiative equilibrium, and represent the observations almost equally well. Accurate observations are required to distinguish between the two types of equilibrium. The wave-length of maximum intensity is further to the violet in convective equilibrium. This may have some bearing on the interpretation of stellar colour temperatures.

2. The same assumption for the equilibrium of sunspots leads to the result that the observed angle- and wavelength-variations of the ratio Spot/Disk may be equally well represented by the assumptions that spot and disk are either both in convective or both in radiative equilibrium. The wavelength-variations resulting from a convective spot and radiative disk, or from a radiative spot and convective disk, are at variance with observation.

Solar Physics Observatory,
Cambridge :
1940 *June*

THE ORIENTATION OF THE EXTRA-GALACTIC NEBULÆ

A. G. Walker, M.A., Ph.D.

1. *Introduction.*—Observations on extra-galactic nebulæ have recently been examined * with the object of discovering whether there is any systematic inclination, and it is an obvious question to ask whether existing relativity theories can predict a law of orientation. These theories have been applied with some success to the study of nebulæ in an ideal system †, but it might be thought that any systematic orientation, and the consequent preferential direction at each point, cannot exist in such a system without implying the existence of preferential regions and so contradicting a fundamental principle common to all relativistic cosmologies. This, however, is not the case, and it will be shown that in an ideal system the inclinations of the nebular axes need not be purely random, and that a precise law is consistent with the rules of relativity and with the Cosmological Principle. This "law" is an alternative to the possibility that orientations are purely random, and is, I believe, the only logical alternative. All relativity theories agree that an ideal system should satisfy the Cosmological Principle, under which no nebula can be preferential, and it is simply this principle which is applied to determine the orientations of nebulæ.

It will be seen that a precise "law" appears, and each nebular axis must be inclined in a particular way, dependent upon its distance and galactic latitude. In turning now from theory to observations, it is recognised that the system of nebulæ is not in detail ideal, and that actual orientations will differ from those predicted owing to many early and subsequent causes which cannot possibly be accounted for. It is reasonable to assume, however, that these causes and their consequences are random, and that the precise law of theory can be replaced by a statistical law, where the "orientation of a nebula" refers to the mean orientation in its neighbourhood, and the "law" refers to the *statistical* dependence of orientation upon position. This is to be understood when in our analysis we use for convenience the language of precision.

The law will be found to depend essentially upon the form of the relativistic model considered, particularly the curvature of the spatial part of the space-time map. In all cases it admits a first-order observational test, and it should be possible from observations to answer certain outstanding

* F. G. Brown, *M.N.*, **98**, 218, 1938, and subsequent papers.

† The application of General Relativity to cosmology is described by R. C. Tolman in *Relativity, Thermodynamics and Cosmology* (Oxford, 1934). An account of Milne's world-model is given by E. A. Milne in *Relativity, Gravitation and World-Structure* (Oxford, 1935). See also W. H. McCrea, *Z. f. Astrophys.*, **9**, 290–314, 1935, for an account of observable relations, and A. G. Walker, *Proc. Lond. Math. Soc.* (2), **42**, 90–127, 1937, for a more general form of Milne's model.

questions concerning the most suitable model for comparison with the universe.

We shall as far as possible use the notation commonly used in the application of General Relativity to cosmology, and well-known results will be quoted. In the same notation we shall refer to Milne's model and to its generalisation.

2. In all relativistic cosmologies the nebulæ correspond to points in a Riemannian 3-space S_3, of constant curvature k which can be taken to be 0, 1 or -1. This space can be referred to dimensionless co-ordinates x, y, z in terms of which the metric takes the form

$$d\sigma^2 = \frac{dx^2+dy^2+dz^2}{(1+\frac{1}{4}kr^2)^2}, \qquad r^2 = x^2+y^2+z^2. \tag{1}$$

The system of nebulæ is then conveniently described by means of a space-time map S_4, a Riemannian 4-space with metric

$$ds^2 = dt^2 - R^2 d\sigma^2, \tag{2}$$

where R is a function of time t. In the General Relativity model, k and the form of R have not so far been determined, though certain information is known resulting from comparisons with observations. In Milne's model, $k=-1$ and $R \equiv t$. In the generalisation of Milne's model, $R \equiv at$, where a is a constant, and k and a have not so far been determined.

At the origin O ($r=0$), the co-ordinate axes may be regarded as fixed by a "base," a triad of three orthogonal vectors, and another similar co-ordinate system is fixed in the same way by any other similar base at O or at any other point of S_3. The metric of S_3 is of the same form (1) in each case, and we say that the space can be rotated and displaced into itself; the complete set of such motions constitutes a six-parameter group * G_6. If now we regard each nebula as having a definite orientation, this is equivalent to considering only one base at each point, the base at any point fixing the orientation at that point. Since we still wish to avoid introducing preferential regions, these bases must be placed throughout the space so that the whole set appears the same from whatever point it is viewed. The set of motions from one base to all the others must therefore constitute a three-parameter group G_3, which will evidently be a sub-group of G_6. Since we wish to have a base at each point of space, G_3 must be transitive. The problem of orientation is thus finally reduced to the problem of finding a transitive three-parameter sub-group of motions in S_3.

This geometrical problem has been solved completely †, and I have found that a real solution exists whatever the value of k. In each case the bases throughout S_3 have been determined, and it is seen that the aggregate always displays symmetry about one of the base vectors at each point. This vector we identify with the axis of the nebula at the point, and we are concerned

* For the application of group theory to cosmology, see A. G. Walker, *Proc. Lond. Math. Soc.* (2), **42**, 90–127, 1937.

† "Certain groups of motions in 3-space of constant curvature", *Quart. Journ. of Maths.*, **11**, 81–94, 1940. This paper will be referred to as G.M.

only with the inclinations of the axes throughout space as observed from one point, taken to be the origin O in calculations.

3. The inclination of the axis at a point P as observed from O is conveniently fixed by two angles θ and ϕ, which are easily observable and which correspond to simple theoretical measures. In so far as observations are concerned, it is convenient to regard the whole of space as Euclidean, the line of sight OP being a straight line. Then if OO' and PP' are the axes at O and P (fig. 1), the angle θ is defined as the angle between the planes $O'OP$ and OPP' measured in the positive sense about OP, and the angle ϕ is defined as $O'\hat{O}P + O\hat{P}P' - 180°$. Briefly, θ is the angle of rotation

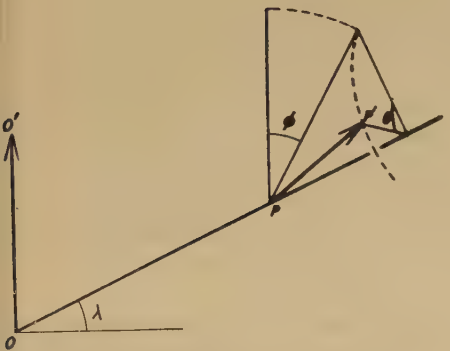

FIG. 1.—*Inclination angles θ and ϕ.*

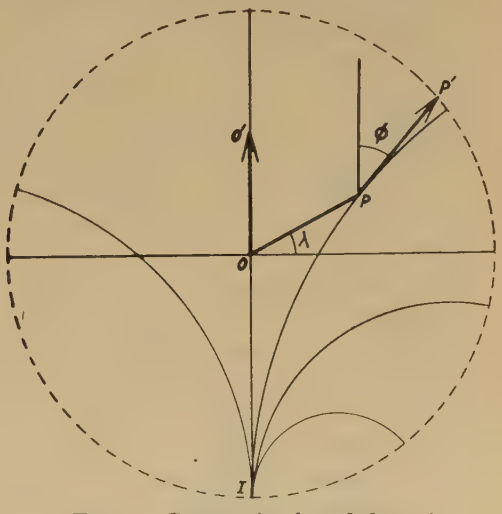

FIG. 2.—*Construction for nebular axis when $k = -1$.*

(of a rigid body) about the line of sight OP, and ϕ is the angle of rotation towards OP, which together will bring the axis at O parallel to that at P.

If the nebula is a discoid or a spheroid, the angle θ is directly observable, for the nebula appears elliptic and $90° - \theta$ is the angle the major axis makes with the meridian. The angle ϕ is easily obtained from observations when the nebula is discoid with a discernible circular central plane. The circle appears as an ellipse whose eccentricity depends upon ϕ but not upon θ, and it is easily verified that if λ is the galactic latitude of the nebula and if e is the observed eccentricity, then $e = \cos(\lambda + \phi)$. This enables ϕ to be determined.

The angle λ requires some explanation, for it has already been implied that the actual orientation of any particular nebula, as, for example, our own galaxy, may deviate widely from the theoretical orientation considered here. It is probable, therefore, that the axis OO' will not be our galactic axis, but must be found by taking the mean inclination of all neighbouring nebular axes. By "galactic latitude" we shall then mean the angle which the line of sight makes with the plane perpendicular to OO'.

Turning to the theoretical side, it is well known that the light paths in

S_4 are null geodesics and that these correspond to geodesics in S_3. We are concerned only with light received at the origin, *i.e.* with the geodesics through O in S_3, and these curves correspond to straight lines through the origin in the Euclidean space E_3 with metric $dx^2+dy^2+dz^2$. This space is conformal to S_3, whence angles in S_3 are given correctly by the angles in the corresponding figure in E_3. Thus, finally, the angles subtended at O by distant objects are given correctly by the corresponding figure in E_3, light paths through the origin being straight lines. In particular, the theoretical values of the inclination angles θ and ϕ can at once be calculated when the direction of the axis is known at any point provided co-ordinates x, y, z are used, since then the whole of space can, as far as O is concerned, be regarded as Euclidean.

4. Since there is symmetry about the axis at the origin, θ and ϕ for a nebula at P will depend at most upon the latitude of P and the "distance" from O. In Euclidean space E_3 the distance from O is r, which serves as a distance parameter although it is not directly observable. It follows from (1) that if k is 0 or 1, r can take all values, and if $k=-1$, r can take values from 0 to 2, the whole space S_3 corresponding in this case to the inside of the sphere $r^2=4$ in E_3. To express calculations in terms of observables, the parameter r can be related * to one of the distance observables, *e.g.* apparent brightness, apparent size, red-shift, etc. For the present purpose, red-shift seems to be the most suitable since observations of red-shift do not require any corrections based upon any particular theory. We shall therefore refer to the observable $Z=D-1$, where D is the Doppler ratio of observed to emitted wave-length.

To find the relation between r and Z, we suppose that light received at O at present time t_0 was emitted at time t at a distance r. Then from (1) and (2), since $ds=0$ along a light path, we have

$$\int_t^{t_0}\frac{dt}{R}=\int_0^r\frac{dr}{1+\frac{1}{4}kr^2}, \tag{3}$$

giving a relation between t and r. The Doppler ratio is $D=(\delta t_0/\delta t)_{\delta r=0}$, whence

$$D=1+Z=\frac{R(t_0)}{R(t)}, \tag{4}$$

and this, with (3), gives implicitly the relation between r and Z.

When Z is small, r also is small, and we have $t_0-t\sim rR_0$ from (3), and $Z\sim(t_0-t)R_0'/R_0$ from (4), where $R'=dR/dt$, and a suffix $_0$ denotes evaluation at time t_0. Hence, to the first order,

$$Z\sim rR_0'. \tag{5}$$

5. $k=0$.—In this case, S_3 is flat and the group G_6 consists of rotations and translations in Euclidean space. It is easily verified that the most general sub-group of the kind required here consists of translations followed

* See W. H. McCrea, *loc. cit.*

by rotations about a fixed direction. The axis of symmetry is therefore always in this fixed direction, *i.e.* the nebular axes are all parallel, and we thus have

$$\theta = \phi = 0. \tag{6}$$

6. $k = -1$.—If the co-ordinates are chosen so that the galactic axis at O is the z-axis, then I have shown * that in this case the inclination of the axis at the point $P(x, y, z)$ is given by the unit vector

$$(1+\tfrac{1}{4}r^2)^{-1}\{(1-\tfrac{1}{4}r^2)(0, 0, 1)+\tfrac{1}{2}z(x, y, z)-\epsilon(-y, x, 0)\}, \tag{7}$$

where ϵ is either 1 or -1, the same for all nebulæ. It is at once seen that this vector and the z-axis make the same angle with OP, whence $\phi = 0$. It can also be verified that the angle θ giving the inclination (7) is

$$\theta = 2\epsilon \tan^{-1} r/2. \tag{8}$$

In this case, therefore, there are two distinct possibilities, given by ϵ, the rotation θ being in either sense about the line of sight. The magnitude of θ depends only upon the distance of the observed nebula, and not upon its latitude.

When applying these theoretical considerations to observations, it can be assumed for most observed nebulæ that r is small, in which case $\theta \sim \epsilon r$ radians. The approximate law relating inclination to distance (red-shift) is thus, from (5),

$$\phi = 0, \qquad \theta \sim \frac{\epsilon Z}{R_0}, \text{ radians}, \qquad \epsilon = \pm 1. \tag{9}$$

7. $k = 1$.—In this case my results show † that the inclination of the axis at any point $P(x, y, z)$ is given by the unit vector

$$\frac{2(z+2)}{x^2+y^2+(z+2)^2}(x, y, z+2)-(0, 0, 1). \tag{10}$$

This vector lies in the plane $O'OP$, so that $\theta = 0$. It can be verified that the remaining angle ϕ is given by

$$\phi = 2 \tan^{-1}\left(\frac{r \cos \lambda}{2 + r \sin \lambda}\right), \tag{11}$$

where λ is the galactic latitude of P.

The dependence of inclination upon position is quite simply illustrated geometrically in the Euclidean space E_3, co-ordinates x, y, z, for the axes throughout this space are tangents to the circles which are coplanar with the z-axis and touch it at the point $I(0, 0, -2)$. This is illustrated in fig. 2 (see p. 625) by a plane section through the z-axis. The point I plays a

* The result given here is a particular form of equation (18) in G.M.

† The results quoted here occur in G.M., sections 7, 8. Since the nebular axis is the axis of symmetry, it is identified with the vector A^i, which is uniquely defined everywhere. We are now taking the axis at O to be the z-axis so that $a^i = \delta_3{}^i$ in G.M.

special part here, but it does not imply the existence of a preferential point in S_3. It lies on the bounding sphere in E_3 (the section of which is drawn as a broken line in fig. 2), and from any point in space it can be regarded as being at infinity. Under the transformation from the above co-ordinate system to the similar system with any other point as origin, the point I is invariant.

As mentioned before it is sufficient to consider r small, and (11) becomes $\phi \sim r \cos \lambda$. In this case, therefore, the approximate law relating inclination to distance and latitude is, from (5),

$$\theta = 0, \qquad \phi \sim \frac{Z}{R_0'} \cos \lambda \text{ radians.} \tag{12}$$

The apparent eccentricity (see section 3) is $e = \cos(\lambda + \phi)$, so that we have approximately

$$e \sim \cos \lambda \left(1 - \frac{Z}{R_0'} \sin \lambda\right). \tag{13}$$

The present case is seen to differ from the other two in that the aggregate of nebular axes does not display symmetry about the galactic plane. It is thus necessary to distinguish between the two senses along the galactic axis.

8. The numerical order of the results obtained in the last two sections can be estimated from (9) and (12), where it is seen in each case that the angle measuring inclination is of the order Z/R_0'. The variable Z is dimensionless, and is, to the order considered here, proportional to the distance Δ by Hubble's law. If v is the recessional velocity of a nebula and c the velocity of light, the Doppler effect gives $Z = v/c$, and from an estimate of Hubble's constant * we have approximately $v/\Delta = H \sim 6 \times 10^{-10}$ (year)$^{-1}$. It follows that Z is of the order 6×10^{-4} per 10^6 light years. It is known from theoretical arguments that H is related to $R(t)$ by

$$H = R_0'/R_0, \tag{14}$$

and several writers have suggested that R_0 probably lies between $1{\cdot}6 \times 10^9$ and 2×10^9 years. It follows that the dimensionless constant R_0' is probably of the order 1. Passing from radians to minutes of arc, we finally have that the angles θ in (9) and ϕ in (12) are of the order

$$2 \text{ minutes of arc per } 10^6 \text{ light years.} \tag{15}$$

9. The best procedure for analysing observations with (6), (9) and (12) in mind is straightforward since θ and ϕ occur independently. The analysis should be in two parts, the first dealing with θ and the second with ϕ. It must be remembered that this analysis can only follow a determination of our own axis OO', which should be made by finding the mean orientation of neighbouring nebulæ. Since the inclinations calculated above are small, nebulæ over large distances can be included for an accurate determination

* See G. C. McVittie, *Cosmological Theory* (Methuen, 1937), Chap. I.

of the axis OO'. All observations must then be corrected so that θ and ϕ are calculated relative to this axis.

In the first place we note that $\theta = 0$ when $k = 0$ and -1, and that θ depends only upon distance when $k = 1$. A correlation should be sought, therefore, between the observables θ and Z, and for this purpose observations from any or all regions of the sky can be used equally and together.* It is expected, from our results, either that θ is purely random, or that θ is, statistically, zero or proportional to Z. If zero, we know that k is 0 or -1, and if proportional to Z, we know that $k = 1$ and we obtain also the value of R_0' from (9).

The second part of the analysis concerns only ϕ, which is zero when $k = 0$ and 1, and depends upon both distance and latitude when $k = -1$. From (12) it appears that a correlation should be sought between $\phi \sec \lambda$ and Z, using observations from any or all regions of the sky. It is expected, from our results, that $\phi \sec \lambda$ is either purely random or is, statistically, zero or proportional to Z. If zero, we know that k is 0 or 1, and if proportional to Z, then $k = -1$ and we can also obtain the value of R_0' from (12). In a more detailed survey, a correlation between ϕ and Z can be sought in each of a number of narrow latitude bands.

10. In conclusion we remark that, since observations of nebulæ extend over distances many times greater than 10^6 light years, the estimate in section 8 shows that the first-order effects considered here are appreciable, and that observations should provide a crucial test of the correctness of our argument. If the inclinations of nebular axes are not purely random, observations should also yield important information concerning the most suitable relativistic model for the universe. There is, firstly, the value of k, giving the sign of the curvature of S_3, and secondly, if † $k \neq 0$, the value of R_0' and hence of R_0 from (14). These quantities have been discussed theoretically but have not so far been determined from observations, since this determination has previously required second approximations to observable laws.

The results mentioned above will either give added support to Milne's model, or decide against it. This model requires $k = -1$, $R_0 = t_0$ and $R_0' = 1$, the last two being consistent with (14) with the observed value of H. If the results are inconsistent with these values, there still remains the generalisation of Milne's model derived from the same theory. Here, k can have any value and $R \equiv at$. Thus R_0' determines a, and $R_0 = a/H \sim at_0$ as required. This generalisation can thus be made to fit all cases.

I wish to acknowledge my indebtedness to Professor E. A. Milne for his valuable criticisms of a rough draft of this paper.

* A remark made in section 3 should be noted, to the effect that when θ alone is being considered, observations on spheroidal as well as discoidal nebulæ can be used.

† If $k = 0$, then from (1) and (2) it is seen that R_0 is arbitrary and H then determines R_0'.

Summary

It is shown that relativity provides an alternative to the possibility that the orientations of nebulæ are purely random. There are three distinct cases, corresponding in relativistic cosmology to the values 0, 1 and -1 of k, the curvature of the spatial part of space-time. In each case the inclination of a nebular axis depends at most upon the distance and galactic latitude of the nebula, and the effects estimated from first-order approximations are well within the present range of observations, being of the order of 2 minutes of arc per 10^6 light years. The predicted relations can be tested statistically from observations in any region of the sky. These tests can also yield information of importance to relativistic cosmology, such as the values of k and the present "radius" of the universe.

THE ELECTRON VELOCITY DISTRIBUTION IN THE PLANETARY NEBULÆ

Yusuke Hagihara

(Communicated by Sir Arthur Eddington, O.M., F.R.S.)

In the current treatments of the physical state of the planetary nebulæ it is always assumed that the electron velocity distribution within them is strictly Maxwellian. I have recently * deduced the criterion for a Maxwellian distribution, and examined to what extent this assumption is admissible. The detailed analysis is limited to nebulæ consisting of hydrogen alone. The frequency function for the electron velocities is assumed to be expansible in a convergent series of Hermite polynomials, and is substituted in Boltzmann's integro-differential equation modified for the presence of free electrons, hydrogen ions and neutral hydrogen atoms repelling or attracting according to the Coulomb law, and also for the occurrence of absorption and emission processes in the field of radiation in the frequency range of the Lyman continuum, together with encounter processes between various constituent particles of different masses and different charges. For the capture and ionisation probabilities the wave-mechanical formula of Gaunt † is adopted. The free-free transitions are omitted because the emitted and absorbed energies in such transitions are considered negligibly small compared with the kinetic energy of the encountering electrons in the usual treatment according to the correspondence principle.‡

The functions representing the rates of change in the number of free electrons in each velocity range through the encounter processes and the radiative processes are also expanded in a series of Hermite polynomials.

We impose the stationary condition, that is the condition for the constancy of the total number of free electrons in the whole velocity range. The steady state condition is satisfied if the relation

$$\mathcal{J}_\nu d\nu = \frac{2h^4\nu^3\sigma_3}{m^3c^3}\frac{N_eN_i}{N_1}[f]_{V^2=2h(\nu-\nu_1)/m}d\nu, \qquad V^2=u^2+v^2+w^2,$$

exists between the intensity $\mathcal{J}_\nu$ of the incident isotropic radiation and the frequency function f for the electron velocities for each value of ν, where N_e, N_i and N_1 are respectively the numbers of free electrons, ions and neutral atoms per unit volume, and $\sigma_3=\sum_{s=1}^{\infty}s^{-3}$. In this case the frequency function

* Hagihara, *Jap. J. Astr. Geophys.*, **17**, Nos. 2–3, 1940, in press.

† Gaunt, *Phil. Trans.*, **229** A, 200, 1929.

‡ Kramers, *Phil. Mag.*, **46**, 836, 1923.

is strictly Maxwellian and the state is to some extent in detailed balancing.* We can, however, scarcely expect the physical state in the nebulæ to be in detailed balancing.

Accordingly, we inquire whether there is another steady state in which the frequency function is not necessarily Maxwellian but is of the form

$$f=\frac{1}{\alpha^3}\beta_{ijk}\phi_{ijk}, \qquad \phi_{ijk}=(-1)^{i+j+k}H_{ijk}\phi_{000},$$

$$H_{ijk}=H_i\left(\frac{u}{\alpha}\right)H_j\left(\frac{v}{\alpha}\right)H_k\left(\frac{w}{\alpha}\right), \qquad \phi_{000}=(2\pi)^{-\frac{3}{2}}e^{-(u^2+v^2+w^2)/2\alpha^2},$$

where $H_i(U)$ is the Hermite polynomial:

$$H_i(U)=U^i-\frac{i(i-1)}{2\cdot 1!}U^{i-2}+\frac{i(i-1)(i-2)(i-3)}{2^2\cdot 3!}U^{i-4}+\ldots$$

A new quasi-steady state is discovered, in which the parameter α varies very slowly, so that any noticeable change requires a time-interval of the order of magnitude $10^7/N_i$ years, and the other parameters remain constant all the time. The non-zero coefficients β_{ijk} up to the second order in the expansion are $\beta_{200}=\beta_{020}=\beta_{002}=\beta_2$.

Let $\psi_1(\nu)$ be the probability for ionisation from the ground state in the field of radiation of unit intensity at the frequency ν, and ν_s be the frequency at the sth series limit; then β_2 (which is a measure of the deviation from the Maxwellian distribution) is computed to be

$$\beta_2=\frac{2}{3}\frac{P}{m\alpha^2 Q}\left\{\int_{\nu_1}^{\infty}h\nu\psi_1(\nu)\mathcal{J}_\nu d\nu-(h\nu_1+\tfrac{3}{2}m\alpha^2)\int_{\nu_1}^{\infty}\psi_1(\nu)\mathcal{J}_\nu d\nu\right\}, \tag{1}$$

$$P=\sum_{s=1}^{\infty}s^{-3}e^{h\nu_s/m\alpha^2}\,\mathrm{Ei}\,(h\nu_s/m\alpha^2)+\beta_2\sum_{s=1}^{\infty}s^{-3}\{2-(3+2h\nu_s/m\alpha^2)e^{h\nu_s/m\alpha^2}\,\mathrm{Ei}\,(h\nu_s/m\alpha^2)\},$$

$$Q=\sum_{s=1}^{\infty}s^{-3}\left\{-\left(\frac{4}{5}\frac{h\nu_s}{m\alpha^2}+\frac{8}{15}\right)+\left[\frac{4}{5}\left(\frac{h\nu_s}{m\alpha^2}\right)^2+\frac{4}{3}\frac{h\nu_s}{m\alpha^2}+1\right]e^{h\nu_s/m\alpha^2}\,\mathrm{Ei}\,(h\nu_s/m\alpha^2)\right\},$$

$$\mathrm{Ei}\,(a)=\int_a^{\infty}e^{-x}dx/x.$$

Here the ionisation from quantum states other than the first is considered negligible compared with the ionisation from the first quantum state, as is proved in one of my previous works.†

A necessary condition for the Maxwellian velocity distribution is by (1),

$$\int_{\nu_1}^{\infty}h\nu\psi_1(\nu)\mathcal{J}_\nu d\nu-(h\nu_1+\tfrac{3}{2}m\alpha^2)\int_{\nu_1}^{\infty}\psi_1(\nu)\mathcal{J}_\nu d\nu=0. \tag{2}$$

This equation shows that the mean kinetic energy of a free electron set free by ionisation is $\frac{3}{2}m\alpha^2$.

* Refers to the theorem by Dirac, *Proc. Roy. Soc.*, A, **106**, 581, 1924.

† Hagihara, *Jap. J. Astr. Geophys.*, **15**, 1, 1938.

The condition for radiative equilibrium has been deduced without the assumption of a Maxwellian velocity distribution in the form

$$\int_{\nu_1}^{\infty} h\nu\psi_1(\nu)\mathcal{J}_\nu d\nu - (X' + h\nu_1)\int_{\nu_1}^{\infty} \psi_1(\nu)\mathcal{J}_\nu d\nu = 0, \tag{3}$$

where X' reduces for the Maxwellian velocity distribution to

$$X = \frac{kT_\epsilon\sigma_3 - h\nu_1 S_5(T_\epsilon)}{S_3(T_\epsilon)} + \frac{kC'' T_\epsilon^2}{CS_3(T_\epsilon)},$$

$$S_n(T_\epsilon) = \sum_{s=1}^{\infty} s^{-n} e^{h\nu_s/kT_\epsilon}\,\mathrm{Ei}\,(h\nu_s/kT_\epsilon), \qquad (n = 3,\ 5)$$

$$C = \frac{2^9\pi^5}{(6\pi)^{\frac{3}{2}}}\frac{\epsilon^{10}}{m^2c^3h^3}\left(\frac{m}{k}\right)^{\frac{3}{2}}, \qquad kC'' = \frac{128\pi^3}{3\sqrt{3}}\frac{\epsilon^6}{c^3(2\pi m)^{\frac{3}{2}}}\frac{k^{\frac{1}{2}}}{h},$$

$$ma^2 = kT_\epsilon, \tag{4}$$

and T_ϵ is the electron-temperature at the point in question in the nebula. The last expression is the same as the one given by Menzel and his colleagues.*

We notice that the conditions (2) and (3) are both independent of the absolute value of the radiation intensity, and determined only by the spectral intensity distribution of the radiation $\mathcal{J}_\nu$.

The value of β_2 for a nebula in radiative equilibrium becomes

$$\beta_2 = \frac{2P}{3ma^2Q}\{X' - \tfrac{3}{2}ma^2\}. \tag{5}$$

These formulæ are applied to the optically thin nebulæ in which the incident radiation consists mainly of the direct radiation from the central star with the Planck intensity distribution. The values of the electron-temperature T_ϵ computed by (3) and (4) for radiative equilibrium in the Maxwellian approximation, the values of the electron-temperature T_ϵ' computed by (2) for the Maxwellian velocity distribution and the values of β_2 computed by (5) for radiative equilibrium in the first approximation are given in the following table, with the temperature T_s of the central star as the argument:—

T_s	T_ϵ	T_ϵ'	β_2 in Radiative Equilibrium
°	°	°	
5 000	4 500	3 200	−·272
7 000	6 200	4 400	−·278
10 000	9 000	6 300	−·280
12 000	10 600	7 500	−·282
15 000	13 300	9 200	−·284
20 000	17 500	12 300	−·293
30 000	25 500	17 800	−·304
50 000	41 000	28 000	−·307
100 000	67 000	47 000	−·309

* Baker, Menzel and Aller, *Ap. J.*, 88, 422, 1938.

The values of T_ϵ are nearly the same as those given by Menzel and his colleagues *, and the values of T_ϵ' are nearly equal to those given by Lambrecht † as the values for radiative equilibrium.

It is evident from this table that the electron velocity distribution deviates from the Maxwellian for the nebulæ in radiative equilibrium, at least when the optical thickness is sufficiently small. Also (5) holds for the nebulæ of any thickness. The existence of the new quasi-steady state for the planetary nebulæ can be inferred unambiguously from this circumstance.

It may be supposed that the situation is similar for the physical state of interstellar matter.‡

Astronomy Department,
Tokyo Imperial University :
1940 *January* 20.

* Baker, Menzel and Aller, *Ap. J.*, **88**, 422, 1938.
† Lambrecht, *Astr. Nachr.*, **268**, 49, 1939.
‡ Eddington, *I.C.S.*, 395, 1926.

THE SPECTRUM OF BRIGHT CHROMOSPHERIC ERUPTIONS

C. W. Allen, D.Sc.

1. *Introduction.*—The discovery that bright chromospheric eruptions on the Sun produce definite effects in the Earth's ionosphere is turning the attention of astronomers particularly to this type of solar disturbance. The nature of the effects indicates that the solar influence is transmitted by ultra-violet light, and that the ultra-violet intensity in the eruption is of the order of a thousand times that normally emitted from the Sun's surface.* The short wave-length radiation suspected of causing the ionspheric disturbances cannot be photographed through the Earth's atmosphere, and hence for the present its nature must be largely a matter of conjecture. However, if such considerable changes occur in the far ultra-violet spectrum, it is reasonable to suppose that some corresponding effects would appear in the spectral regions that can be seen and photographed. It was for the purpose of studying such effects that the eruption spectra described in this paper were obtained.

In a recent paper † Richardson and Minkowski have given a list of lines appearing in the complete eruption spectrum from 3300 A. to 11,500 A. However, their list does not include many lines that are frequently emitted in eruptions ‡, and hence further observation is necessary. Very bright eruptions are necessary to show up most of these extra lines, although at least one of them (5169·052 of Fe^{+}) can be seen in practically any eruption.

2. *Observations.*—The observations were made with the 3-prism spectrograph of the Commonwealth Solar Observatory in conjunction with the Sun telescope.§ The eruptions were set on the slit to give the brightest emission in $H\alpha$ or $H\beta$. The majority of the observations were photographic but some regions have been studied visually. Practically the whole of the visible spectrum has been covered either by photograph or visually, but only a fraction of these observations was made on eruptions which were bright enough to show up the emission lines. Only those plates and visual observations considered to present some useful information are described here. In consequence the spectrum described is discontinuous and some regions are duplicated. This duplication is useful in demonstrating the consistency of the results and the similarity of the spectra of different eruptions. The ten-inch spectrograms cover about 100 A. in the violet and about 300 A. in the green.

It is well known that eruption spectra contain strong emission lines,

* Martyn, Munro, Higgs and Williams, *Nature*, **140**, 603, 1937.
† R. S. Richardson and R. Minkowski, *Ap. J.*, **89**, 347, 1939.
‡ L. d'Azambuja, *l'Astronomie*, **53**, 97, 1939.
§ C. W. Allen, *Mem. Comm. Sol. Obs. Canberra*, **1**, No. 5, 1934.

and the evidence of the spectrohelioscope suggests that the level represented by the emission is well above the reversing layer. It is not certain that the level is so high that the eruption emission spectrum can be regarded as having a completely separate existence from the ordinary Fraunhofer spectrum, but this conception leads to consistent results and is the most convenient way of describing the eruption spectrum. We therefore regard the spectrum in the area representing an eruption on the Sun's disc as a Fraunhofer spectrum—perhaps somewhat modified—on which is superimposed the eruption spectrum consisting mainly of emission lines but also capable of producing absorption lines (as in the case of *He*). It is this eruption spectrum that we wish to observe.

The spectrograms were first examined with an eyepiece. Any strong emissions could be seen at once, and frequently an apparent filling-in of the Fraunhofer absorption line would indicate weak emission. The latter could be detected more easily by passing the plate through the microphotometer both in the region of the eruption and in a comparison region of normal Fraunhofer spectrum. The depth of the Fraunhofer line with superimposed emission would not be as great as that of the normal line, and very faint emission could be detected in this way.

There were, however, some sources of uncertainty. The use of the microphotometer for detecting faint emission requires the assumption that the Fraunhofer spectrum is the same below the eruption as in the comparison spectrum. When the eruption occurs among sunspots or is very close to the limb this cannot be certain. Also some evidence given in section 6 shows that the Fraunhofer intensities themselves are influenced by the eruption. This effect, however, is hardly sufficient to be confused with real emission. Another possibility is that the ϵ factor in the formation of Fraunhofer lines * is increased in the neighbourhood of eruptions. This would produce an effect in the centre of very strong Fraunhofer lines, and might possibly be responsible for the apparent emission in *Ca* 4226, *Fe* 4383 and other lines.

Taking these points into consideration we must regard the reality of all emission lines marked intensity 1 in the lists as somewhat doubtful, while intensities 2 and 3 are also open to doubt if superimposed on very strong Fraunhofer lines.

Several sections of eruption spectra are shown in figs. 1 to 9 (Plate 3).

3. *Results.*—The emission lines detected in the eruptions selected for study are shown in Table I. The wave-lengths and identifications are taken mainly from the Revised Rowland Table †, but some identifications for Fe^{+} are quoted from a paper by Wyse.‡ The identifications are intended to refer to the eruption emission lines. The Flash intensities are averaged from intensities published by Mitchell §, Menzel ||, and Pannekoek and

* A. S. Eddington, *M.N.*, **89**, 620, 1929; B. Strömgren, *Zs. f. Astrophys.*, **10**, 237, 1935.

† Mount Wilson Observatory, 1928.

‡ A. B. Wyse, *Lick Obs. Bull.*, **18**, No. 492, 129, 1938.

§ S. A. Mitchell, *Ap. J.*, **71**, 1, 1930.

|| D. H. Menzel, *Pub. Lick Obs.*, **17**, 1931.

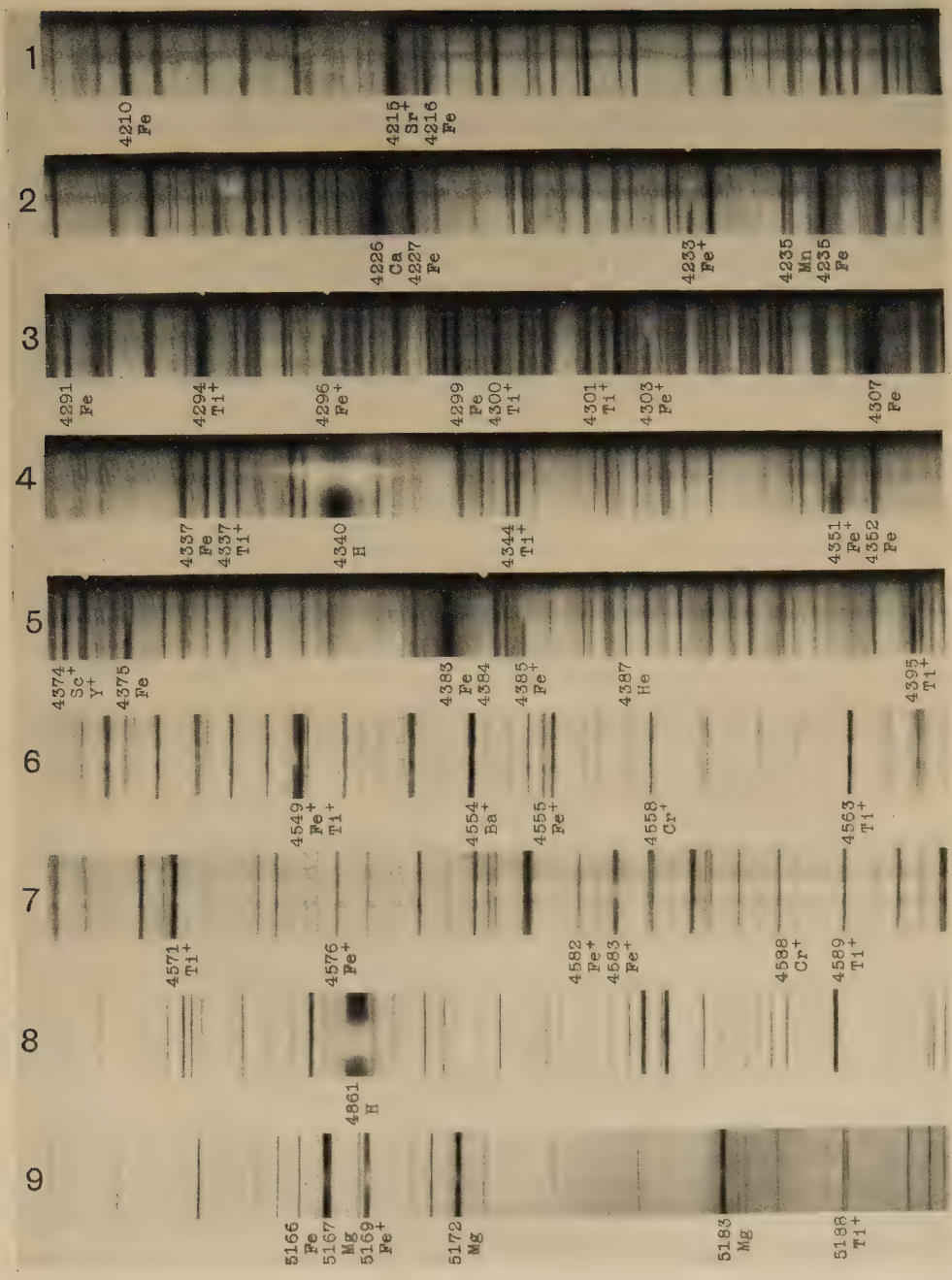

Figs. 1 to 9.—Eruption Spectra.

TABLE I

List of Emission Lines detected in Eruption Spectra

Region of Spectrum. Date of Eruption	Wave-length	Element	Flash Intensity	Per cent. Freq. in Metallic Promi-nence	Eruption Intensity		*T* (or *t*)	
					(*a*)	(*b*)	(*a*)	(*b*)
3922–4010	3933·684	*Ca*+	300		200		(28?)	
1938 Feb. 11	3968·494	*Ca*+	200		150		(20?)	
05h 05m	3970·078	*H*	120		50 w		(20?)	
4065–4169	4077·726	*Sr*+	80			6		35
1938 Apr. 11	4101·750	*H*	140			200 w		14?
23h 40m	4122·667	*Fe*+	6			1		6
4153–4267	4161·801	*Sr*+	...		1		...	
1939 Sept. 7	4167·279	*Mg*	5		1		5	
00h 40m	4173·466	*Fe*+	16		10		6	
	4174·919	*Fe*	4		1		4	
	4177·705	*Fe*+	...		2		...	
	4178·863	*Fe*+	15		15		4	
	4184·000		4		1		4	
	4198·29	*Fe*	6		1		6	
	4199·107	*Fe*	9		1		9	
	4202·042	*Fe*	9		1		9	
	4206·704	*Fe*	5		1		5	
	4210·37	*Fe*	5		1		5	
	4215·545	*Sr*+	60		4		30	
	4216·193	*Fe*	5		6 s		2	
	4226·742	*Ca*	38		3 r		23	
	4227·442	*Fe*	5		1		5	
	4233·171	*Fe*+	32		40		6	
	4235·951	*Fe*	10		1		10	
	4238·818	*Fe*	5		1		5	
	4246·838	*Sc*+	50		1		50	
	4250·799	*Fe*	10		1		10	
	4254·348	*Cr*	25		1		25	
	4258·168	*Fe*+	6		1		6	
	4258·326	*Fe*	4		1		4	
	4260·488	*Fe*	13		1		13	
4286–4416	4287·886	*Ti*+	8			1		22
1939 Sept. 7	4289·731	*Cr*	14			2		30
00h 40m	4290·228	*Ti*+	18			1		49
	4291·475	*Fe*	3			1		8
	4294·10	*Ti*+*Fe*	18			2		33
	4296·580	*Fe*+	9			15 s		7
	4299·252	*Fe*	5			1		14
	4300·055	*Ti*+	22			3		33
	4301·929	*Ti*+	8			1		22
	4303·181	*Fe*+	6			20		4
	4307·914	*Fe*	20			3 r		30
	4312·877	*Ti*+	12			1		33
	4314·093	*Sc*+	12			1		33

TABLE I—*continued*

Region of Spectrum Date of Eruption	Wave-length	Element	Flash Intensity	Per cent. Freq. in Metallic Prominence	Eruption Intensity		*T* (or *t*)	
					(*a*)	(*b*)	(*a*)	(*b*)
	4314·27	*Fe*+	...			2		...
	4314·979	*Ti*+	15			1		41
4323–4454	4325·777	*Fe*	15		...	2 r	22 +	30
1937 Oct. 7	4330·710	*Ti*+	6		...	1	9 +	16
03h 00m	4337·057	*Fe*	4		...	1	6 +	11
	4337·927	*Ti*+	18		...	1	25 +	49
	4340·477	*H*	160		250 w	500 W	15?	25?
	4351·769	*Fe*+	16		20	40	5	8
	4369·408	*Fe*+	3		...	2	5 +	6
	4375·946	*Fe*	8		1	15 s	10	6
	4383·559	*Fe*	15		...	3 r	22 +	24
	4384·319	*Fe*+	3		...	2	5 +	6
	4385·389	*Fe*+	8		2	20	7	5
	4387·901	*He*	3		...	2	5 +	6
	4395·042	*Ti*+	35		1	3	42	55
	4399·780	*Ti*+	12		...	1	18 +	33
	4404·763	*Fe*	12		...	2 r	18 +	24
	4415·137	*Fe*	9		...	2	12 +	16
	4416·829	*Fe*+	8		2	10	7	8
	4427·319	*Fe*	10		1		12	
	4435·158	*Fe*	6		1		7	
	4443·814	*Ti*+	28		1		34	
Visual	4471·54	*He*	80			10		(28)
4508–4664	4508·293	*Fe*+	12		4		6	
1939 Sept. 6	4514·430		3		1		3	
04h 00m	4515·345	*Fe*+	11		3		6	
	4520·231	*Fe*+	12		5		6	
	4522·640	*Fe*+	18		15		5	
	4531·160	*Fe*	4		1		4	
	4533·973	*Ti*+	30		1		30	
	4534·173	*Fe*+	...		1		...	
	4541·525	*Fe*+	6		1		6	
	4549·476	*Fe*+	42		30		8	
	4549·640	*Ti*+	...		1		...	
	4554·038	*Ba*+	40		1		40	
	4555·894	*Fe*+	18		10		6	
	4563·768	*Ti*+	27		1		27	
	4571·982	*Ti*+	32		1		32	
	4576·342	*Fe*+	7		1		7	
	4583·841	*Fe*+	25		30		5	
	4629·344	*Fe*+	20		10		6	
4721–5044	4861·344	*H*	200	100		200		12?
1937 Dec. 21	4891·504	*Fe*	9	...		1		6
01h 00m	4923·932	*Fe*+	35	74		15		7
	5012·077	*Fe*	4	...		1		3
	5018·452	*Fe*+	28	62		20		5

TABLE I—*continued*

Region of Spectrum Date of Eruption	Wave-length	Element	Flash Intensity	Per cent. Freq. in Metallic Promi-nence	Eruption Intensity		*T* (or *t*)	
					(*a*)	(*b*)	(*a*)	(*b*)
5097–5381	5105·547	*FeCu*	3	...	1		2	
1938 Jan. 4	5110·409	*Fe*	4	...	1		3	
$04^h\ 15^m$	5166·286	*Fe*	2	...	1	...	2	3+
1939 July 6	5167·330	*Mg*	18	81	8	8	5	7
$00^h\ 00^m$	5169·052	*Fe*+	22	89	40	60	3	4
5160–5460	5172·700	*Mg*	30	90	10	10	8	11
1939 Sept. 15)	5183·621	*Mg*	40	90	12	12	9	12
(visual)	5197·578	*Fe*+	10	30	2	6	5	4
$01^h\ 00^m$	5227·194	*Fe*	6	6	2	4	3	3
	5234·632	*Fe*+	12	42	2	4	7	6
	5269·552	*Fe*	12	12	3	6	5	6
	5270·33	*CaFe*	6	7	1	3	4	4
	5276·001	*Fe*+	15	43	3	6	7	7
	5316·622	*Fe*+	20	89	8	20	6	5
	5328·053	*Fe*	8	5	1	6	6	4
	5328·544	*Fe*	6	...	1	4	4	3
	5362·871	*Fe*+	10	25	...	3	9+	6
	5371·503	*Fe*	8	4	1	3	6	4
	5429·708	*Fe*	10	3	...	3	9+	6
	5455·626	*Fe*	8	1	...	2	8+	6
Visual obs.	5875·64	*He*	80	100	50		(12)	
from various	5889·977	*Na*	25	91	6		(11)	
eruptions	5895·944	*Na*	20	91	6		(9)	
	6456·396	*Fe*+	15	...	1		(15)	
	6562·816	*H*	200	100	800		(10?)	
	6678·10	*He*	20	68	20		(5)	

Minnaert *, and are adjusted to Mitchell's intensity scale. The metallic prominence frequencies are the percentage number of times that the line was mentioned in an arbitrary selection of about 300 metallic prominences observed at Kodaikanal.† The eruption intensity column is divided into two sections in order to include overlapping regions of spectrum and to show the discontinuities in the regions observed. The intensities are eye-estimates on a scale for which 100 represents intensity equivalent to about 0·4 A. of the Sun's continuous spectrum, and 1 indicates that emission could be detected only with difficulty. Some description of the appearance of the emission lines is also given by the following nomenclature : w = wide, W = extended wings ("bombs"), s = sharp, r = reversed (*i.e.* apparent absorption within emission line). The last column contains *T* or *t*, which is intended to indicate the relative enhancement of lines in an eruption

* A. Pannekoek and M. Minnaert, *Photometry of the Flash Spectrum*, Amsterdam, 1928.

† *Kodaikanal Observatory Bulletins.*

relative to the chromosphere. They are defined in the next section. The normalised value T is given where available ; otherwise the column contains t and the values are in parentheses.

4. *Comparison with the Flash Spectrum.*—Since an eruption takes place above the reversing layer it might be expected that its spectrum would be similar to that of the Flash. Table I supports this general similarity. The question then arises whether the eruption spectrum is merely a Flash

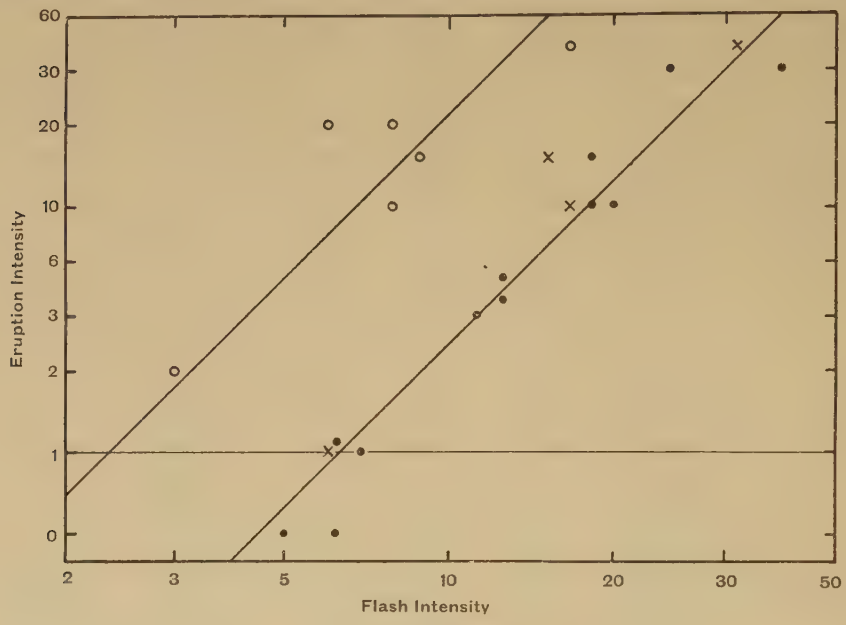

FIG. 10.—*Fe*+ *lines.*

○ 4286–4416 A.
● 4508–4664 A.
× 4153–4267 A.

spectrum of greater intensity, or whether certain sets of lines or certain elements are enhanced relative to others.

An examination of Table I will show that *Fe*+ lines appear much more strongly in an eruption than most other lines of comparable Flash intensity (*e.g.* compare *Fe*+ 4303 with *Ti*+ 4330). Thus one might say that *Fe*+ lines are enhanced in eruptions. An attempt has been made to determine the enhancement of each line numerically in the following manner.

The eruption intensities were plotted logarithmically against the Flash intensities for individual elements in each section of Table I. In the case of *Fe*+ there was a fairly close relation between eruption and Flash intensity. The logarithmic eruption intensity scale was then contracted until the points lay approximately on a 45° slope (see fig. 10). The symbol t is defined as the Flash intensity at the point where the graph cuts eruption intensity 1. It is the brightness in the Flash of a line that would just be detected in an eruption. The greater the intensity in the eruption relative to the chromosphere the smaller the value of t ; we may therefore use it to

define the enhancement of the eruption line. By marking off a 45° slope on the graph it is possible for every observation to give a value for t. When the line is absent from the eruption a minimum value of t is available.

Although the t values are comparable for one plate they are dependent on the brightness of the particular eruption and also on any wave-length variation in Mitchell's Flash intensities. In an attempt to make all plates and regions comparable it has been assumed that the enhancement of the Fe^+ lines is constant throughout the spectrum. In order to normalise the t values they were multiplied by a factor to bring the mean Fe^+ values to 6 for each plate. These normalised t values are denoted T. Justification for this procedure is to be found in the fact that the Ti^+ lines are also brought into consistent agreement with a mean T of about 33. Values for other elements are given in Table II, together with excitation and ionisation potentials.

TABLE II

Mean Values of T (index of enhancement in eruption)

Element (Ionised)	Fe^+	Ti^+	Sr^+	Ba^+	Sc^+	Cr^+	Zr^+	La^+	Y^+
T	6	33	33	40	40	12 +	20 +	30 +	40 +
Effective number of lines	45	24	2	2	6	4	3	2	4
Upper E.P. (volts)	5·5	4·0	3·0	2·6	3·4	6·7	3·7	3·0	3·2
First I.P.	7·83	6·81	5·65	5·19	6·57	6·74	6·92	5·59	6·5
Second I.P.	16·5	13·6	10·98	9·96	12·80	16·6	13·97	11·5	12·3

Element (Neutral)	*He*	*Fe*	*Mg*	*H*	*Ca*	*Cr*	*Mn*
T	6	3 to 30	8	15?	25	28	10 +
Effective number of lines	2	50	7	4	3	2	4
Upper E.P. (volts)	23·9	2 to 6	5 to 7	13	3 to 5	3	5
First I.P.	24·48	7·83	7·61	13·54	6·09	6·74	7·40
Second I.P.	54·18	16·5	14·97	...	11·82	16·6	15·70

For the ionised elements Fe^+ and Ti^+ all lines give the same value of T within experimental error. For each of the other ionised elements the T values are also in agreement, but there are not enough lines available for the mean value of T to be reliable. The great enhancement of the Fe^+ lines is the most noticeable feature of the eruption spectrum.

The T values for the neutral elements are more complex. The figures for hydrogen are doubtful owing to the necessity of extrapolation in fig. 10. In *Fe* there are enough lines to study the agreement of the T values, and we find definite disagreement which cannot be explained as observational error. Thus, for example, in fig. 5 it is seen that 4375 A. is much stronger in the eruption than 4383 A., whereas its Flash intensity and Fraunhofer intensity are much less. In fig. 11 the values of T for *Fe* are plotted against the upper excitation potentials, and it is apparent that below 4·2 volts T is in the neighbourhood of 5, while above 4·2 volts it is frequently much greater (perhaps always greater since lines of intensity 1 are doubtful).

Apparently *Fe* lines whose upper excitation potentials are below 4·2 volts are strongly enhanced in eruptions.

There are not enough data to test whether any such relations occur in any other neutral elements. Since the T variation for the *Fe* lines seems to be associated with the excitation potential, it would appear that the consistency of T for the ionised elements may be due to the fact that the upper E.P.'s do not vary greatly for the lines available for study.

5. *Comparison with Metallic Prominences, "Hot Spots" and Stellar Emission Lines.*—Comparison of eruptions with the chromosphere has

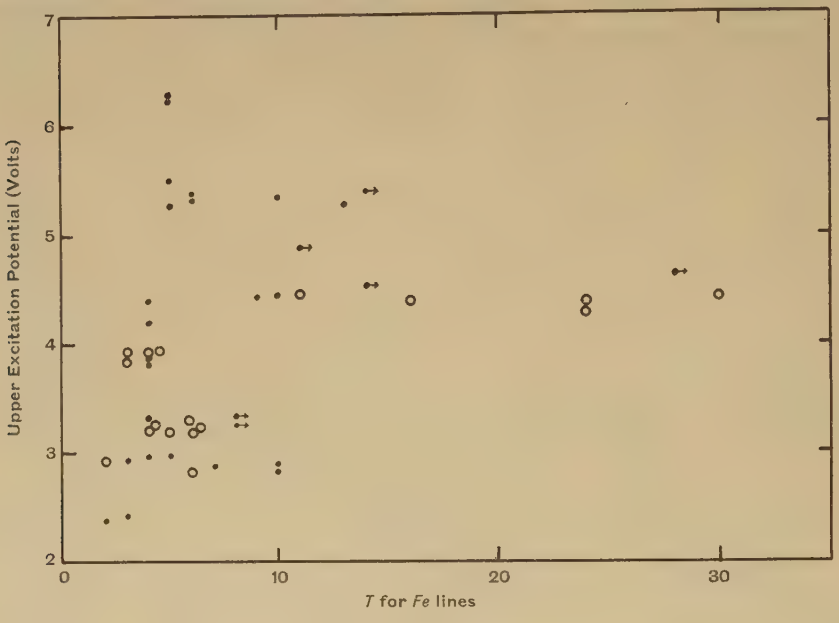

FIG. 11.

● Eruption Intensity = 1.
○ Eruption Intensity > 1.
•→ Not observed in Eruption.

revealed that the Fe^+ lines and some of the *Fe* lines are strongly enhanced in the former. It is now of interest to discover whether the Fe^+ and *Fe* lines receive similar enhancement in other regions of unusual excitation on the Sun's surface.

It might be supposed that an eruption seen on the Sun's limb would appear as a bright low prominence, and that the eruption lines would be emitted. Prominence spectra have been studied at Kodaikanal for many years, and the results have shown that a small percentage of prominences exhibit metallic lines. The fact that metallic prominences are frequently bright and eruptive leaves little doubt that they often represent eruptions seen on the Sun's edge. The *Kodaikanal Bulletins* do not give intensities of the metallic lines, but presumably these may be judged from the frequencies with which they are observed. Percentage frequencies are given in Table I. It is found in general that the percentage frequencies for Fe^+ lines are far

greater than the figure representing Flash intensity, while for Ti^+ and Ba^+ they are less. Thus for ionised lines we find similarity between metallic prominences and eruptions. This similarity, however, does not extend to the neutral elements. We find that the metallic prominence does not show the same enhancement for the low E.P. *Fe* lines as the eruption.

Occasionally regions of the Flash spectrum have shown signs of unusual excitation. Such a region has been called a "Hot Spot" by Cillié and Menzel *, and it is quite possible that this excitation is in some way associated with an eruption. From Cillié and Menzel's observations of intensity within the Hot Spot it is possible to determine the relative enhancement of the different elements. Table III is taken from their paper, where the column 49*b* refers to the Hot Spot and 49*a* to the normal chromosphere. Here again Fe^+ leads the ionised elements, and there is some similarity to

TABLE III

Element	*He*	*H*	Fe^+	Cr^+	*Fe* E.P. > 4·2	Mn^+	Ti^+	*Fe* E.P. < 4.0	*Cr*	Sc^+
Log intensity 49*b*–49*a*	+·40	+·14	+·05	−·03	−·09	−·10	−·11	−·12	−·20	−·22
Number of lines	12	10	4	9	19	5	29	16	4	6

the order of elements shown in Table II. However, there is not the same difference between high E.P. and low E.P. *Fe* lines as in eruptions. Similar observations made by a recent Harvard-M.I.T. eclipse expedition have been studied by Hemmendinger.† Details are not yet available, but the relative weakening of Ba^+ and *Ca* that is mentioned is similar to our eruption results.

The behaviour of *Fe* and Fe^+ is rather similar in the spectrum of eruptions and some bright-line stars.‡ In long-period variables of classes Me and Se several low-level *Fe* lines are emitted, while bright Fe^+ lines are also present. This is only a general similarity, however, and there are differences in individual lines. 4307·91 A., for example, is conspicuous in these stars but in eruptions is not as strong as 4375·95 A.

6. *The Fraunhofer Spectrum below an Eruption.*—It has been observed that there is not generally any increase in the continuous spectrum intensity in eruptions.§ There is, however, a detectable change in the relative intensity of Fraunhofer lines. This was revealed by the microphotometry of spectra inside and outside the eruption area. The depths of lines were measured on the tracing and not converted into true intensities. The brightest eruptions are not included since too many lines are obscured by emission. The results are shown in Table IV. The elements and values influenced by real emission are in parentheses, and for the others the figures can be taken as indicating the relative intensity of Fraunhofer lines below eruptions compared with the normal Sun's surface. The values have been

* G. G. Cillié and D. H. Menzel, *H.C.O. Circular* 410, 1935.
† H. Hemmendinger, *Phys. Rev.*, 55, 1119, 1939.
‡ P. W. Merrill, *Ap. J.*, 65, 286, 1927.
§ R. S. Richardson and R. Minkowski, *Ap. J.*, 89, 347, 1939.

normalised to give 1·0 for neutral elements, and we find very consistently that the ionised Fraunhofer lines are stronger below an eruption.

TABLE IV

Element	*Ca*	*Cr*	*Mn*	*Ni*	*Ti*	(*Mg*)	*Zn*	*Co*	*V*	*Fe*	(*H*)
Depth $\frac{\text{Eruption}}{\text{Normal}}$	1·01	0·99	1·00	1·00	0·98	(0·59)	1·04	0·93	1·00	0·99	(0·10)
Number of lines	14	21	10	41	25	5	2	3	12	167	3

Element	Sc^+	Ti^+	Cr^+	(Fe^+)	Ba^+	Y^+
Depth $\frac{\text{Eruption}}{\text{Normal}}$	1·09	1·06	1·10	(0·74)	1·05	1·08
Number of lines	6	19	4	13	2	2

Making the same analysis for the *Fe* lines of various excitation potentials we obtain Table V. There is a consistent increase of Fraunhofer intensity below an eruption with increased excitation potential.

TABLE V

E.P. of *Fe* Lines (Volts)	0 to 1	1 to 2	2 to 3	3 to 4	4 to 5
Depth $\frac{\text{Eruption}}{\text{Normal}}$	0·90	0·94	0·99	1·01	1·04
Number of lines	15	13	71	52	16

The increase of intensity for ionised lines and the increase with excitation potential both agree in demonstrating an increase of excitation temperature in the reversing layer below an eruption. The amount of this increase may be determined roughly by assuming that the change in the number of atoms is proportional to the change in the depth of the lines on the microphotogram. The usual excitation formula used with the results of Table V leads to an increase of temperature of about 100° K.

Summary

High dispersion spectrograms of bright eruptions on the Sun's disc have been obtained. 116 emission lines have been detected and tabulated in various discontinuous regions of the spectrum from 3922 A. to 6700 A.

The intensities of the eruption lines when compared with those of the Flash spectrum reveal that all Fe^+ lines and all low E.P. *Fe* lines are strongly enhanced in eruptions. The enhancement of Fe^+ lines is also detected in metallic prominences and "Hot Spots," but this is not the case for the low E.P. *Fe* lines. Emission lines in some stellar spectra are similar to those in eruptions.

No satisfactory explanation of the results has been found.

Small variations detected in the intensities of Fraunhofer lines from areas in eruption may be explained if the excitation temperature of the reversing layer is increased by about 100° K.

Commonwealth Solar Observatory,
Canberra, Australia :
1940 *May.*

SOME PROBLEMS CONCERNING THE DISTRIBUTION OF SUNSPOTS OVER THE SUN'S DISC

G. H. A. Archenhold, Ph.D.

1. *Introduction.*—This paper is mainly concerned with the distribution of sunspots as a function of longitude from the central meridian. Hitherto this question has been investigated only as regards the centres of whole groups.* It has been shown by Mrs. Maunder † that the number as well as the total areas of groups diminish from the Sun's centre towards the limb. The decrease is more marked for numbers, which fall by 81 per cent., than for areas, which decline by 72 per cent. It follows from this that smaller groups are more affected by the so-called foreshortening than bigger ones. Small groups, just large enough to be seen when near the centre of the disc, will escape observation if they happen to be in the limb zones. Mrs. Maunder did not discuss the nature of the decrease in numbers and areas from centre to limb in detail. Her interest was directed towards the asymmetry revealed between the eastern and western hemisphere of the Sun as regards the number, areas, births and deaths of groups.

A statistical examination of the dependence of visibility of groups in different zones upon their size is rendered more difficult by the complexity of groups. A group of a given area, for instance, may consist of one big spot or of several small ones. Since the two alternatives are not equivalent as regards the visibility of the group near the limb, the area alone does not characterize a group sufficiently. To avoid difficulties arising from the complexity of groups we prefer to study the distribution of individual spots.

2. *The Observational Data.*—The material used is taken from the Greenwich Photoheliographic Results. The daily results up to the year 1915 give the details of position and area of single spots and of the more important individual spots composing the groups. In this paper we define the spot's longitude from the central meridian as L.

3. *Longitude Area Diagrams.*—Diagrams have been constructed which show the distribution of spots of different size as a function of L. The abscissa of the diagrams represents the longitude from central meridian, the ordinate represents the area. Every sunspot is plotted for each day it has been observed. The areas used are already corrected for foreshortening in the Greenwich Results.

Longitude area diagrams have been drawn for the years 1889, 1898, 1899 and 1900. The results of this paper are based mainly on these diagrams. There is no need to reproduce the diagrams, which contain more than 5000 spots and have a very large scale. Their chief purpose was to facilitate the numerical work.

* A compilation of papers on this subject is given by Miss Hazel Marie Losh in *Publ. of the Observatory, Michigan*, **7**, 127, 1938.

† *M.N.*, **67**, 451, 1907.

4. *The Geometrical Foreshortening Curve.*—We define the area of a sunspot as it appears on the photographic plate and expressed in units of one millionth of the Sun's visible hemisphere as its "apparent size." This is not identical with the "projected area" used in the ledgers of sunspot groups in the Greenwich Publications since the latter area is expressed in millionths of the Sun's disc. The apparent area multiplied by the secant of the projection angle is the *corrected area.* The latter may not coincide with the area of the spot if viewed normally. We define the *normal area* as the area which would be measured if the spot were viewed in the direction normal to the Sun's surface.

There exists a well-marked lower limit of the corrected size of observed sunspots. Near the centre of the disc spots of an area equal to one millionth of the Sun's visible hemisphere are numerous. Near the limb (beyond $\pm 80°$) no spot smaller than ten millionths has been detected during the period on which the longitude area diagrams have been based. The curve representing the smallest corrected areas of observed sunspots as a function of the distance from the Sun's centre will be referred to as the *geometrical foreshortening curve.*

Assuming that the apparent size of a spot which might be detected on the photographs must have a certain minimum value, it is clear that due to the geometrical foreshortening the corrected area of the smallest detectable spots must increase from the centre of the disc towards the limb. If the visibility of a spot depended upon the apparent size only, the minimum corrected area would be proportional to the secant of the angular distance from the Sun's centre. Since, however, the apparent shape of a spot approaching the Sun's limb becomes more and more elongated and other conditions of visibility may change also, it is by no means sure that the secant law is valid right up to the limb.

From the longitude area diagrams we get an approximation to the foreshortening curve by neglecting the difference between the longitude from central meridian and the angular distance from the Sun's centre. This difference, depending on the latitude and longitude of the spot and on the latitude of the centre of the Sun's disc, diminishes quickly from centre to limb. The years chosen for plotting the diagrams were those before sunspot minima. According to the small equator distance of spots in those years, the maximum value of the difference, which occurs near the central meridian, was limited. Since, moreover, the chief functions with which we shall be concerned vary only a little near the centre, but more near the limb, no serious error is introduced by the neglect of the difference mentioned.

The second line of Table I gives for different values of L the corrected area of the smallest spots measured on the photographs of the Sun. The corresponding apparent size is given in the third line of the Table. The third line of Table I indicates that the secant law for the geometrical foreshortening curve holds up to a value of about $L = 75°$. Above 80° the smallest visible spots have at least double the apparent size of that necessary for a spot near the central parts of the disc. The failure of the secant law is probably

a consequence of the condition that the minor axis of a just detectable sunspot must have a certain minimum size, for which we have derived a value of 1″·4. The last line in the Table gives the values for the corrected areas of a circular spot assumed to have an apparent minor axis of 1″·4. The agreement between the calculated and the observed values is sufficient to support the assumption on which the theoretical data are based.

TABLE I

The Corrected and Apparent Size of the Smallest Sunspots observed on Greenwich Plates during the Years 1889 *and* 1898 *to* 1900

L	0°	45°	60°	70°	75°	80°	85°
Corrected area	1	1	1·8	2	4	10	33
Apparent size	1	0·7	0·9	0·7	1·0	1·7	2·9
Theoretical area	(0·3)	(0·5)	1	2	4	9	35

First line : Longitude from central meridian.
Second line : Corrected area of smallest visible spot.
Third line : Apparent size calculated by dividing the corrected area by sec *L*.
Fourth line : Theoretical area of a circular spot having an apparent minor axis of 1″·4.
(The unit of area used throughout this paper is 1 millionth of the Sun's visible hemisphere. A circular spot of unit area would show a diameter of 2″·7 when situated in the centre of the disc.)

This lower limit of size may be thought to refer to plates of best quality only, but the statistical average is found to be only slightly higher. A discussion of the data, which cannot be given here for reasons of space, suggests that the figures in the second line of Table I are representative of the geometrical foreshortening curve.

5. *The Physical Foreshortening.*—In fig. 1 is given the frequency of sunspots of corrected area 1 to 20 millionths for (*a*) the central zone −10° to +10°, and (*b*) zones 60° to 70° east and west of the central meridian. A comparison of these curves reveals a great difference between the numbers of spots of equal corrected size in the limb and central zones. One finds, for instance, that the number of spots of corrected area 5 millionths is 12 and 52 respectively. Since the areas are already corrected for geometrical foreshortening, the cause of the difference must be something else. As will be seen from the figure, the curve *b* fits fairly well into curve *a*, if the former is shifted by about 10 units of the abscissa to the right. It seems therefore that the corrected areas of the spots in the zones 60° to 70° from the central meridian appear 10 units of area smaller than they would appear in the central zone. If that is true, the smallest spots of a corrected area of 2 millionths seen in the 60° to 70° zone have in reality a normal area of 12 millionths. We define the difference between the corrected area of a spot at longitude *L* and its normal area as *physical foreshortening*.

A statistical method for determining the physical foreshortening will be based on the assumption that the number of sunspots of a given normal area is the same in all longitudes from central meridian. We denote by

$N(L, c)\Delta L$ the number of spots between $L - 1/2\Delta L$ and $L + 1/2\Delta L$ whose corrected area is equal to or bigger than c millionths of the Sun's hemisphere. In the central zone, $L = 0°$, normal and corrected areas are identical. We

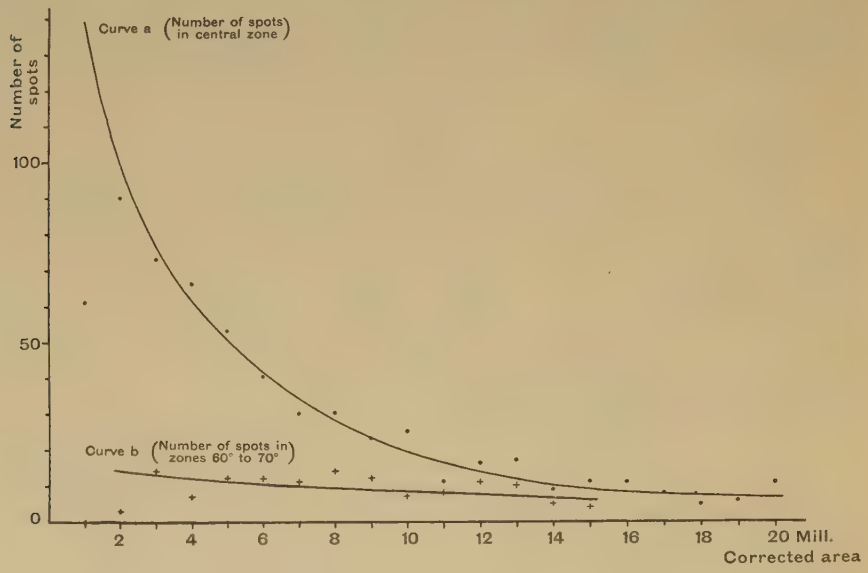

FIG. 1.—*Number of spots of corrected area* 1 *to* 20 *millionths* :—
(*a*) *in the central zone* $-10°$ *to* $+10°$ (*dots*).
(*b*) *in the zones* 60° *to* 70° *East and West from central meridian* (*crosses*).

denote briefly $N(0, c) = N_0(n)$. On account of the assumption made, it follows that if

$$N(L, c) = N_0(n), \qquad (1)$$

the corrected area c at longitude L is equivalent to the normal area n.

The function $N_0(n)$ has been determined by counting in the longitude area diagrams the spots equal to or bigger than n in the central zone $-10°$ to $+10°$ and dividing by 20. Table II gives the values of $N_0(n)$ for suitable steps of n.

TABLE II

Number of Spots equal to or bigger than n millionths in the Central Zone

n	1	11	21	31	41	51	101	151	201	251	301
$N_0(n)$	44·3	17·8	12·3	9·3	7·8	6·9	4·5	2·1	1·9	1·3	1·0

The values of $N(L, c)$ have been derived similarly for longitude zones of 5° or 10° width and suitable steps of c. As can be seen from Table II, the numbers of spots decrease quickly with growing spot sizes. To improve the accuracy of the values $N(L, c)$ for $c > 50$, the longitude area distribution of all spots bigger than 50 millionths has been determined in the additional years 1890, 1897, 1901 and 1902, so that the results of the eight years 1889–1890 and 1897–1902 could be used.

The procedure of finding the normal area n corresponding to a corrected area c at longitude L was to interpolate according to formula (1) that value of n that gives the same number of spots $N_0(n)$ as is observed at longitude L down to a corrected size c, i.e. $N(L, c)$. In fig. 2 the derived normal areas corresponding to corrected areas of 201, 151, 101, 51, 31, 11 and 1 millionth are given as a function of longitude from the central meridian.

It appears that the physical foreshortening at a certain longitude is slightly dependent upon the size of the spots, since the curves in fig. 2 are

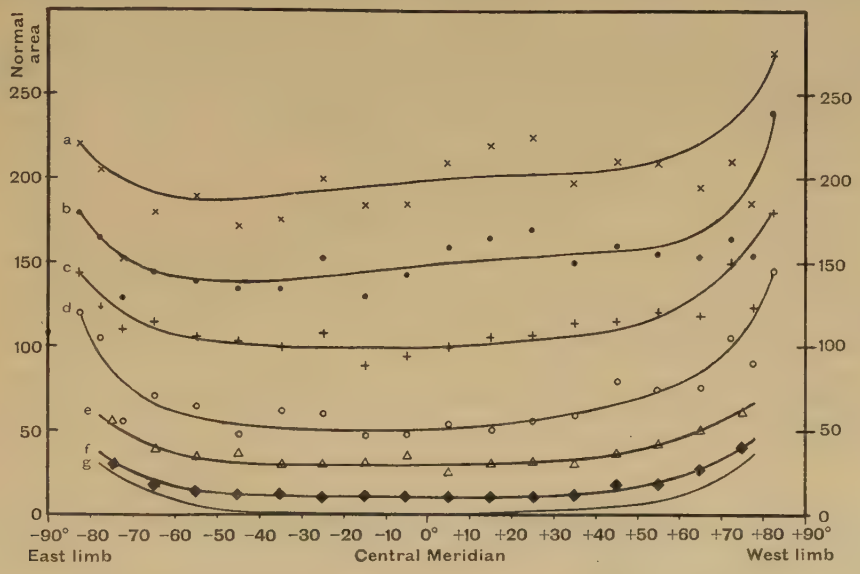

FIG. 2.—*The physical foreshortening. The curves give the normal area of spots of a corrected area :—*

200 *millionths* (*curve a*) ×		50 *millionths* (*curve d*) o	
150 ,, (*curve b*) •		30 ,, (*curve e*) △	
100 ,, (*curve c*) +		10 ,, (*curve f*) ◆	

and the physical foreshortening of spots of the smallest visible size (*curve g*).

not parallel. The dependence is different for eastern and western longitude, and the asymmetry between the physical foreshortening East and West is more distinct for bigger spots. Since, however, the numbers of spots of large area are relatively small, this result may still be uncertain. It is, however, quite clear that the physical foreshortening is not proportional to the area. It is therefore impossible to correct the geometrical foreshortening factor used in the reduction of the observations in such a way as to allow for the physical foreshortening. It is further very unlikely that the cause of the difference between corrected and normal size may be found in purely observational facts such as the scattering of light in the Earth's atmosphere or optical contrast phenomena.

6. *The Curve of Visibility.*—We define as curve of visibility the function which gives the normal size n_0 of the smallest photographed spots at longitude L. Applying formula (1), we have to use on the left side of the

equation the total number of spots at longitude L, which may be denoted $N(L)$. Table III gives the numerical values of the function $N(L)$ derived

Table III

Number of Spots Visible at Eastern and Western Longitude L.

L	87°·5	82°·5	77°·5	72°·5	65°	55°	45°	35°	25°	15°	5°
$N(-L)$	0·3	4·4	8·8	13·8	18·6	27·2	34·6	38·5	42·7	46·5	44·0
$N(+L)$	0·3	3·7	8·4	10·3	15·9	21·4	26·0	32·6	41·7	44·0	44·6

from the same material as Table II. Corresponding values of L and n_0 to satisfy (1) are now determined by comparison of Tables II and III. The resulting values of n_0 as a function of L (East and West) are given in Table IV.

Table IV

The Curve of Visibility

L	87°·5	82°·5	77°·5	72°·5	65°	55°	45°	35°	25°	15°	5°
$n_0(-L)$	(400)	103	34	24	10	5	3	2	1	1	1
$n_0(+L)$	(400)	116	37	27	13	8	6	4	1	1	1
10 *sec* $L-9$	(220)	(68)	37	24	15	8	5	3	2	1	1

Up to longitudes of 77°·5 these values can be represented approximately by the formula

$$n_0 = 10 \sec L - 9. \qquad (2)$$

To facilitate a comparison of the curve of visibility with the geometrical foreshortening curve, both the curves are drawn in fig. 3. The difference between the two curves, which is mainly due to physical foreshortening, appears as a very striking fact.

7. *The Model of a Sunspot.*—The physical foreshortening, which means that a sunspot appears smaller if looked at from a greater angle of observation even after its area is corrected for the geometrical foreshortening, implies a structural feature of sunspots.

If a sunspot has the shape of a flat dish or funnel, then it should show an increase in corrected area when approaching the limb, because the depth to which an observer can look into the Sun decreases with increasing inclination of the line of sight. To satisfy the observational facts presented in this paper we must conclude, however, that the cross-section of a sunspot decreases in the higher levels of the Sun's surface. This conception is in agreement with certain theories of spots (see Minnaert and Wanders, *Zs. f. Ap.*, **5**, 297, 1932).

8. *Discussions of the Reality of the Observed East-West Effect.*—We proceed now to discuss if the eastern excess of sunspots may be considered to be real. The numbers of individual spots as well as of groups observed on the eastern and western half of the Sun in the years 1888 to 1915 * have been tabulated and are summarised in Table V. After the counting had

* From 1916 onwards data of individual spots have not been published in the Greenwich Results.

been made, it was found that part of the figures concerning the numbers of groups have already been given by Pocock * and Akesson.† The results agree very well with those published by Akesson. In the case of large differences as found, for instance, for the year 1906 our figures have been checked independently. Pocock's figures are slightly distorted, since he counted those groups twice which were observed from the last days of one year to the first days of the following year, and for which data are given in two consecutive volumes of the Greenwich publications. Neither author has given figures for individual spots. Our own tabulation shows that the

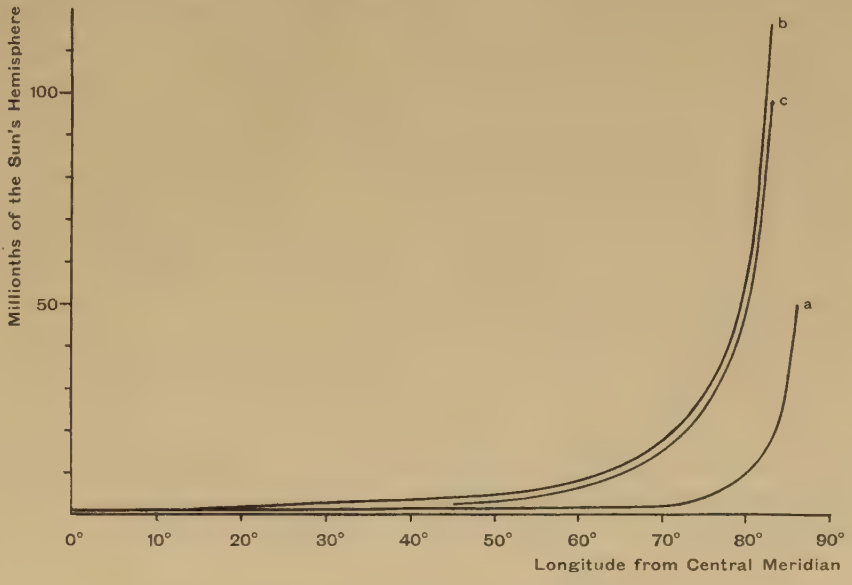

FIG. 3.—*Curve a: The geometrical foreshortening curve.*
Curve b: The curve of visibility.
Curve c: The physical foreshortening.

eastern excess is smaller for spots than it is for groups. This may be due partly to the effect mentioned in section 9. On the other hand, the East-West effect cannot be expected to be the same for spots and groups since the ratio of spots per group is smallest near the limb where the East-West effect is biggest.

Estimates of the dispersion or "natural uncertainty" of the numbers of spots and of groups may throw some light on the question if the eastern excess is big enough to establish the reality of the East-West effect. If sunspots showed a random distribution so that the probability of a spot being situated on the eastern hemisphere is p, the dispersion σ would be given by

$$\sigma = \sqrt{Np(1-p)} = \sqrt{N_E(1-p)}, \qquad (3)$$

where N denotes the total number of spots East *plus* West, and $N_E = Np$ the mean value of sunspots on the eastern hemisphere.

* *M.N.*, **74**, 54, 1918. † *Meddelanden Lund*, Serie II, No. 11, 1914.

It is obvious that the assumption of a random distribution, on which formula (3) is based, does not hold in the case of the actual distribution of sunspots. Firstly, sunspots often remain on the same side of the central meridian for some consecutive days, and secondly, they are clustered together into groups. To allow for these facts, we introduce a factor c, writing

$$\sigma_c = c\sqrt{N_E(1-p)}. \qquad (4)$$

The value of the factor c depends upon the frequency distribution of the number of spots per group. This distribution is probably a function of the sunspot cycle, since the average number of spots per group is 2·5 in years with less than 500 observed groups, and 3·1 in years with more than 1000 observations. As a first approximation we shall regard c as constant. The procedure to derive the factor c was as follows. For each year the deviation of the observed number of eastern spots from the expected value $N_i p$ was determined (N_i denoting the total number of spots in a particular year). This deviation was then expressed in units of the theoretical scatter $\sqrt{N_i p(1-p)}$. The root mean square of these values, which form a normal error law distribution, gives the result c (*spots*) = 2·6. The factor c derived in the same manner for groups is c (*groups*) = 1·1.

In Table V the numbers of spots and groups for the two complete cycles 1889–1901 and 1902–1913, as well as for the whole period 1888–1915, are given incolumns 2 and 3. Column 4 contains the difference East *minus* West, column 5 the natural uncertainty of this value calculated from formula (4) under the assumption that $p = 1/2$. Column 6 shows how many times the East *minus* West difference exceeds the natural uncertainty.

TABLE V

The Observed Eastern Excess of Sunspots and Groups

Years	Number		E. *minus* W.	Natural Uncertainty σ_t	E. *minus* W. / σ_t
	East	West			
			Sunspots		
1889–1901	25513	24261	+1252	590	+2·1
1902–1913	16826	16517	− 191	482	−0·4
1888–1915	45387	44229	+1158	780	+1·5
			Groups		
1889–1901	8120	7469	+ 651	144	+4·5
1902–1913	6378	6023	+ 355	127	+2·8
1888–1915	15831	14724	+1107	204	+5·4

It will be seen from the table that the East-West effect for spots is not large as compared with the natural uncertainty. In the second cycle there are even more spots West than East. The reality of the East-West effect of *groups* is well established by the eastern excess being more than five times the dispersion or natural uncertainty.

Since the result derived in Table V does not prove the reality of the East-West effect of spots, we have made a further analysis by investigating the ratio West to East for different zones of the Sun's disc. It is known from Mrs. Maunder's figures that the asymmetry between East and West is biggest when the limb zones are compared. From Mrs. Maunder's Table V (*loc. cit.*, p. 456) we have formed the ratio of the numbers of groups in corresponding eastern and western longitudes. These values are represented by dots in fig. 4. The West to East ratio of the numbers of individual

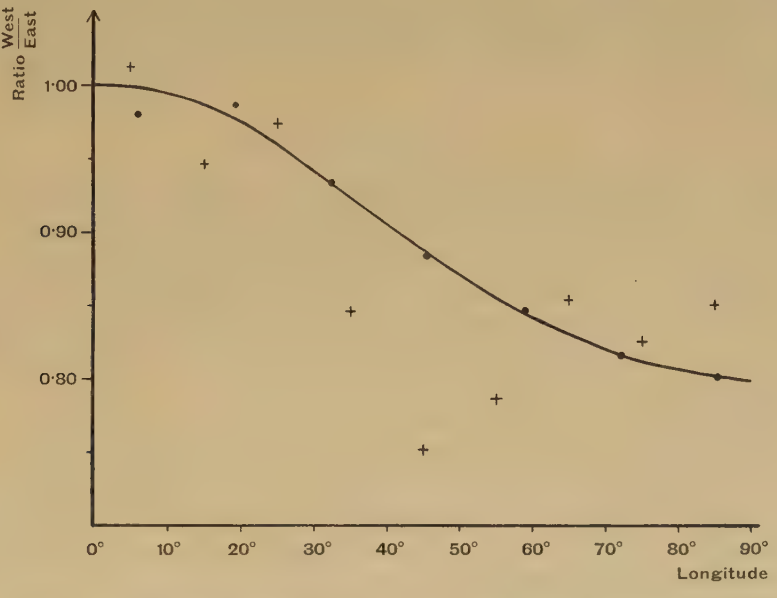

FIG. 4.—*The ratio of numbers of spots (dots) and of groups (crosses) on the western and eastern half of the Sun as a function of longitude.*

spots as it follows from the numbers $N(L)$ in Table III of the present paper is given by crosses in fig. 4. It should be mentioned here that the period for which the $N(L)$ are derived shows a slightly bigger eastern excess than the whole Maunder cycle. The curve is drawn to fit the values derived for groups. It may be seen that the same curve approximates to the crosses which represent the East-West effect of spots. This seems to indicate that there is an East-West effect also for individual spots.

This East-West difference can be explained by a slight difference of the physical foreshortening curve for eastern and western longitudes, which amounts to the small percentage of about 20 per cent. only of the physical foreshortening itself. It may be hoped that a theory which explains the physical foreshortening may also explain the East-West effect by taking into account two points already suggested by Mrs. Maunder :

1. That the axes of sunspots generally may slope downwards from West to East.
2. That the surface behind a sunspot is heaped up.

These assumptions can be supported as follows. It is well known that the rotation of the Sun is faster in higher levels. The axis of a spot must therefore, at least in its higher parts, become inclined from West to East. The observations of Hydrogen and of Calcium flocculi give evidence that the main bulk of the flocculi is mostly following the visible spots, and the same observation has been made as regards faculæ.*

9. It may be added that included in the East-West effect is a relatively small factor due to the systematic difference in size between the leader and follower spots of bipolar groups. This effect has been investigated in detail, but the numerical evaluation is omitted here for reasons of space. It is concluded that about a tenth of the Maunder effect might be explained in this way.

Summary

Studies of the distribution of sunspots over the Sun's disc give evidence that the area of a sunspot already corrected for geometrical foreshortening is affected by a physical foreshortening. The numerical values of this foreshortening are determined for spots of various sizes. The physical foreshortening increases from centre to limb and slightly from small to large spots. At longitude 65° it amounts to about 10 units of area, at longitude 80° to about 50 units.

These results have some bearing on the structure of sunspots.

Numerical values of the geometrical foreshortening curve and of the curve of visibility are derived from Greenwich observations. These curves, which give the corrected and the normal size of the smallest visible spots respectively, have the character of instrumental constants and will change with the method of observation.

The Maunder effect amounts to an eastern excess of $7{\cdot}5 \pm 1{\cdot}4$ per cent. (mean error) for groups in the period 1888 to 1915. The East-West asymmetry of spots amounts to $2{\cdot}6 \pm 1{\cdot}7$ per cent. (mean error) for the same period. The reality of the East-West asymmetry for spots could be shown by comparing the numbers of spots in smaller corresponding eastern and western zones. The numerical difference between the East-West effect for groups and for spots is attributed to the fact that the number of spots per group is biggest near the central meridian where the asymmetry is smallest. About a tenth of the Maunder effect for groups is attributed to the bigger size of leading members of sunspot groups as compared with the followers.

The physical cause of the Maunder effect can be found in the slope of the axes and the preponderance of faculæ on the eastern side of sunspots. The East-West asymmetry of the size of sunspots accounting for the Maunder effect is a small percentage only of the physical foreshortening.

Finally, it follows from the derived curve of visibility that a sunspot group contributes the less to the statistical "character" figure the nearer it is to the limb. The consequences as regards the observed births of spots will be treated in another paper.

* Rodés, *Boletin del Observatorio Del Ebro*, **25**, fasc. 1, 1935.

In conclusion, I should like to express my thanks to Professor F. J. M. Stratton for the kind interest he has taken in this paper. I am also grateful to J. C. Dobbie and W. Moss, with whom I had helpful discussions, and to H. R. Hulme, H. W. Newton and A. D. Thackeray who have read the manuscript. [The latter have edited the paper in the author's absence.]

Solar Physics Observatory,
Cambridge.

THE EFFECT OF ABSOLUTE MAGNITUDE ON STAR COLOURS

A. Hunter, Ph.D., and E. G. Martin

(Communicated by the Astronomer Royal)

1. *Introduction.*—It is well known that a considerable range of colour exists amongst stars of given spectral type; this range is largest for the earliest and the latest spectral types. Since in stars of late spectral type redness is associated with high luminosity and blueness with low, it is generally tacitly assumed that the difference of colour between giants and dwarfs is due to their difference in absolute magnitude. With early-type stars, where, broadly speaking, redness is again associated with high luminosity, there has, however, existed a difference of opinion as to the cause of the dispersion in colour: one school of thought attributing it to differential space absorption, *i.e.* to an effect of distance, and the other to an absolute magnitude effect. The question is difficult to decide amongst the early-type stars because their distances and absolute magnitudes are not known with any great certainty. This is also true of the late-type giants, but reliable values are available for late-type dwarfs, and the range of absolute magnitude in any sub-type is much greater than for early-type stars. There is, however, an *a priori* reason for attributing the reddening in early-type stars to space absorption: these stars are highly concentrated to the Milky Way, where, by analogy with external galaxies seen "edge-on," such absorption would be expected. The later-type stars are much less concentrated and accordingly it is more reasonable to rely on an explanation involving difference of absolute magnitude rather than on one involving difference of absorption.

If observations are confined to groups of stars of exactly the same apparent magnitude, no distinction whatsoever can be drawn between the causes, since in this case absolute magnitude is completely correlated with distance. To distinguish clearly between the causes, then, we must investigate the colours of stars which differ widely amongst themselves in apparent magnitude; this is, unfortunately, limited by observational conditions. For determining the colour excess of a given star, we need its colour (colour index, gradient, effective wave-length, etc.) and its spectral type (for determining the deviation of this colour from the normal colour for stars of that spectral type). It is essential that spectral types used for this latter purpose should be directly estimated; spectral types deduced from colour indices or similar measures are worthless because of the range of spectral type to a given colour. Thus the data are limited in the first place by the necessity of securing observed colours and spectral types. For

the purpose of explaining the observed reddening, whether as an effect of distance or of absolute magnitude, reliable distances and absolute magnitudes are required, and these again are rarely available for early-type stars.

We have endeavoured to separate the two effects by examining the colours and magnitudes of members of galactic clusters. Such clusters are usually at distances of 100 to 2000 parsecs, and cover from a few square degrees to a fraction of a square degree. Assuming that the clusters are not greatly elongated in the line of sight, the separate components are at a constant distance to within at most a few per cent., generally very much less. The most luminous members of the closer clusters are sufficiently bright to allow a range of the order of three spectral classes before spectral types and colours cease to be available.

It should therefore often be possible to determine whether or not the colour excess of a cluster member depends upon its absolute magnitude. It is the object of the present paper to estimate the size of such an absolute magnitude effect if it exists. This question is discussed at length in sections 5 and 6 below, where correlation coefficients are deduced between colour excess and absolute magnitude.

2. *Data Used.*—Table I contains references to the material used later in the paper. The source named is always the *original* source, but in many cases the index number, which refers to the list of publications at the bottom of the table, indicates the most convenient source, which often merely quotes the data.

3. *Physical Scatter of the Colour Indices.*—Before proceeding to the actual calculation of correlation coefficients we must decide whether the available observations are such that any significance may be attached to the coefficients when they are obtained. In any one cluster, the colour indices of the individual stars are naturally correlated closely with their spectral types. If there were no experimental error in either co-ordinate, it might be expected that the diagram connecting colour index and spectral type would show no scatter, *i.e.* all stars of the same spectral sub-type would have the same colour index. In fact, however, the diagram does show a considerable scatter.

The following experimental errors will contribute to the observed scatter :—

(*a*) errors in the spectral types,
(*b*) errors in the photographic magnitudes, and
(*c*) errors in the visual magnitudes.

Internal evidence will in general be available for the calculation of (*a*), (*b*) and (*c*) separately. When combined, these give the total scatter to be expected from observational inaccuracies. Comparison of this experimental scatter with the scatter actually observed will then show whether there is any residual scatter needing further investigation.

The most favourable case to examine will be one in which the experimental error is small. The Pleiades have been so well observed (see Table I) that many series of accurate colour indices and spectral types are

available. Trumpler's * investigation enables the cluster members to be distinguished from background or foreground stars. Using his classification, good spectral types and colour indices for over a hundred cluster stars have been obtained by combining the material shown in Table I. In general the various magnitude systems are not strictly comparable ; where the necessary corrections are not explicitly given by the authors, the photographic magnitudes were corrected by graphical means to the scale and zero-point of Hertzsprung † ; the visual magnitudes to the scale and zero-point of the Harvard visual system. The resulting colour indices are practically on the International Scale.

TABLE I

Cluster	Photographic Magnitude	Visual Magnitude	Spectral Type
Pleiades	Hertzsprung [1] Hertzsprung [2] Gaultier [3] Harvard [4] Shapley and Richmond [5]	Müller and Kampf [14] Graff [15] Shapley and Richmond [5]	Harvard [16] Harvard [17] Schwassmann [18]
20 Clusters	Zug [6]	Zug [6]	Trumpler [6]
N.G.C. 752 (*a*)	Jungkvist [7]	Jungkvist [7]	Jungkvist [7]
,, (*b*)	Heinemann [8]	Heinemann [8]	Jungkvist [7]
Præsepe (*a*)	Vanderlinden [9]	Vanderlinden [9]	Harvard [9] Schwassmann [9]
,, (*b*)	Haffner and Heckmann [10]	Haffner and Heckmann [10]	Harvard [9] Schwassmann [9]
Hyades (*a*)	Göttingen [11]	Harvard [11]	Harvard [11]
,, (*b*)	Hertzsprung [12]	Hertzsprung [12]	Kohlschütter [12]
N.G.C. 663	Wallenquist [13]	Wallenquist [13]	Trumpler [6]
N.G.C. 7654	Wallenquist [13]	Wallenquist [13]	Trumpler [6]

References

[1] *A.N.*, **186**, 177, 1911.
[2] *A.N.*, **200**, 137, 1915.
[3] *Bull. Soc. Astr. France*, **15**, 491, 1901.
[4] *H.A.*, **89**, 51, 1932.
[5] *M.W. Cont.*, 218.
[6] *L.O.B.*, **16**, 119, 1933.
[7] *Medd. Obs. Upsala*, **52**, 1931.
[8] *A.N.*, **227**, 193, 1926.
[9] *Étude de l'Amas de Præsepe*, Gembloux, 1933.
[10] *Veroff. Göttingen*, No. 55, 1937.
[11] *Pub. Ap. Obs. Potsdam*, No. 63, 1911.
[12] *A.N.*, **211**, 289, 1920.
[13] *Medd. Obs. Upsala*, **42**, 1929.
[14] *A.N.*, **150**, 193, 1899.
[15] *Hamburg. Abhandl.*, **2**, 3, 1920.
[16] *L.O.B.*, **10**, 110, 1921.
[17] *H.B.*, 764, 1922.
[18] *Hamburg. Mitt.*, **6**, 129, 1930.

* *L.O.B.*, **10**, 110, 1921.

† *A.N.*, **200**, 137, 1915.

The spectral types depend on two or three determinations for the brighter stars ($3^m.0$–$9^m.0$ pg.) and on one or two for the fainter stars ($9^m.0$–$14^m.0$ pg.). Photographic magnitudes are from three or four catalogues for the brighter stars and from one or two for the fainter ones. Two determinations of visual magnitude are available practically throughout the whole range. A main catalogue was prepared by combining the various observations in approximate accordance with their probable errors, these latter either being given explicitly by the authors or being derivable from the individual observations they publish for the various stars. This final catalogue contains 107 stars for which good spectral types, photographic magnitudes and visual magnitudes are available. There is a natural separation between the 43 brighter early-type stars (B5–A7, $3^m.0$–$9^m.0$) and the 64 fainter late-type members (F4–K1, $9^m.0$–$14^m.0$) which also divides the observations as regards order of accuracy. For any one star the separate values in the three parts of the catalogue differ from their weighted means by amounts which yield, on the average, the probable errors in the following table :—

	Bright Group	
		m m
Spectral type	± ·028 class =	± ·016 ± ·0026
Photographic magnitude		± ·020 ± ·0017
Visual magnitude		± ·029 ± ·0024

	Faint Group	
		m m
Spectral type	± ·173 class =	± ·053 ± ·0010
Photographic magnitude		± ·063 ± ·0031
Visual magnitude		± ·038 ± ·0029

where the probable error of a spectral class has been converted to its equivalent in colour index (magnitudes) by means of the appropriate part of the colour index-spectral type diagram. The probable errors of the magnitudes are very close to the values calculated by combining the probable errors published in the various catalogues. Combining the probable errors of the above table and comparing the total experimental error thus obtained with the observed probable error, deduced directly from the scatter of the plotted points on the colour index-spectral type diagram, we have

	Bright Group		Faint Group	
	m	m	m	m
Calculated	± ·039	± ·0023	± ·091	± ·0025
Observed	± ·080	± ·0090	± ·111	± ·0093
Residual	± ·070	± ·0104	± ·064	± ·0165

It is thus evident that the observed scatter exceeds that attributable to observational errors by an amount of the order of ± $0^m.07$; this is best shown in the bright group, where the observations are very good, but even the relative inaccuracy of the material in the fainter group cannot conceal the existence of a physical scatter there too. The precision of the dispersions is indicated by the probable errors attached to them. These were computed

in the usual way from the deviations of the separate probable errors from their mean.

The same effect is present in the other material. The following table collects the observed and calculated probable errors, together with the residual scatters, for all the material of Table I with the exception of the last three entries. These latter give a calculated scatter which is actually larger than the observed, indicating no residual scatter; the clusters are therefore omitted from the treatment in section 4. It is probable, however, that the error published by Wallenquist for his colour indices underestimates their precision in the central portion of the clusters, which is the part for which Zug's spectral types are available.

		Observed	Calculated	Residual
		m	m	m
Pleiades, bright		± ·080	± ·039	± ·070
faint		± ·111	± ·091	± ·064
20 Zug's Clusters		± ·124	± ·100	± ·073
N.G.C. 752	(*a*)	± ·059	± ·046	± ·038
	(*b*)	± ·106	± ·068	± ·082
Præsepe	(*a*)	± ·056	± ·037	± ·042
	(*b*)	± ·078	± ·059	± ·051
Hyades	(*a*)	± ·066	± ·059	± ·030
			Weighted mean	± ·068

We conclude that there is a physical scatter of about ± $0^m.07$ which evidently cannot be due to space reddening proportional to distance. Whether it is due to an absolute magnitude effect is investigated in the next section.

4. *Method of Treatment of Data—(a) Derivation of Correlation Coefficient.*—The ideal method of treating the data would be to separate the material in each cluster into the separate sub-types, and then to examine each sub-type for a relation between colour index and apparent magnitude (with these restrictions this is equivalent to searching for a relation between colour excess and absolute magnitude). None of the clusters of Table I, however, contains a sufficient number of stars to make this possible. It would, of course, be possible to combine together the various sub-types in any one cluster, but this procedure tacitly assumes an absolute magnitude effect which is independent of spectral type. The alternative is to treat the data sub-type by sub-type, combining together the material in the different clusters. Serious lack of homogeneity in the spectral classifications thus combined would raise doubts as to the legitimacy of this procedure, since the size of the absolute magnitude effect may depend on the system of classification used. However, direct comparisons between several systems have been made (see column 4 of Table I), and show that no systematic differences exist at any magnitude, though the accidental scatter of estimation is greater for faint than for bright stars. This method has therefore been adopted: though it is not ideal, combination of some sort is necessary in

order to attain statistical significance, and the first method outlined above introduces an assumption which is clearly and seriously wrong.

For any one sub-type, the mean apparent magnitudes in two clusters at different distances will, of course, be different owing to inverse-square dimming ; and the mean colour indices will differ owing to space reddening. If, however, we difference the separate values from the cluster means and deal subsequently with the resulting "magnitude excesses" and "colour excesses", these values will be automatically freed from these two effects. This method will be possible so long as any given sub-class is represented in a cluster by at least two stars ; otherwise we shall in fact be dealing with individual stars at different distances. This use of colour excesses and magnitude excesses instead of the original colour indices and apparent magnitudes in effect transfers the points representing the various cluster members on a colour index-apparent magnitude diagram to a common origin, without, of course, altering any relation which may exist between the co-ordinates, *i.e.* any absolute magnitude effect.

Grouping in this way in each sub-type the data for the various clusters, correlation coefficients were calculated for each group between colour excess and magnitude excess. If a correlation coefficient so found differs insignificantly from zero it will, of course, indicate that the colours of the stars in that particular sub-type do not depend upon their absolute magnitudes ; a positive correlation coefficient indicates that the most luminous stars are the bluest ; a negative coefficient means that the intrinsically bright stars tend to be red.

(*b*) *Derivation of Absolute Magnitude Effect.*—The size of the absolute magnitude effect (*i.e.* the amount of reddening per magnitude increase of luminosity) can be derived in two ways. Working directly from the original data, perhaps the most natural way is by a least-squares solution of equations of the form

$$\Delta C = c\Delta m,$$

where ΔC and Δm are respectively the colour excess and magnitude excess defined in 4 (*a*) above. The value of c for each sub-type can, however, be obtained directly from the correlation coefficient r already calculated, since the least-squares line is simply the regression line of colour index on absolute magnitude, whose slope is

$$c = r\frac{\sigma_2}{\sigma_1},$$

where σ_2 and σ_1 are respectively the standard deviations of ΔC and Δm. Values of c for each sub-type were calculated by the second method and checked by the first.

The choice of the regression line of colour index on absolute magnitude assumes that all the scatter of the observations is introduced by errors in the colour indices, the absolute magnitudes being assumed free from errors. These assumptions are not strictly true, but are nearly so, since the absolute magnitudes (in this case, the apparent magnitudes) will have a higher accuracy than the colour indices, which are differences of two

determinations of magnitude. In default of a better method, then, we are forced to adopt this.

5. *Results from Galactic Clusters.*—In Table II the second and third columns give the total range in colour index and photographic absolute magnitude for each sub-type. (Because of scarcity of material, certain neighbouring sub-types have been combined, an attempt being made to keep similar sub-types together and to keep the number of stars in a group not less than 20.) The fourth and fifth columns give the corresponding values of the coefficients of correlation and of the absolute magnitude effect, the latter being expressed in units of international colour index per magnitude increase of luminosity. The probable errors of r were computed from the usual formula p.e. $= \cdot 6745 \frac{1 - r^2}{\sqrt{n}}$, where n is the number of stars. The probable errors of c were obtained from the residuals from the formula $\Delta C = c\Delta m$.

TABLE II

Type	Range in C.I. (m)	Range in M. (M)	Correlation Coefficient	c	No. of Stars
O9–B2	0·59	2·99	+·16 ± ·12	+·030 ± ·024	28
B3	·35	1·57	+·14 ·13	+·029 ·030	24
B4	·36	2·98	−·31 ·14	−·058 ·032	20
B5	·81	2·46	+·03 ·12	+·008 ·030	30
B6, 7	·77	1·52	−·12 ·13	−·048 ·053	26
B8	·62	4·22	+·23 ·08	+·038 ·015	63
B9	·98	2·72	+·47 ·06	+·156 ·025	67
A0	·72	2·59	+·04 ·07	+·024 ·012	102
A1	·72	2·49	+·02 ·12	+·007 ·046	30
A2	·66	2·61	+·24 ·08	+·060 ·020	57
A3	·91	2·16	+·20 ·11	+·076 ·037	37
A4, 5	·93	2·49	+·31 ·09	+·069 ·019	51
A8, F0	·66	2·65	+·20 ·11	+·033 ·016	37
F2	·44	2·49	+·02 ·09	+·003 ·015	55
F5	·47	1·41	−·13 ·09	−·035 ·023	59
F6, 7, 8	·55	2·17	+·39 ·08	+·110 ·023	50
F9, G0, 1	·68	4·62	+·04 ·09	+·008 ·019	53
G2, 3	·58	1·60	+·29 ·11	+·087 ·035	31
G5	0·76	4·10	−·52 ·08	−·124 ·021	35
G8, K0	1·02	2·87	−·17 ± ·13	−·059 ± ·041	24

Amongst early B-type stars the correlation coefficients can hardly be given any statistical significance; they are not large compared with their probable errors and are, moreover, variable in sign. From about B8 to A5 the values become definitely positive and in most cases exceed their probable errors. By the time F-type stars are reached, the values have decreased

again, and amongst late G types a tendency to negative sign is apparent, though the number of stars of these types is not as great as in the earlier groups.

These general conclusions are confirmed by the actual coefficients c of the absolute magnitude effect given in the fifth column, the rise from negligible values amongst early B-type stars to a positive maximum near A3, and the gradual fall to negative values again amongst the late G types being clearly visible.

It is not possible at present to obtain from galactic clusters any information about the effect of absolute magnitude on the colours of stars of still later types (K and M), since the limiting apparent magnitude needed to observe such stars in clusters is too faint. In order to extend the investigation to later types, we must resort to other methods of attack, even though this involves a certain amount of uncertainty as to the results.

6. *Other Evidence—Late-type Stars.*—If we now no longer confine ourselves to groups of stars at the same distance (*i.e.* galactic clusters) we must use whatever data there are available for stars in different regions of the sky and trust to published parallaxes for obtaining absolute magnitudes. The greatly increased range of absolute magnitude (10 magnitudes for M stars) so introduced will, however, tend to compensate for the use of differing distances and the consequent uncertainty due to inexact parallaxes. The procedure used for the M stars was as follows. Of the Mt. Wilson list * of absolute magnitudes of 410 stars of type M, some 300 were selected either as being more than 20° away from the Milky Way or as being nearer than 50 parsecs ; these stars are presumably not seriously affected by space reddening. In effect, this process of selection retains the dwarfs in the list whilst rejecting giants affected by space reddening ; even so, two-thirds of the remaining stars are giants. For the purpose of the correlation, absolute magnitudes, spectral types and colour indices are required, of which only the first two can be taken directly from the list. The colour indices require visual and photographic magnitudes. For the giant stars, good visual magnitudes are available in the H.D. Catalogue, but for dwarfs, visual magnitudes are uncertain : the single-decimal magnitudes in the H.D. Catalogue (corrected B.D. and Co.D. values) are individually unsatisfactory for the derivation of colour indices. As regards the photographic magnitudes, no catalogue covers the whole sky as does the H.D. Catalogue with visual magnitudes. From 0° to 30° Dec.† and north of $57\frac{1}{2}°$ ‡, catalogues of good photographic magnitudes are available, but the magnitude limit of these lists is such that they usually cover only the giant M stars. The position is therefore this : that homogeneous photographic magnitudes for dwarf M stars are in general available only if they happen to have been observed in a Selected Area § ; and this fact reduces the number of M dwarfs usable for the correlation from about 100 to 12. The

* *M.W. Cont.*, 319, 1926.
† *Göttingen Aktinometrie*, 1910 ; *Yale Transactions*, **10**, 1934 ; *ibid.*, **9**, 1933.
‡ Harvard Mimeogram.
§ *Harvard Annals*, **101**, 1918.

incompleteness of photographic magnitude catalogues even reduces the number of giants from 200 to 105.

Collecting these 12 dwarfs and 105 giants into sub-types, correlation coefficients between colour index and absolute magnitude were calculated as before. These coefficients, together with the corresponding values of c, are given in Table III, in which the columns have the same significance as

TABLE III

Type	Range in		Correlation Coefficient	c	No. of Stars		
	C.I.	M.			Giant	Dwarf	Total
	m	M					
Mo	1·07	10·0	$-\cdot37 \pm \cdot12$	$-\cdot036 \pm \cdot014$	20	5	25
M1, 2	1·28	9·4	$-\cdot19 \pm \cdot10$	$-\cdot031 \pm \cdot019$	37	2	39
M3	1·07	10·4	$+\cdot12 \pm \cdot13$	$+\cdot018 \pm \cdot023$	24	2	26
M4, 5, 6	1·22	13·0	$-\cdot16 \pm \cdot13$	$-\cdot014 \pm \cdot012$	24	3	27

in Table II. The correlations are evidently small but show a distinct negative tendency; the values of c are probably significantly negative in at least the early M types.

Next an attempt was made on the K stars, where the smaller range of absolute magnitude, although it makes any correlation found somewhat less convincing, does at least provide a hope that homogeneous colour indices can be derived for the dwarfs. Further, the early results of Seares * suggest that there is a bigger difference of colour index between giants and dwarfs amongst K stars than amongst M stars, although a more recent publication from Harvard † does not commit itself on the point.

All the Ko stars in the Greenwich Astrographic Zone with proper motions greater than 5″ per century, and all brighter than 5·5 visual magnitude, are on the Greenwich parallax observing list, and up to the present 214 results have been obtained. This programme thus comprises all bright Ko giants between $+64°$ and the North Pole (this region is mostly clear of the Milky Way), and many dwarfs down to absolute magnitude $+7$. This latter limit corresponds to an apparent magnitude a little too faint for visual and photographic magnitudes to be always available, but satisfactory colour indices could be derived from Harvard visual and Greenwich photographic magnitudes ‡ for 136 stars in all, ranging in absolute magnitude from -2 to $+7$. Absolute magnitudes were obtained by using the Greenwich parallaxes corrected by the method described in *M.N.*, **86**, 687, 1926, the corrections being derived from a distribution curve utilising Ko stars alone. The correlation found between colour index and absolute magni-

* *M.W. Comm.*, No. 59, 1919.

† *H.A.*, 89, No. 6, 1935.

‡ *Photographic Magnitudes of Stars brighter than* $9^{m}\cdot0$, *Greenwich*, 1913–14.

tude was -0.25 ± 0.05 ; the corresponding value of c is $-0^{m}.030 \pm 0.007$ per magnitude. These values are probably significant. The value of c represents an upper limit to the size of the effect, since all the reddening has been attributed to it, whereas some may in fact be due to space reddening. The latter effect should not, however, be overestimated, since the range of distance in the Greenwich Ko stars is not large, only 10 of the 136 stars being more distant than 150 parsecs.

7. *Discussion of Results.*—The results from galactic clusters (O9–Ko, Table II) together with those for the late-type stars (Ko–M6, section 6) now make information available as to the size of the absolute magnitude effect over the whole range of spectral types. The final results are shown in Table IV, in which the grouping of spectral types is not entirely arbitrary,

TABLE IV

Type	c	No. of Stars
O9–B7	$-.005 \pm .012$	128
B8–Ao	$+.066$ $.026$	232
A1–A5	$+.057$ $.009$	175
A8–F8	$+.024$ $.021$	201
F9–Ko	$-.018$ $.029$	143
Ko	$-.030$ $.007$	136
Mo–M6	$-.017$ $.008$	117

but whilst preserving a rough equality in the number of stars per group, is in accordance with certain theoretical considerations discussed below. The values of c are means of the separate values in Tables II and III, weighted according to the number of stars in the sub-types ; the probable errors given measure the deviations of the separate values from the group means. Down to Ko the results refer, strictly speaking, to stars in galactic clusters, but until any reason can be shown why such stars are peculiar as regards dependence of colour on absolute magnitude, they may be taken as applying to the stars as a whole.

In discussing the results in Table IV it must be remembered that they have been derived throughout in terms of ordinary colour indices, viz. differences between photographic and visual (or photovisual) magnitudes. The distinction between these colour indices and gradients (which are more fundamental in the sense that they refer to the continuous background and are therefore unaffected by strong absorption lines) has been pointed out in a previous paper.* Certainly the size of the effect, and possibly even its existence, will depend on how the star colours are measured ; and we emphasise again that the results of Table IV refer only to colour indices.

In early B-type stars and for types beyond F the effect is small, not only as regards the probable errors, but also in an absolute sense. The difference of colour index between a giant and a dwarf Mo star of absolute magnitudes 0.0 and $+10.0$ respectively will be only a fifth of a magnitude. At the well-marked maximum between B8 and A5 the values are, however,

* R. d'E. Atkinson, A. Hunter and E. G. Martin, *M.N.*, **100**, 196, 1940.

much larger : two A2 stars differing in luminosity by four magnitudes will be a quarter of a magnitude different in colour index.

It is significant that a positive maximum occurs near A0, where, as is well known, the contribution of hydrogen line absorption to stellar spectra is a maximum. Colour indices measured in the ordinary way integrate wide wave-length ranges in the blue-violet and the yellow. Only the shorter wave-length region is much affected by hydrogen lines, however, so that all stars of types close to A0 will be made to appear redder by the blue-violet absorption than would be the case if integration were avoided. The least luminous stars, which show the strongest hydrogen absorption, will be most affected by this process and will appear the reddest. This corresponds to a positive coefficient for the absolute magnitude effect, as is indeed observed. This, then, explains the sign of c in stars showing strong hydrogen absorption. The fact that a maximum of c occurs near A0 can be explained by reference to Miss Williams's work * on the total absorption of the hydrogen lines in A stars. Examination of her Table I shows that the hydrogen absorption remains small and fairly constant amongst the most luminous A stars (it subsequently rises to a maximum at F5), but that it is much larger for the less luminous stars, and shows a sharp maximum for A0–A2 dwarfs. Accordingly, the difference of hydrogen absorption between giants and dwarfs in the blue-violet, which on the above view of the matter is what results in their difference of colour index, reaches a maximum in the early A types, as is in fact observed. The rise of intensity of the H and K lines towards later types will not produce a similar effect, since these lines are not sensitive to absolute magnitude.

In so far as the negative values of c in the later-type stars are real (only the result for K0 stars exceeds three times its probable error), the existence of an effect which makes giants redder than dwarfs is in harmony with ionisation theory. The low pressures in the atmospheres of giants will allow them to reach a given level of excitation, *i.e.* a given spectral type, at lower temperatures than dwarfs, so that giants will actually be expected to be cooler and therefore redder than dwarfs of the same sub-type. This corresponds to a negative absolute magnitude effect. That the effect is indeed due to differences of continuum intensities and not, as is suggested above for early-type stars, to line absorption is confirmed by the fact that in G-type stars a clear separation into giants and dwarfs can be made on the basis of the size of their spectrophotometric gradients.† Clearly the size of the absolute magnitude effect due to a real temperature difference will depend on how closely the criterion of spectral type is a pure temperature one : for instance, the separation of G-type stars into giants and dwarfs by the size of their gradients is much more pronounced on the basis of H.D. types than if M.W. types are used.‡ It should be remarked here that the K0 stars used in this investigation (see section 6) are H.D. types,

* *H.O.C.*, 348, 1929.
† *M.N.*, **100**, 189, 1940.
‡ *Observatory*, **63**, 38, 1940.

whereas the M stars are classified on the M.W. system. For this reason alone the numerical value of c in M-type stars will be expected to be smaller than that at Ko, so that not much significance can be attached to the minimum at Ko.

If the above explanation is correct, the need for caution in applying the results to all sorts of colour measurements is apparent. Stellar gradients, for instance, should be quite unaffected by the first process, but as sensitive as colour indices to the second; so that, on the basis of gradients, the positive maximum near A2 would be expected to disappear, though the negative values around type K should persist. Direct evidence on this point will presumably have to await gradient measures on cluster stars.

8. *Comparison with Previous Results.*—The early investigations of Sticker * on the subject of an absolute magnitude effect, using the colour indices of the *Göttingen Aktinometrie*, suggested that amongst B and A stars, the more luminous stars tend to be bluer than the faint ones, whereas F, G, K and M stars show a negative value of c, the maximum effect occurring in the K stars ($c = -0^m.06$ per magnitude). No account was, however, taken of interstellar absorption, and Raimond † finds that at least 70 per cent. of Sticker's stars are affected by absorption. Correction for this effect considerably reduces Sticker's estimates of the absolute magnitude effect, the value of c for the K stars becoming only $-0^m.04$ per magnitude.

Becker ‡ comes to much the same conclusion from an investigation of his own photoelectric colour indices for 738 stars. Here again, however, the stars are at different distances and interstellar absorption may invalidate the results.

E. T. R. Williams §, using 53 bright B-type stars at different distances, makes a solution allowing simultaneously for space absorption and for absolute magnitude effect. She concludes that the absolute magnitude effect is quite negligible for this spectral type, being only $+0^m.006 \pm 0.005$ in units of international colour index per magnitude increase of luminosity.

Dufay and Ssu-Pin Liau ||, in attempting to correlate Becker's colour indices with spectroscopic absolute magnitudes for the O6–B2 stars, obtain a correlation coefficient of $+0.16 \pm 0.09$ (p.e.) and conclude that no relation exists for stars of these types. In a later publication ¶ they allow for the effect of space absorption and obtain for the same stars a negligible correlation coefficient ($+0.04 \pm 0.09$).

Raimond ** investigates the colours of some 1200 stars of all spectral types, avoiding the effect of interstellar absorption by confining his selection to stars away from the galactic equator. He finds a small positive absolute magnitude effect in A, F, G and M stars, but an appreciable negative

* *Veroff. Bonn*, 23, 1930.
† *Gron. Pub.*, 46, 17, 1934.
‡ *Zs. f. Ap.*, 5, 101, 1932.
§ *Ap. J.*, 75, 393, 1932.
|| *C.R.*, 196, 1372, 1933.
¶ *Ann. d'Astrophysique*, 1, 230, 1938.
** *Gron. Pub.*, 46, 1934.

coefficient $c = 0^m.062 \pm 0.007$ for the K stars, when stars of absolute magnitude between $+1.5$ and $+2.5$ are excluded.

A recent paper from Greenwich * in describing the "dwarf reddening" in B8–A2 stars gives a diagram (fig. 2) from which a value of c for these stars may be obtained. This diagram connects the absolute magnitudes of 30 stars with the difference between their "reduced" colour indices and gradients, *i.e.* with the reddening due to hydrogen absorption in their spectra. This reddening is given as $+0.13$ on the gradient scale, or $0^m.08$ in international colour index, per magnitude increase of luminosity.

Thus the results of Sticker, using photographic colour indices, and Becker, using photoelectric colour indices, agree qualitatively with ours in spite of their different effective wave-lengths and their inclusion of interstellar absorption. Miss Williams's zero value for B-type stars is not surprising, since 90 per cent. of her stars are of types earlier than B8 (see Table IV); and the stars used by Dufay and Ssu-Pin Liau are of similarly early type. Raimond's results are in agreement as to the negative value in K stars, but though his figure is positive near A0, there is no sign of the sharp maximum there; on the other hand, the earlier Greenwich result near A0 is even a little larger than our present value.

Summary

The observed range of colour amongst stars of any one spectral type is sometimes attributed to differential absorption in space, sometimes to an effect of luminosity, *i.e.* to an absolute magnitude effect. The two causes can be separated if we eliminate the first by confining our attention to stars at the same distance and in the same direction in space, *e.g.* to stars in galactic clusters. A preliminary examination shows that the dispersion of colour in cluster stars of any one sub-type is of physical origin, since it is larger than can be explained by observational errors. It is possible, then, that colour may correlate with absolute magnitude. Using published colour indices and photographic magnitudes for 879 stars in 24 clusters, correlation coefficients were derived between colour index and absolute magnitude for 20 sub-types between O9 and K0. To extend the investigation to later spectral types (dwarf stars of these types not being observable in clusters), colours and absolute magnitudes of 253 individual K- and M-type stars suffering little space absorption were used; this process, though introducing some uncertainty as to the accuracy of the absolute magnitudes, permits the use of a large range in luminosity. The correlation coefficients found are small at all spectral types, but are probably significant at A (where they are positive) and possibly also at K (where they are negative). These results are confirmed by calculating, sub-type by sub-type, the amount of reddening per magnitude increase of luminosity. The paper suggests reasons why in early-type stars the larger colour indices should be associated with low luminosity, whilst at later types it is the giants which are relatively red.

* *M.N.*, **100**, 196, 1940.

SPACE REDDENING IN THE GALAXY

A. Hunter, Ph.D., and E. G. Martin

(Communicated by the Astronomer Royal)

1. In the last few years material has been accumulating, at Greenwich and elsewhere, on the colours of early-type stars. It is now certain that many of these stars are extremely red for their spectral types, though the cause of this reddening is still a matter of controversy. In the foregoing paper*, dealing with one side of this controversy, we have given reasons for believing that there is no effect of absolute magnitude on the gradients of early-type stars. In this paper we adopt the hypothesis that the reddening shown in the gradients of such stars is due to a widespread general space absorption. (The term "general space absorption" here and throughout the paper refers to *selective* absorption which is not localised in any particular region.) Close examination of the data suggests certain refinements of this simple hypothesis, and in a modified form the theory is shown to explain the facts reasonably well.

2. *Material Used.*—The values of the spectrophotometric gradients of early-type stars determined at Greenwich, when combined with reliable parallaxes, should provide material for the derivation of selective absorption coefficients. In attempting to analyse in galactic longitude, however, and dividing the Greenwich material into, say, 20° longitude groups, it is evident that the number of stars in each group is too small for much confidence to be placed in the separate results. There are, however, several collections of photoelectric measures of the colours of early-type stars which correlate sufficiently closely with gradient to be combined with the Greenwich values and thus to afford a larger catalogue. The following series were used to compile such a catalogue for this investigation :—

Greenwich Colour Temperatures (*M.N.*, **100**, 189, 1940)	146 stars.
Elvey (*Astrophys. J.*, **74**, 298, 1931)	114 ,,
Stebbins and Huffer (*Publ. Washburn Obs.*, **15**, 217, 1934)	273 ,,
Bottlinger (*Veröff. Berlin-Babelsberg*, **3**, 4, 1923)	143 ,,
Becker (*ibid.*, **10**, 3, 1933)	112 ,,

It might appear from the preponderance of photoelectric colour indices in the above material that this quantity and not gradient should be used as the basis of the investigation. Gradients have, however, been preferred as being measures of the continuous spectrum at specific wave-lengths, rather than integrations over wide ranges of wave-length, including absorption lines and bands whose effect varies with spectral type and with absolute magnitude.

* A. Hunter and E. G. Martin, *M.N.*, **100**, 656, 1940.

In order to convert the photoelectric colour indices into gradients, each series was plotted against the Greenwich values. In each case two divergent correlation curves were formed, abnormally red stars lying upon one and stars of normal colour upon the other. Examples of these curves have been given and their significance discussed in a previous paper *, where the divergence is attributed to the effect of absorption lines on colour indices. For the present purpose it is sufficient to remark that since the relation between photoelectric colour indices and gradients is in general double-valued, to any one catalogue value of a colour index there will correspond two possible gradient values. When the spectral type is taken into consideration, there is, however, rarely any doubt as to the right value to adopt. For instance, inspection of fig. 1 of the paper referred to will show that a star whose colour index according to Elvey is $-0^{m}.20$ may have a gradient of either $+0.90$ or of $+0.25$, according to whether it is a "reddened" early B-type star or a "normal" A2 star, *i.e.* according to whether its spectrum shows a small or large amount of hydrogen absorption. The value for an early B-type star of this colour index will therefore be converted quite unambiguously to gradient by using the correlation line for reddened stars. Towards the smallest values of colour index the two lines begin to coalesce : here, although there is naturally some doubt as to which line to use for any given star, the resulting difference of gradient is so small that the only effect of an error will be to increase slightly the scatter of the final gradients. There remain in the colour index catalogues a few late B stars and Ao stars which are appreciably reddened but do not show "*c*" characteristics in their spectra. No examples of such stars have been observed at Greenwich, and accordingly gradients are not available for deciding empirically where they lie on the various (*C*, *G*) diagrams. If they show normal amounts of hydrogen absorption they will presumably lie on short lines parallel to the "reddened" line branching from the "normal" curve at points corresponding to their spectral types ; if, on the other hand, they show small absorptions (*e.g.* if they are really super-giants whose "*c*" characteristics are obscured by rapid rotation) they will lie on the line containing the other reddened stars. There are, however, only nine such stars in the whole of the final catalogue, and their colour indices have been reduced to gradients as if they were in the latter category ; the fact that where intercomparisons between the various catalogues are possible the resulting gradients agree well, suggests that this procedure has involved no serious error. In any case, the final results will be negligibly affected if future observations show that the wrong procedure has been followed for these nine stars. We may thus say that having constructed correlation diagrams for stars for which both gradients and photoelectric colour indices have been measured, we can then use them to convert colour index into gradient where only the former has been directly observed. In this way the photoelectric colours of each series were converted into gradients.

A comparison of the computed gradients for each series with the

* R. d'E. Atkinson, A. Hunter and E. G. Martin, *M.N.*, **100**, 196, 1940, figs. 1, 3 and 4.

Greenwich values gave the following probable errors of the intercomparison in units of gradient :—

		Weight
Elvey	± ·053	9
Stebbins and Huffer	± ·066	6
Bottlinger	± ·081	4
Becker	± ·108	2

and the weights given are approximately proportional to the inverse squares of these probable errors.

In order to assess on this system the weight to be given to the gradients directly observed at Greenwich, the independent evidence of E. T. R. Williams * was used. This suggests that Greenwich should be weighted some three times as heavily as Bottlinger. Accordingly a weight of 12 was applied to the Greenwich results, and a weighted mean gradient computed for each star. The final weight for this mean can evidently vary, according to the number of catalogues in which the star appears, from 2 to 33. In order to avoid unnecessary complication, however, a summary method of weighting was adopted using weights 1, 2 and 3 respectively for groups whose true weights lie in the ranges 2–11, 12–21 and 22–33. The final catalogue contains gradients for 396 stars of H.D. type A0 or earlier, and provides sufficient material for analysis into longitude groups.

The mean probable error for a single entry deduced from the residuals of the separate values from their adopted weighted means is ± ·047. This figure agrees well with that obtained from the known probable errors of the separate catalogues, viz. ± ·048.

3. *Derivation of Gradient Excesses.*—Having obtained, as described in section 2, weighted mean gradients for 396 early-type stars, a gradient excess GE for each star was derived by subtracting from its gradient the value for the "normal" star of that spectral class. The normal gradients used are as follows :—

O6	−·21	B0	−·15	B5	−·07	A0	+·01
O7	−·20	B1	−·13	B6	−·05	A1	+·03
O8	−·18	B2	−·12	B7	−·04	A2	+·04
O9	−·17	B3	−·10	B8	−·02	A3	+·06
		B4	−·09	B9	−·01		

and were deduced by plotting the gradients of stars more than 15° from the galactic equator against their spectral types and reading smoothed values from the curve so obtained. The spectral types used for this purpose were generally those of the Victoria classification, but a few were from *Mt. Wilson Contr.*, 262, or *Ap. J.*, 64, 262, 1926. For the very few remaining stars the only type available was taken from the H.D. Catalogue. Galactic co-ordinates were taken from *Lund Annals*, vol. 3.

The scatter of the separate points from the smooth curve is represented by a probable error of ± ·059, the difference between this value and ± ·048, which takes into account only the probable error of the gradients themselves,

* *Harvard Circ.*, 348, 1929.

being due to errors of estimation of spectral type and to physical scatter in the gradients of any one sub-type. Each sub-type contains on the average 12 "normal" stars, so that the probable error of a mean normal gradient in the above table is $\pm \cdot 059/\sqrt{12} = \pm \cdot 017$. The gradient excess of a catalogue star is the difference between its gradient and the mean "normal" gradient appropriate to its spectral type. Its probable error will therefore be obtained by combining $\pm \cdot 059$ and $\pm \cdot 017$, giving $\pm \cdot 061$. This is the mean probable error of a single gradient excess for all the catalogue stars; the separate values are: for gradients of weight 1, $\pm \cdot 074$; weight 2, $\pm \cdot 049$; weight 3, $\pm \cdot 046$.

4. *Correlation of Gradient Excess with Distance.*—The stars were next divided into groups covering 20° of galactic longitude: 0°–19°, 20°–39°, etc. The group 200°–219° was extended to take in a few stars beyond, so that the group covers 200°–223°. Only 4 determinations of gradient were available between 223° and 310°, as this region is too far south for detailed investigation at any of the observatories concerned. This circumstance reduces the number of stars used from 396 to 392. The groups 300°–319°, 320°–339°, 340°–359° were not large enough to reduce separately and were combined to give one result for the region 310°–359°. Each group contains stars of all galactic latitudes from the galactic equator outwards, though most of the stars are naturally within ± 60° of the galactic equator.

There is no great range of apparent magnitude in the groups, and consequently it is difficult to decide whether the reddening should be attributed to selective absorption proportional to distance or to an absolute magnitude effect. The suggestion has been made in section 1 above that the latter effect is not likely to be of importance when gradients of early-type stars are considered. Fortunately it is possible to confirm this from the present data.

If there were no range of apparent magnitude whatever, the two causes could not be distinguished at all, since in this case absolute magnitude would correlate completely with distance. There does exist, however, a small range, and this fact can be used to confirm the hypothesis of space reddening. For this purpose, five of the longitude groups containing stars showing the heaviest gradient excesses were selected. For each group two correlation coefficients were derived; one (R_1) between gradient excess and distance, and the other (R_2) between gradient excess and absolute magnitude. Absolute magnitudes and distances were taken from Schlesinger's *Bright Star Catalogue*. The figures exhibited below show that in each group the correlation coefficient is numerically larger between gradient excess and distance than between gradient excess and absolute magnitude.

	R_1(GE, r)	R_2(GE, M)
° °		
60– 79	+·30	+·03
100–119	+·54	−·35
120–139	+·36	−·19
140–159	+·61	−·47
310–359	+·56	−·35

These results confirm our conclusion that the reddening is not due to an absolute magnitude effect: the correlation shown here between gradient excess and absolute magnitude is not to be regarded as physically significant, but as due to the combined effect of a real correlation of gradient excess with distance and a high correlation of distance with absolute magnitude.

5. *Distances Used.*—The material has therefore been treated as if all the reddening were due to differential absorption in space. For the derivation of accurate coefficients of selective absorption, reliable distances of the stars are needed. For stars of such early types, it must be admitted that good parallaxes are not yet available, and that published distances are often in serious disagreement. The values in the *Bright Star Catalogue* used (for a minor purpose) in section 4 above are from determinations of all kinds, trigonometric, spectroscopic and dynamic. Though the resulting figures no doubt represented the best values obtainable at the time (1930), they are probably not as homogeneous as could be desired. More recent values by the several methods are separately given in the 1935 Yale Catalogue. Trigonometric parallaxes, though presumably correct on the whole, are individually unreliable, as is shown by the frequency of occurrence of negative results. Spectroscopic distances involve apparent magnitudes, which for distant stars, and particularly for reddened ones, presumably need correcting for absorption. Nevertheless, the spectroscopic method does at least make estimates available for all the B- and early A-type stars of this investigation, which is more than can be said for any other method; so that, however sceptically we may regard the values, we are forced to use them. The main difficulty arises with the most distant stars: the distances corresponding to the smallest spectroscopic parallaxes quoted in the Yale Catalogue (0″·003, 0″·002, 0″·001) are 333, 500 and 1000 parsecs, and there the range ends. Obviously little confidence can be given to individual distances of this sort. It is just with these most distant stars of the very earliest types, however, that the method of deducing distances from interstellar line intensities finds its application. Plaskett and Pearce * remark that "the intensity of the interstellar lines may be considered as giving the most reliable known method of obtaining the individual distances and absolute magnitudes of the stars in which they appear. These stars are the most distant of any class observed, and, because of this distance and the relative failure of the spectroscopic or other methods in obtaining individual values, the intensity method is particularly useful." For types later than B5, however, these distances (hereinafter referred to as "K-line distances") are not available, since the interstellar absorption cannot generally be disentangled from calcium absorption in the stellar atmosphere. Again we are forced to fall back on spectroscopic distances, though fortunately these are probably more reliable here than for the very earliest types.

We have therefore proceeded as follows. Where K-line distances are available, they have been used; where they are not available, we have used spectroscopic distances. The resulting solutions have been kept distinct

* *Publ. D.A.O.*, 5, 201, 1933.

from one another, since although the two groups of distance may be on a homogeneous basis amongst themselves, the two scales are not in agreement (see section 10). Of the 392 stars of the main catalogue, 84 appear in the D.A.O. list of K-line intensities. For these stars the distances used were computed from the relation

$$r = 259(I - 1{\cdot}51),$$

where I is the published K-line intensity and r is the distance in parsecs.

The spectroscopic distances for the remaining 308 stars will be affected by absorption, since they are obtained from estimated absolute magnitudes by the use of apparent magnitudes which are too faint. The values of m in the ordinary relation

$$M - m = 5 - 5 \log r$$

will be too large, leading to an overestimate of r. An idea of this overestimate can be obtained from the size of the gradient excess of the stars considered. It now seems well established * that the selective absorption in magnitudes varies with the wave-length according to the law

$$A_\lambda = \frac{A_1}{\lambda}. \qquad (A_1 = \text{constant for a given star.})$$

Let us assume that all the absorption is selective and obeys this law. Let the true monochromatic magnitudes of a star at the wave-lengths λ_r, λ_b at which Greenwich gradients are measured be m_r, m_b. The corresponding values observed in the presence of selective absorption will be $m_r + A_1/\lambda_r$, $m_b + A_1/\lambda_b$. The change of gradient produced by the selective absorption will be, by definition of gradient,

$$0{\cdot}921 \frac{\Delta m_r - \Delta m_b}{1/\lambda_r - 1/\lambda_b},$$

whence

$$\mathrm{GE} = 0{\cdot}921 A_1.$$

Thus the absorption in magnitudes at say $\cdot 545\ \mu$ (visual magnitudes) is

$$\begin{aligned} A_{\cdot 545} = A_1/{\cdot}545 &= \mathrm{GE}/(0{\cdot}921 \times {\cdot}545) \\ &= 2{\cdot}00\mathrm{GE}. \end{aligned}$$

Allowing for this absorption, the equation for deducing the distances from spectroscopic absolute magnitudes becomes

$$M - m + 2\mathrm{GE} = 5 - 5 \log r,$$

and the distances used for the 308 stars mentioned above were obtained from this equation, using the spectroscopic parallaxes of the 1935 Yale Catalogue.

6. *Correction for Galactic Latitude.*—Before proceeding to the calculation of selective absorption coefficients, we must make some assumption as to the distribution of the reddening material about the galactic plane. This assumption must, at the present state of our knowledge, be almost purely

* Stebbins, Huffer and Whitford, *Ap. J.*, 90, 212, 1939.

arbitrary. We know, however, by analogy with external galaxies, that the density of the absorbing material increases rapidly towards the galactic plane, more rapidly than does the star-density. An exponential distribution law of the form assumed by Williams * (this is similar to the empirical law found for the falling-off of star-density by Oort †) was adopted :

$$\rho = \rho_0 e^{-2|z|/T},$$

where ρ is the density at a distance z parsecs from the galactic plane, ρ_0 is the density in that plane, and T is the thickness of a uniform layer of density ρ_0 which would produce the same reddening as the assumed layer, for light traversing it from pole to pole. Van de Kamp's determination $T = 210$ parsecs was adopted, though, as mentioned below (section 8), a subsequent solution was tried, for a few groups, using a larger value.

We define the effective reddening path of light from a star of galactic longitude l as the distance at which the star would have to be placed in the galactic plane at longitude l so that its light should suffer the amount of reddening it is actually observed to suffer. This effective path for a star of galactic latitude b at a distance r from the Sun will obviously be less than r because of the decrease of density of the reddening material away from the galactic plane. Any relation between gradient excess and distance should evidently employ these effective paths P reduced to the galactic plane, instead of geometrical distances r; the coefficients of selective absorption then obtained from the relation will refer to absorption in the galactic plane. The effective path P will be

$$P = \int_0^r e^{-2|z|/T} dr = \int_0^r e^{-(2r \sin |b|)/210} dr = \frac{105}{\sin |b|}(1 - e^{-(r \sin |b|)/105}).$$

For a star in the galactic plane, $P = r$; for a distant star in the direction of the galactic pole, $P = 105$ parsecs. Using this formula, the effective path P was computed for each star from its galactic latitude and the value of r obtained as described in section 5.

7. *Derivation of Selective Absorption Coefficients.*—Having thus obtained gradient excesses GE (section 3) and effective distances P (section 6) for each of the 392 stars in the main catalogue, equations of the form

$$\mathrm{GE} = \beta P$$

were used to derive values of the selective absorption coefficient β in the galactic plane. Each star will give a value of β for its own particular galactic longitude, and the values weighted as described below ‡ were combined into the groups of section 4. The material for the 308 stars for which spectroscopic distances were used was reduced separately from that for the 84 K-line stars.

The separate values of β in any one longitude group will not be of equal weight, since errors in the gradient excesses and the effective distances will

* *Ap. J.*, 79, 404, 1934.
† *B.A.N.*, 6, 249, 1932.
‡ We are indebted to the Astronomer Royal for the method of weighting.

affect each star differently. Let ϵ_{GE}, ϵ_P and ϵ_β respectively be the probable errors of the observational quantities GE, P, and of their ratio β. Then

$$\epsilon_\beta^2 = \left(\frac{\partial\beta}{\partial \mathrm{GE}}\right)^2 \epsilon_{GE}^2 + \left(\frac{\partial\beta}{\partial P}\right)\epsilon_P^2$$

$$= \frac{1}{P^2}\epsilon_{GE}^2 + \frac{\mathrm{GE}^2}{P^4}\epsilon_P^2$$

$$= \frac{\epsilon_{GE}^2}{P^2} + \beta^2\frac{\epsilon_P^2}{P^2}.$$

The value of this quantity depends on whether the distances used are K-line distances or spectroscopic. For interstellar distances the quantity ϵ_P/P is a constant, since the probable error of a K-line distance is closely proportional to the distance itself. The dispersion in estimated distance, due to accidental errors in measuring the K-line intensity and to irregularity in the distribution of the absorbing calcium ions, has been shown * to be 0·16 times the distance. This corresponds to $\epsilon_P/P = \frac{1}{9}$ nearly. Adopting this value, we obtain

$$\epsilon_\beta^2 = \epsilon_{GE}^2/P^2 + \beta^2/81,$$

and the weight of β (the reciprocal of this quantity) was computed for each equation by substituting the appropriate values of ϵ_{GE} (·074, ·049, or ·046 according to the strength of the gradient determination—see section 3), of P (the K-line distance computed as in sections 5, 6), and of β (the weighted mean absorption coefficient for the group). Since the weights need to be known before this last quantity can be ascertained, a series of successive approximations is necessary. First, a straight mean for β was used to calculate approximate weights; a provisional weighted mean based on these weights was then used to adjust the weights slightly; and so on until the last adjustment of the weights produced no alteration in β. Usually three such approximations were needed. This process gives a final weighted mean β in each longitude group.

For spectroscopic distances the quantity ϵ_P/P is again a constant, since the probable error of a spectroscopic parallax is proportional to the parallax itself. The constant of proportionality is usually taken as 20 per cent. (this corresponds to a probable error of $0^m.4$ in the estimate of absolute magnitude), but this refers to stars of much later types than B. In fact it may be doubted whether the probable error of the spectroscopic absolute magnitude of a B-type star is much better than $0^m.6$, which corresponds to about 33 per cent. In any case, the final weighted means are not at all sensitive to the exact value assumed for ϵ_P/P, so adopting $\epsilon_P/P = \frac{1}{3}$ we obtain

$$\epsilon_\beta^2 = \epsilon_{GE}^2/P^2 + \beta^2/9.$$

The weight of β is the reciprocal of this and was computed as before for each equation and the weighted group mean derived.

* Plaskett and Pearce, *D.A.O.*, 5, p. 206 ff.

In both cases the weight of β depends mostly on the first term ; the second term is constant for all stars in a group, but is small because β is small. The numerator of the first term depends on the weight of the gradient determination and does not vary from star to star by a factor of more than three. Roughly speaking, then, the weight of β will be proportional to P^2. However, at large distances the weight does not increase as rapidly as P^2, because of the effect of the second term.

8. *Results.*—The results of the investigation are given in Tables I and II. Column 3 of Table I gives the values of β obtained from the 84 stars for which K-line distances were used. For some longitudes the material was so scanty that neighbouring groups were combined. The results from the stars with spectroscopic distances are given in column 3 of Table II. Here, with a total of 308 stars, no further combination of the groups was necessary. The probable errors of β were obtained from the differences between the separate values of β in any group and the group mean. On the evidence of these probable errors, the differences between the values of β for the various longitudes are more than would be expected from mere accidental deviations from a constant value. We are therefore led to suspect a real variation with longitude, a deduction which is confirmed by the similarity of the coefficients in the two tables.

TABLE I

K-line Distances

Long.	First solution, before rejection		Second solution, after rejection	
	No. of stars	β per kps.	No. of stars	β per kps.
°–°				
0–19, 20–39	8	+0·58 ± 0·21	7	+0·24 ± 0·09
40–59	11	+0·61 ± 0·11	10	+0·43 ± 0·06
60–79	20	+0·67 ± 0·11	18	+0·43 ± 0·06
80–99, 100–119, 120–139	13	+0·59 ± 0·09	12	+0·53 ± 0·08
140–159	8	+0·62 ± 0·08	8	+0·62 ± 0·08
160–179, 180–199, 200–223	18	+0·05 ± 0·06	17	−0·05 ± 0·04
310–359	6	+1·30 ± 0·28	6	+1·30 ± 0·28

From the existence of large gradient excesses in certain stars (neither on the galactic equator nor particularly distant) it was recognised, before the solutions were attempted, that a relation assuming proportionality between effective distance and gradient excess could not entirely satisfy this abnormal reddening. This is shown graphically for a typical longitude group, viz.

TABLE II

Spectroscopic Distances

Long.	First solution, before rejection		Second solution, after rejection	
	No. of stars	β per kps.	No. of stars	β per kps.
° °				
0–19	14	+0·40 ± 0·16	14	+0·40 ± 0·16
20–39	37	0·00 ± 0·12	34	−0·26 ± 0·08
40–59	27	+0·45 ± 0·12	26	+0·38 ± 0·09
60–79	26	+0·31 ± 0·45	25	−0·01 ± 0·09
80–99	29	+0·42 ± 0·22	26	+0·22 ± 0·09
100–119	28	+1·48 ± 0·46	25	+0·54 ± 0·17
120–139	34	+0·77 ± 0·27	31	+0·26 ± 0·16
140–159	22	+1·23 ± 0·36	21	+0·71 ± 0·18
160–179	37	−0·27 ± 0·09	36	−0·42 ± 0·03
180–199	22	+0·10 ± 0·11	22	+0·10 ± 0·11
200–223	9	−0·11 ± 0·11	9	−0·11 ± 0·11
310–359	23	+1·72 ± 0·38	21	+1·35 ± 0·26

80°–99°, in fig. 1 (p. 680), where gradient excesses for the 29 stars concerned are plotted against their effective spectroscopic distances. The dotted line represents the weighted mean for the group ; its slope has obviously been greatly affected by the three large excesses towards the top of the diagram. The weighted residuals (*i.e.* residual × $\sqrt{\text{weight}}$) of the values of β for these stars from the group mean are in fact 10, 11 and 13 times their internal probable errors. Such large residuals occur far more frequently than they should in practically all groups. There is no reason to doubt the probable errors of the gradient excesses ; those of the distances (and particularly of the K-line distances) are not so certain, but they are not likely to be so far in error as to produce these large residuals as often as they do occur. The question therefore arises as to how far the separate values of β are measures of the same physical quantity, *i.e.* how far is the taking of a mean justified over extensive regions of the sky? An idea of the answer to this question can be obtained from the size of the negative residuals which occur. Taking first the 308 stars with spectroscopic distances, the negative weighted residuals fit the average internal probable error better than do the positive ones : the largest is less than 6 times its probable error, whereas there are 18 values of β with positive residuals larger than this. A residual of this size occurs in a Gaussian distribution once in about 7000 times ; it has actually occurred on the negative side once in 300 times, but on the positive side once in 17 times. Amongst the stars with K-line distances, the largest negative residual is nearly 9 times its probable error, whereas there are 6 positive residuals (1 in 14) exceeding this limit. It is thus the large positive

residuals which are most troublesome ; the negative ones can reasonably be explained as accidental if the distances (especially the K-line distances) are not so accurate as they are claimed to be. The implication is evidently that a few stars are reddened not by general space absorption only, but also by a very local absorption, or by some intrinsic effect. On this view of the matter the solutions in column 3 of Tables I and II have exaggerated the value of β by including a few stars which are not reddened by general space absorption alone. If in fact two causes (general space absorption and this other local effect) are operating to produce the observed reddening, we must now adopt a criterion which will distinguish between the two, and then exclude the abnormally reddened stars and re-solve the equations. Any rejection criterion is bound to be more or less arbitrary, and there will always be border-line cases where discrimination between what should and what should not be excluded is difficult. But a legitimate view of the matter seems to be this : negative residuals, which are presumably in the nature of accidental errors, occur, when spectroscopic distances are used, with values up to 6 times the internal probable error, and when K-line distances are used, up to 9 times. It is reasonable to suppose that positive residuals of these sizes could also arise from observational errors. If, then, we reject any value of β which diverges from its group-mean by more than 6 (or 9, respectively) times its probable error, the remaining values should be, if not completely homogeneous, at least much more nearly so than when no rejections are made.

The fifth columns of Tables I and II give the weighted mean values of β after this method of rejection has been applied ; the value for 80°–99° is represented in fig. 1 by the full line. The difference between the numbers in columns 2 and 4 gives in each case the number of stars rejected from the initial solutions.

The results in Tables I and II are based on an effective thickness $T = 210$ parsecs for the absorbing layer. It will be of interest to see how they are affected when a different thickness is assumed. For this purpose the value $T = 310$ parsecs suggested by Williams * was tried for the regions 80°–99° and 100°–119° using spectroscopic distances. The values of β for this distribution become respectively $+0.23 \pm 0.09$ and $+0.51 \pm 0.16$, as compared with $+0.22$ and $+0.54$ in Table II. The coefficient of space reddening is thus not particularly sensitive to the value assumed for T, and the matter was carried no further.

The results also tacitly assume that the Sun is in the plane of symmetry of the reddening material. It is possible, of course, that this is not so, but there appears to be no information yet available on this point. Hertzsprung†, using 68 Cepheid variables, has found that the Sun is 40 parsecs north of the galactic plane. More recently, Seares ‡ has found a figure of 40–50 parsecs as the Sun's distance from the plane of the local cluster, and one of 0 ± 8 parsecs from the plane of systems of stars brighter than the 16th and 18th apparent magnitude. There seems no reason for identifying

* *Ap. J.*, 75, 393, 1932. Note added in proof.

† *A.N.*, 196, 207, 1913. ‡ *Ap. J.*, 67, 124, 1927.

the plane of the absorbing material with one rather than the other of these systems, but as a trial solutions were carried through for the regions 80°–99° and 100°–119°, assuming the Sun to be 40 parsecs north of the plane of the reddening material. The results for the two groups are:

$$\beta = +0{\cdot}27 \pm 0{\cdot}10 \qquad 80°–99°$$
$$\beta = +0{\cdot}64 \pm 0{\cdot}20 \qquad 100°–119°.$$

These values differ so little from the original values that it was not considered worth while to pursue the matter further, particularly as the position

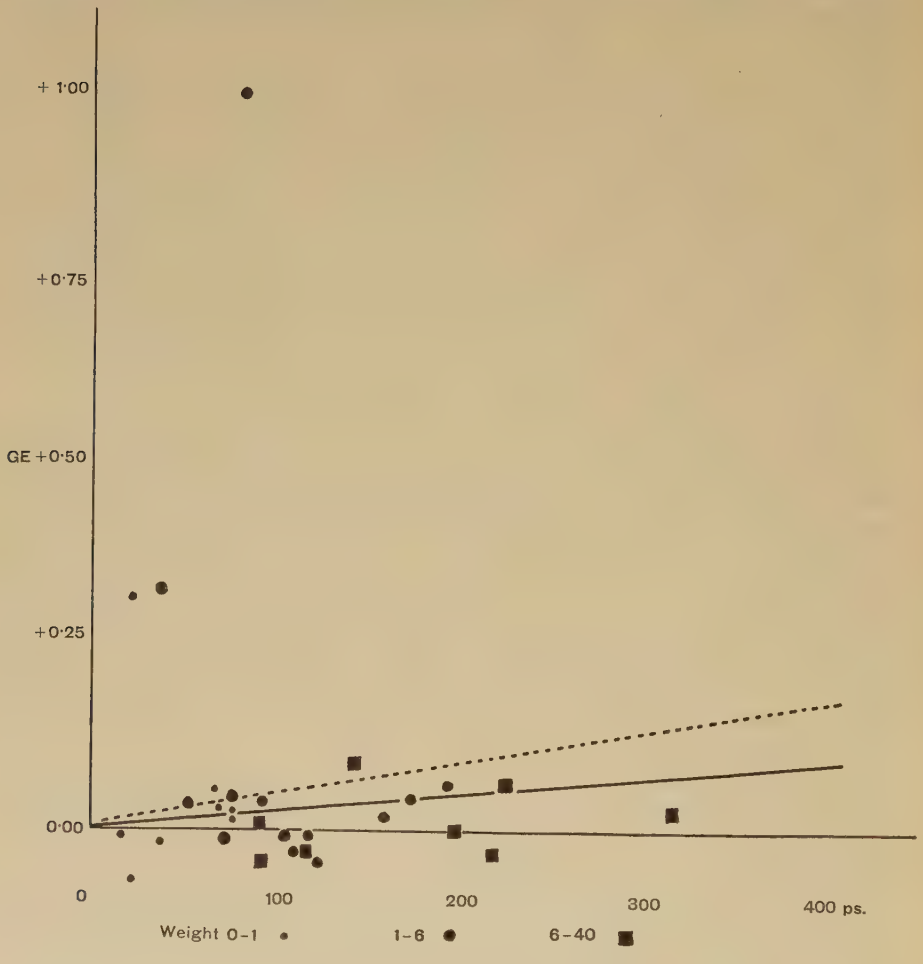

Fig. 1.

of the Sun with respect to the plane of the reddening material is at present so uncertain.

9. *Discussion of Results.*—The histograms of fig. 2 show how the reddening coefficients vary with galactic longitude. For comparison with our values, fig. 2 (*a*) gives the results of Stebbins and Huffer*, who

* *Publ. Washburn Obs.*, 15, 217, 1934.

determined β on the assumption that all their observed reddening is space reddening. Their results, which are based on spectroscopic distances corrected for absorption, should therefore be comparable with those in

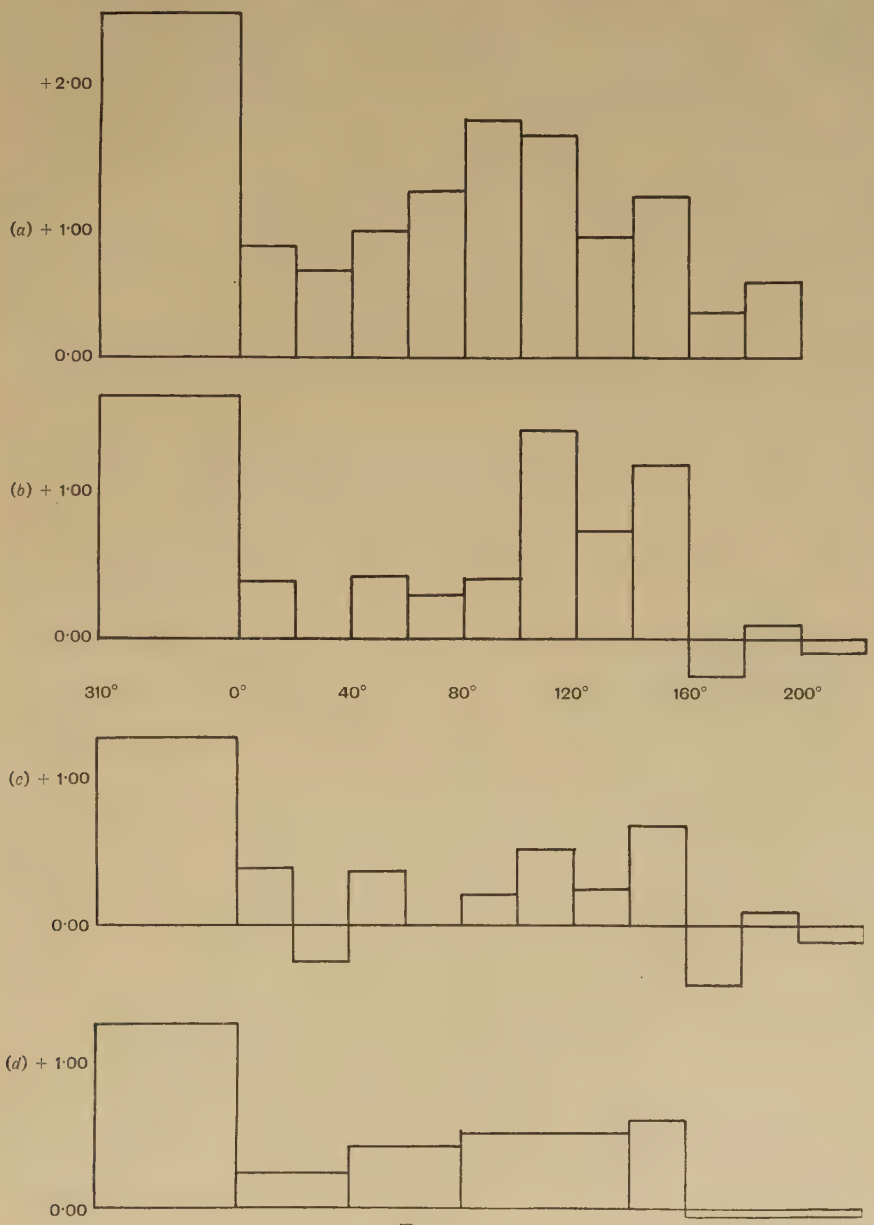

FIG. 2.

Table II, column 3, except that they were working in terms of a photo-electric colour index which is numerically 3·6 times smaller than a gradient. The ordinates of fig. 2 (*a*) therefore give the values of β quoted by Stebbins and Huffer multiplied by 3·6. Fig. 2 (*b*) gives the values of Table II,

column 3. There is a general agreement in the run of the coefficients with longitude, but the actual figures are considerably higher for Stebbins and Huffer. This is at first sight surprising, since they included in their solution all stars within 5° of the galactic plane, without attempting a latitude correction. The method in section 6 of the present paper reduces the geometrical distances of such stars to smaller "effective distances" in the galactic plane, and would therefore, if applied, still further increase the Washburn values of β. The discrepancy no doubt lies in the method of weighting. Stebbins and Huffer give equal weights to all values of β in obtaining their group means. Our method of weighting (section 7) gives small weights to stars with large values of β, since these values are so sensitive to errors of distance and of gradient excess ; it therefore results in smaller group means. If unweighted group means are computed for our material, the values of β are much increased and do in fact become comparable with those of Stebbins and Huffer. There is thus no inexplicable difference between figs. 2 (*a*) and 2 (*b*).

The high value of β near 350°, stated by Stebbins and Huffer to be a weak determination, is confirmed by the present value. It is perhaps significant that this direction is that of the centre of the galaxy.

Figs. 2 (*c*) and 2 (*d*) give the values of β from spectroscopic and K-line distances respectively after the exclusion of abnormally reddened stars according to the criteria of section 8. The diagrams appear to show a general agreement, as to order of magnitude and variation with longitude, which is discussed further in section 10.

10. *Abnormally Reddened Stars.*—Tables I and II each contains two series of results which are not in agreement : one with and one without rejection of heavily reddened stars. If the hypothesis of local reddening advanced in section 8 is not accepted, the two solutions can be reconciled in only one way, viz. by assuming that the parallaxes of the reddened stars are systematically too great. (The possibility that the other co-ordinate, gradient excess, is seriously in error, is quite out of the question.) If in fig. 1, for example, the reddened stars at the top of the diagram were really much farther away, they could, of course, be put on to the mean line. The size of the correction needed, however, gives reason for doubting whether such an explanation can possibly be correct : we must on the average increase the distances of the stars excluded from the spectroscopic second solution by a factor of 37 before they will fit the solution. This involves brightening their absolute magnitudes by nearly 8^m. Such drastic changes in the absolute magnitude scale are so unlikely that we must examine whether it is not possible to obtain external evidence confirming our assumption that these stars are abnormally reddened rather than systematically farther away than we thought.

Table III is a list of the 24 stars rejected from the second solutions in Tables I and II. The fifth column gives the gradient excess of each star, the sixth its distance r used in computing the effective path by the formula of section 6, the seventh and eighth the values of the reddening coefficients per kiloparsec for the star and for the longitude group in which it falls. The

TABLE III

Name or B.S. No.	Spectral Type	l	b	GE	r	β for Star	β for Group	Suggested Sources of Reddening
		°	°		ps			
γ Cass	B0*nne*	91	− 2	+ ·32	22	1·60	+0·22	XVI *e*
53 Cass	B8*s*	98	+ 2	·98	83	12·25	0·22	*c*
5 Pers	B8*s*	101	− 4	·74	125	6·17	0·54	*c*
ϕ Pers	B0*ne*	99	−11	·34	38	9·71	0·22	*e*
1035	*c*B8	109	+ 4	1·01	100	10·63	0·54	*c*
o Pers	B2*k*	128	−17	+ ·47	340	2·14	+0·53	VIII
1148	A0*s*	104	+14	·99	22	49·50	0·54	
ζ Pers	B1*s*	130	−16	·55	83	7·86	0·26	VIII *c*
48 Pers	B3*e*	121	− 2	·26	62	4·33	0·26	*e*
χ Auri	B3*ss*	144	+ 1	·92	111	8·36	0·71	*c*
θ' Orio	O7*k*	176	−19	+1·31	180	9·36	−0·05	
o Auri	A0*ns*	129	+12	·77	36	24·06	+0·26	
13 Mono	*c*B9	172	+ 1	·26	167	1·60	−0·42	*c*
χ Ophi	B3*em*	326	+20	·94	67	17·10	+1·35	XIV *e*
β Lyra	B8 + B2	30	+14	·28	250	1·47	−0·26	*e c*
20 Aqil	B3*n*	355	− 9	+ ·62	111	6·20	+1·35	
2 Vulp	B0*nn*	24	+ 4	·48	200	2·57	−0·26	
7678	B0*ssk*	37	− 1	1·40	1760	1·92	+0·24	XX *e c*
29 Cygn	A0*n*	42	0	·35	67	5·22	+0·38	
55 Cygn	B2*sk*	54	+ 1	1·09	720	1·60	+0·43	XV *e c*
9 Ceph	B2*sk*	70	+ 7	+ ·81	910	1·48	+0·43	XX *c*
13 Ceph	B8*s*	68	+ 1	1·81	63	30·16	−0·01	IV
30 Pegs	B7	36	−42	·64	111	8·53	−0·26	
26 Ceph	B1*k*	76	+ 5	·87	1420	2·56	+0·43	IV

TABLE IIIA

κ Cass	B0*k*	88	0	+ ·61	200	0·64	+0·22	*e c*
6946	B3*k*	348	− 1	1·02	125	2·08	+1·35	XIX
9 Sgte	O7*fk*	24	− 5	·56	333	0·57	−0·26	
P Cygn	B1*qk*	43	+ 1	1·15	71	0·66	+0·38	*e*
8119	O9*sk*	66	+ 7	·57	333	0·86	−0·01	IV
8243	B1*sk*	68	+ 6	+ ·59	200	0·88	−0·01	
8327	O9*sk*	70	+ 6	·99	27	1·65	−0·01	
14 Ceph	O9*nk*	69	+ 1	·50	167	0·32	−0·01	IV
19 Ceph	O9*k*	66	− 3	·41	250	0·37	−0·01	IV
λ Ceph	O6*nfk*	71	+ 2	·72	167	0·51	−0·01	
9052	B0*k*	83	− 6	+ ·65	250	1·14	+0·22	XX

average residual in β, obtained from the difference between columns 7 and 8, is ·935, whereas for the 368 stars incorporated in the final solutions, the average (taken without regard to sign) is ·097. We are, therefore, in the position that the hypothesis of general space reddening explains, with satisfactorily small probable errors, any reddening shown by 94 per cent. of the stars, but for the remaining 6 per cent. the residuals are 10 times greater than for the rest. Moreover, since these residuals cannot be explained as due to errors of distance, we must attribute them to abnormal reddening, perhaps due to local obscuration, either in the immediate neighbourhood of the stars concerned, or in the line of sight; or to some intrinsic property of the stars. Absorption by an extended chromosphere, for instance, might well produce reddening, and it has been suggested that this may occur in stars whose spectra exhibit "*c*" characteristics * or a tendency to show emission lines.†

Dealing first with the question of obscuration, Table IV contains references to known absorbing clouds or nebulæ which appear close in the sky to any of the stars in Table III. The non-selective and selective absorptions are given in columns 6 and 7 respectively; the latter are in units of international colour index, but may be approximately converted to gradient form by multiplying by 1·6. It is not sufficient for this explanation, of course, that a star should be in the same direction as a cloud; it must also be within or behind the cloud. Reliable distances are not always available for the clouds, but in some cases there seems definite evidence that absorbing matter is interposed between us and one of the abnormally red stars. In these cases, cross-references to the serial numbers in column 1 of Table IV are given in the last column of Table III, and it will be noticed that with 9 of the 24 stars are associated known regions of obscuration.

Thus over one-third of the reddened stars appear to be within or beyond known obscuring clouds. It must be remembered, however, as Hubble has pointed out, that obscuration is not necessarily accompanied by selective absorption. In any case, the reality of the explanation must be controlled by finding the proportion of all the stars, reddened or unreddened, which can be similarly associated with known nebulosity. For this purpose, the whole of the stars in the working catalogue were compared, with regard to position and distance, with a table showing all known obscuring regions, exactly as the reddened stars of Table III were examined with the aid of Table IV. Of the 392 stars, 48 appear to be associated with nebulosity, *i.e.* 12 per cent. as compared with 38 per cent. of reddened stars. Thus although the association of the reddened stars with regions of nebulosity is somewhat rough and ready, an equally rough method of control applied to all the stars of the catalogue yields a percentage of significant associations which is three times smaller. The reality of the effect seems therefore to be undoubted; but its magnitude can be only partially assessed, as information is meagre as to the selective absorption in the separate clouds (see column 7, Table IV). Remembering, however, that the absorptions

* Payne, *Stars of High Luminosity*, p. 120.

† Greaves and Martin, *M.N.*, 98, 438, 1938.

shown must be increased by a factor of 1·6 to bring them to units of gradient, it can be said, at any rate of the Perseus and Cygnus clouds, that they will explain a large proportion of the residual reddening.

TABLE IV

No.	Long.	Lat.	Region	Distance, ps.	Absorption		Area (sq. deg.)	References
					Non-selective	Selective		
					m	m		
I	24°	−1°	Cygn	500	3·0	...	...	Miller.
II	38–44	+1 to −8	Cygn	150–700	0·4–2·0	...	25	Balanowskaja.
III	43	0 to −5	Cygn	800	1·5	0·44	...	Schalén.
IV	70	0	Ceph	210	0·3	0·06	39	Schalén, Struve.
				450	0·6	0·15		
				800	1·5			
V	77	+18	...	500	1·5	...	4	Slocum, Sitterly.
VI	90	+30	Pole	200	0·5	...	4	Shapley.
VII	129	−13	ξ Pers	260–480	2·1	0·90	...	Greenstein, Balanowskaja.
				1100	1·5–2·0			
VIII	129	−17	o Pers	120	2·0	...	...	Greenstein, Shajn.
IX	135	−5	Auri	125	1·8 / 1·1	0·44	20	Schalén. Greenstein.
X	138	−14	Taur	140	1·1	...	large	Greenstein.
XI	170	+3	S Mono	410–575	2·1	...	...	Andrews.
XII	175	−20	Orio	300–400	1·5–2·0	...	...	Asklöf, Bok.
XIII	234	0	Vela	600	2·0	...	100	Greenstein, Bok.
XIV	320–0	0 to +40	Ophi	100–150	0·9	...	1000	Greenstein.
XV	54	0	55 Cygn	...	...	...	...	N.G.C. 6989, 6991
XVI	91	−1	γ Cass	...	...	...	...	I.C. 59, 63.
XVII	129	−11	ξ Pers	...	...	...	1	N.G.C. 1499.
XVIII	177	−18	θ Orio	...	...	...	...	N.G.C. 1976.
XIX	348	−1	B.S. 6946	...	...	...	...	I.C. 1287.
XX	In *Ap. J.*, 87, 159, 1938, Greenstein lists 38 B-stars immediately surrounded by obvious obscuring clouds.							

Turning now to the other possibilities: the reddened stars are labelled "*e*" or "*c*" in the last column of Table III, where so indicated on the one hand by Merrill and Burwell's catalogue of bright-line stars (*Ap. J.*, **78**, 87, 1933), or on the other by Merrill's catalogue of supergiants (*Ap. J.*, **81**, 351, 1935) or by Miss Payne's book (*Stars of High Luminosity*, Appendix A, 1930). Reference to Table III shows that 7 of the 24 abnormally red stars are classified as having bright-line spectra, *i.e.* 29 per cent. as compared with 12 per cent. of the 392 stars in the final catalogue. Of the 24 stars, 10 show "*c*" characteristics, *i.e.* 42 per cent. as compared with 7 per cent. of the catalogue stars. This might at first sight be attributed to an effect of

absolute magnitude, but a plot for all the "*c*" stars of the catalogue shows no correlation between absolute magnitude and reddening. On the other hand, such intrinsically bright stars will on the average be at a greater distance than the others, and will therefore be more likely to be affected by local obscuration. A similar line of reasoning applies to the bright-line stars, which, as Gerasimovič * has shown, are more luminous than absorption-line stars.

The stars of Table III are those excluded from the solutions because no distances which can reasonably be assigned to them will make their reddenings fit the mean β for their longitude groups. Examination of the catalogue shows that many of the most heavily reddened stars are not in Table III ; they are not excluded because they are assigned K-line distances which are very large. It thus becomes of interest to examine the spectroscopic distances for the 84 K-line stars of the catalogue. When this is done it is at once evident that the K-line distances are of the order of 6 times the spectroscopic values for the same stars. Values of β obtained from the K-line stars might therefore be expected to be 6 times smaller than from stars with spectroscopic distances ; whereas, as a comparison between (*c*) and (*d*) of fig. 2 shows, the agreement is quite good. The reason for this is simply that the group of K-line stars contains two-thirds of the most heavily reddened stars ; in fact, the average reddening is about 6 times bigger amongst the K-line stars. Use of the K-line distances therefore obtains an agreement between the values of β at the expense of introducing a discrepancy in the scale of absolute magnitudes. This disagreement between the spectroscopic and K-line absolute magnitudes may seem surprising when it is recalled that Plaskett and Pearce † claim that their absolute magnitudes, derived from K-line intensities and thus eventually from the galactic rotation, agree to within a magnitude with those derived by other means, *e.g.* spectroscopically or from mean parallaxes. There is no doubt about the discrepancy for our 84 stars, however : their K-line absolute magnitudes are on the average four magnitudes brighter than the spectroscopic values. The difference can be at least partially explained by noting that the apparently bright early B-type stars of Plaskett and Pearce's list are absolutely bright on the basis of their K-line intensities. The 84 stars used in the present investigation are apparently brighter than most of those observed by Plaskett and Pearce, and are therefore given absolute magnitudes considerably brighter than the mean. Whatever the reason for the discrepancy, however, the fact remains that it exists ; and obviously many stars whose gradient excesses would be regarded as abnormally large on the basis of spectroscopic distances have been included in the solutions of Table I, where they are put much farther away by the intensity of their interstellar lines. These stars (11 in number) are listed in Table IIIA, which is in the same form as Table III. We may say that of the 392 stars in the final catalogue, 35 (those in Tables III and IIIA together) would be excluded as abnormally reddened on the basis of spectroscopic distances.

* *H.B.*, 849, 1927.
† *D.A.O.*, 5, 289, 1933.

Eleven of these (Table IIIA) are not excluded from the solution in Table I since their K-line intensities place them sufficiently far away for their redness to be reasonably explained as due to distance. Six of the remaining twenty-four (those with *k* attached to their spectral types in column 2 of Table III) are so heavily reddened that not even increasing their distances by a factor of six from spectroscopic to K-line values will explain their abnormal gradient excesses. Table IIIA thus consists of stars which are abnormally reddened on the basis of spectroscopic distances, but are not particularly so if K-line distances are accepted. In this latter case, however, they are 4^m brighter than their spectral types would suggest. Of the twenty-four stars in Table III, fourteen are either so close as to show no interstellar lines or so red that even their K-line distances cannot explain their gradient excesses : these are undoubtedly abnormally reddened. The remaining ten are late B-type stars for which K-line distances are not available, but it is unlikely that the distances of many could be sufficiently increased to describe them as normally reddened, since such an increase would involve brightening their absolute magnitudes by 8^m. We therefore describe all the stars of Table III as abnormally reddened.

Summary

A catalogue of gradients of 392 early-type stars is compiled by combining with Greenwich measured gradients the results of four series of photo-electric colour index measurements. A linear correlation between gradient excess and distance is used to deduce from each star a selective absorption coefficient β in the galactic plane, assuming an exponential decrease of density of the reddening material away from that plane. Weighting the separate values of β in approximate proportion to the square of the distances of the corresponding stars, mean coefficients are deduced for twelve groups of galactic longitude between 310° and 223°. Spectroscopic distances are used for 308 stars ; distances inferred from the intensity of the interstellar K-line for the remaining 84. The two series of reddening coefficients so derived agree well with each other, though the two scales of distance show discrepancies corresponding to a difference of 4^m in the absolute magnitude scales. These coefficients will not, however, account for the very heavy reddening of 35 stars, and other explanations are sought. Local obscuration seems to play a part in a large proportion of these cases, though the reddening is also correlated with the appearance of "*e*" and "*c*" characteristics in the spectra.

STAR-STREAMING IN RELATION TO SPECTRAL TYPE FROM THE CAPE PHOTOGRAPHIC PROPER MOTIONS

W. M. Smart and T. R. Tannahill, M.A., B.Sc.

1. In a previous paper * (referred to, in the sequel, as STI) we have made an analysis, on the two-streams hypothesis, of the proper motions of stars of all spectral types in the Cape Astrographic Zone † ($-40°$ to $-52°$), the limit of magnitude being 9·0 on the C.P.D. scale.

The present paper gives a similar analysis for the spectral subdivisions A5–F5, F8–G5, K0–M, and also for all the stars (11,448 in number) in the spectral range A5–M.

Owing to the high concentration of the O–A3 stars to the galactic equator it was found impracticable to obtain reliable results for these early-type stars.

For the details of the 16 regions into which the zone was divided and for details of the methods employed the reader is referred to STI.

2. In Table I the results are given of the analysis of the proper motion frequency-curves of the individual regions ; hV_1 and hV_2 are the projections of the space-velocities, hW_1 and hW_2, of the two drifts on the tangent plane at the centre of the region (in terms of the theoretical velocity-unit $1/h$) ; θ_1 and θ_2 are the position angles of the axes of the drift-curves ; N_1 and N_2 are the numbers of stars belonging to the two drifts.

Even in the more sparsely populated regions the observed frequency-curves and the deduced theoretical curves show much the same degree of accordance which is apparent in the diagrams of STI.

3. *The Drift-Constants.*—Table II gives the values of the drift-constants obtained by combining the results shown in Table I ; the weights accorded to the individual regions are the same as in STI. In this table X_1, Y_1, Z_1 denote the equatorial linear components of the space-velocity, hW_1, of Drift I ; A_1, D_1 are the equatorial co-ordinates of the drift-apex and N_1 is the total number of stars in the drift. The second part of the table gives the corresponding quantities for Drift II.

* *M.N.*, **100**, 30, 1939.

† *Proper Motions of Stars in the Zone Catalogue of 20,843 Stars*, 1936.

TABLE I

Analysis of Drift-Curves

Drift I

Region	A5–F5			F8–G5			Ko–M			A5–M		
	hV_1	θ_1	N_1	hV_1	θ_1	N_1	hV_1	θ_1	N_1	hV_1	θ_1	N_1
		°			°			°			°	
I	1·20	85	80	1·00	90	150	0·85	80	98	1·00	85	342
II	1·20	70	67	1·10	65	120	1·25	70	61	1·20	67½	242
III	1·30	55	85	1·20	47½	127	0·85	40	128	1·10	50	340
IV	1·00	10	95	1·20	15	115	1·40	20	65	1·20	15	275
V	1·50	342½	159	1·00	345	110	1·00	340	130	1·20	345	400
VI	1·50	315	126	1·50	315	82	1·50	315	136	1·50	315	343
VII	1·90	287½	185	1·50	290	106	1·50	287½	185	1·70	287½	476
VIII	1·70	272½	128	1·60	275	111	1·60	277½	187	1·60	275	427
IX	1·90	255	150	1·90	262½	163	1·70	260	191	1·80	257½	532
X	1·85	240	142	1·50	235	165	1·50	242½	191	1·60	240	498
XI	2·00	225	138	1·80	225	144	1·40	225	149	1·70	225	431
XII	1·90	200	98	1·70	195	128	1·80	200	150	1·80	197½	376
XIII	1·60	180	96	1·40	175	140	1·30	172½	145	1·40	175	380
XIV	1·90	155	61	1·10	140	106	1·45	145	138	1·40	145	305
XV	1·10	130	87	1·25	115	136	0·95	120	95	1·10	120	318
XVI	1·30	90	63	1·25	105	112	1·00	110	142	1·10	105	317

Drift II

Region	A5–F5			F8–G5			Ko–M			A5–M		
	hV_2	θ_2	N_2	hV_2	θ_2	N_2	hV_2	θ_2	N_2	hV_2	θ_2	N_2
		°			°			°			°	
I	0·55	220	55	0·70	230	110	0·30	210	90	0·55	235	250
II	0·60	240	58	0·70	210	117	0·60	215	90	0·60	215	271
III	0·50	210	69	0·45	195	144	0·50	200	65	0·50	200	278
IV	0·50	190	105	0·50	185	136	0·15	170	155	0·40	185	396
V	0·35	220	111	0·70	175	94	0·40	200	129	0·50	190	333
VI	0·45	200	98	0·40	200	112	0·30	190	158	0·40	200	368
VII	1·00	180	74	0·35	180	83	0·65	175	121	0·70	180	278
VIII	0·60	150	77	0·50	165	90	0·50	195	151	0·50	170	317
IX	0·45	160	71	0·50	180	120	0·45	180	156	0·50	170	319
X	0·40	170	90	0·40	140	118	0·55	180	128	0·45	160	336
XI	0·70	150	81	0·60	180	118	0·60	180	167	0·65	175	366
XII	0·50	170	122	0·60	180	93	0·60	180	132	0·60	175	347
XIII	0·70	155	149	0·30	180	131	0·50	200	135	0·50	180	416
XIV	0·50	140	178	0·60	175	153	0·45	230	116	0·40	180	447
XV	0·35	220	79	0·50	200	147	0·40	190	136	0·45	200	362
XVI	0·40	185	86	0·35	200	175	0·80	235	101	0·50	215	362

TABLE II

The Drift-Constants

Drift I

	A5–F5	F8–G5	Ko–M	A5–M
X_1	−0·028 ± 0·054	−0·019 ± 0·042	−0·029 ± 0·052	−0·022 ± 0·045
Y_1	+1·677 ± 0·041	+1·533 ± 0·038	+1·442 ± 0·047	+1·538 ± 0·041
Z_1	−0·220 ± 0·067	−0·136 ± 0·053	−0·099 ± 0·064	−0·144 ± 0·056
A_1	91°·0 ± 1°·8	90°·7 ± 1°·6	91°·1 ± 2°·1	90°·8 ± 1°·7
D_1	− 7°·5 ± 2°·3	− 5°·1 ± 2°·0	− 3°·9 ± 2°·5	− 5°·3 ± 2°·1
hW_1	1·692 ± 0·042	1·539 ± 0·038	1·446 ± 0·046	1·545 ± 0·041
N_1	1760	2015	2191	6002

Drift II

	A5–F5	F8–G5	Ko–M	A5–M
X_2	+0·182 ± 0·033	+0·046 ± 0·028	+0·040 ± 0·037	+0·092 ± 0·024
Y_2	−0·141 ± 0·030	−0·139 ± 0·025	−0·086 ± 0·033	−0·131 ± 0·022
Z_2	−0·619 ± 0·040	−0·670 ± 0·034	−0·587 ± 0·046	−0·649 ± 0·030
A_2	322°·2 ± 7°·7	288°·4 ± 10°·9	295°·2 ± 21°·2	304°·9 ± 8°·4
D_2	−69°·4 ± 2°·9	−77°·7 ± 2°·2	−80°·4 ± 3°·1	−76°·2 ± 2°·0
hW_2	0·661 ± 0·039	0·686 ± 0·034	0·595 ± 0·046	0·668 ± 0·029
N_2	1503	1941	2030	5446

An increase, with advancing spectral type, of hW_1 may be noted.

We call attention here to an error in STI (p. 37), where the probable error of the declination of Drift II is given as ± 13°·5 ; it should be ± 2°·4.

Using the data of Table II we have calculated the values of hV_1, hV_2, θ_1 and θ_2 for the individual regions ; in the great majority of cases there is satisfactory agreement between these calculated quantities and the values shown in Table I, the degree of accordance being similar to that shown in Tables III and IV of STI.

4. *The Vertex of Star-Streaming and the Solar Motion.*—From the results of the previous section we obtain (i) the position—(α_0, δ_0) in equatorial co-ordinates and (G_0, g_0) in galactic co-ordinates—of the vertex of star-streaming, (ii) the relative speed hU of the drifts, (iii) the position (A_0, D_0) of the solar apex in equatorial co-ordinates, (iv) the solar speed hU_0, and (v) the ratio $N_1 : N_2$ of the populations of the two drifts. The results are shown in Table III.

As in previous investigations of a similar nature concerning stars of all spectral types, the vertex for the several spectral subdivisions is found to lie on the galactic equator, with a longitude about 15° greater than the usually accepted value for the galactic centre.

Table III

The Vertex of Star-Streaming and the Solar Motion

	A5–F5	F8–G5	Ko–M	A5–M
a_0	270°·6 ± 2°·0	272°·2 ± 1°·7	272°·6 ± 2°·4	273°·8 ± 1°·8
δ_0	−12°·3 ± 2°·5	−18°·2 ± 2°·2	−17°·7 ± 3°·0	−16°·8 ± 2°·2
G_0	344°·5	340°·2	340°·6	342°·0
g_0	+2°·8	−1°·2	−1°·4	−1°·8
hU	1·873 ± 0·052	1·756 ± 0·049	1·606 ± 0·060	1·747 ± 0·048
A_0	265°·3	268°·9	269°·5	267°·5
D_0	+25°·6	+29°·2	+25°·3	+27°·3
hU_0	0·934	0·817	0·780	0·838
$N_1 : N_2$	1·173	1·038	1·080	1·102

The last line of Table III shows that the stars are almost equally divided between the two drifts. The result obtained in STI for the ratio $N_1 : N_2$, which took account of the O–A3 stars, was 1·41 ; it appears to be conclusive that the reason for the high ratio just mentioned is the inclusion of the early-type stars and not, as was tentatively suggested in STI, the comparative uncertainty in the Drift II constants.

5. *Calculation of the Ellipsoidal Constants from the Stream-Constants.*— A method * has been described by one of us for deriving the ellipsoidal constants from the stream-constants. This method is strictly applicable if the populations of the two streams are equal, a condition which is sufficiently realised in the present case. The results are given in Table IV, where G_0 is, as before, the longitude of the vertex and K/H the ratio of the axes of the velocity ellipsoid. Jackson's results, obtained by means of Schwarzschild's automatic method from the same material, are included for comparison—they are shown in parentheses.

Table IV

The Ellipsoidal Constants

	A5–F5	F8–G5	Ko–M	A5–M
G_0	344°·7	339°·6	339°·1	339°·5
	(348·1)	(342·1)	(340·3)	(343·0)
K/H	0·62	0·63	0·67	0·64
	(0·55)	(0·56)	(0·65)	(0·62)

Summary

1. The Cape photographic proper motions of stars of spectral types A5–M have been analysed, in three spectral groups A5–F5, F8–G5, Ko–M, and also in the aggregate, according to the two-streams theory.

2. The drift-constants, the vertex of star-streaming and the solar motion have been found for the several spectral groups.

* W. M. Smart, *M.N.*, **99**, 561, 1939 ; see also STI.

3. The longitude of the vertex is, on the average, about 15° higher than the longitude of the galactic centre.

4. The stars in each spectral group are divided almost equally between the two drifts.

5. The ellipsoidal constants have been derived, and they are in good agreement with Jackson's values derived from the same data by a different method. In particular, the ratio of the axes of the velocity ellipsoid for the A5–M stars is found to be 0·64.

University Observatory,
Glasgow, W.2 :
1940 *May* 7.

THE VARIABLE EXTENT OF THE ATMOSPHERE OF ZETA AURIGÆ

Arthur Beer, Ph.D.

In a previous paper * I discussed the first Cambridge spectra of this unique star system, obtained during its 1934 eclipse. Continued observations in 1937 dealt with the subsequent eclipse, but they were made difficult by the low altitude of the star and by cloudy periods. Although the next eclipse, from 1939 December to 1940 January, would have been excellently situated, clouds unfortunately prevented any systematic observations in England. It thus appears desirable to make the best possible use of the 1937 material. The present note is intended to draw attention to the very remarkable behaviour of the K line of *Ca*II, which (since it is produced in the extensive atmosphere of the K5 giant) indicates significant changes in the structure of this star's atmosphere.

The importance of this star for so many astrophysical questions has produced an extensive literature in recent years, exceeding ninety papers.† To them we may refer concerning all general data of this star system.

The new spectroscopic material to be discussed covers about a month before the beginning of the 1937 eclipse, *i.e.* April 21·85.‡ Twelve plates were obtained at the Solar Physics Observatory, Cambridge, between March 22 and April 12, and one on April 19, using the 2-prism spectrograph attached to the 25-inch Newall telescope, giving a dispersion of 31 A./mm. at K. The plates were Ilford Astra II. Three objective prism plates from the Norman Lockyer Observatory at Sidmouth fill the gap for April 17 and 18, while five similar spectra from the Vatican Observatory, Rome, include the period April 15–21. Two earlier Cambridge plates, of March 15 and March 18, are too weak to show any traces of the expected chromospheric K line, which, however, appears clearly and with increasing strength on the next plates, obtained on March 22 and later. The passage of the B8 star behind the atmosphere of the K5 giant had therefore commenced at least 30 days before the predicted date of total eclipse of the B component. These observations already indicated that the chromosphere had expanded since the eclipse of 1934.§

The spectrophotometric investigation of the new material was again performed with the recording microphotometer of the Solar Physics Observatory at Cambridge. Two sets of tracings obtained with different

* A. Beer, *M.N.*, **95**, 24, 1934.

† See *M.N.*, **96**, 360, 1936, and **97**, 349, 1937. Another interesting star system of similar conditions, VV Cephei, has recently been discovered by D. B. McLaughlin and analysed by V. Goedicke in *Michigan Publ.*, vol. viii, No. 1, 1939.

‡ G. Järnefelt, *Annales Acad. Scient. Fennicæ*, Ser. A, **53**, No. 1 (p. 20), Helsinki, 1939.

§ See preliminary note in Circular No. 651 of the I.A.U., Copenhagen, 1937.

arrangements of the instrument were combined. In determining the contours of the chromospheric K line, allowance was made, of course, for the shallow depression caused on the tracings by the K line of the K5 star. Table I gives plate number (No.), time of mid-exposure (t), mean equivalent width of the K line (EW) and the column (O – C), which is explained further below.

Table I

No.	t	EW in A.	(O – C)
T655	1937 March 22·91	0·31	+0·09
656	26·81	0·35	−0·03
657	27·80	0·42	0·00
658	28·81	0·49	+0·03
659	30·81	0·40	−0·15
660	31·82	0·52	−0·07
662	April 3·93	0·72	0·00
664	6·82	(0·45)	—
665	7·80	0·94	+0·06
666	8·80	0·95	+0·02
667	11·80	1·05	0·00
668	12·83	1·07	−0·02
669	19·85	2·45	—

It is obvious that the values EW show individual fluctuations, which appear to be partly real, as for instance a minimum at about March 31. The observation of April 6, however, would be better omitted, as plate T664 is too dense to permit reliable spectrophotometric results. Concerning an explanation of possible irregular intensity variations of K, we refer to an interesting note by Christie *, who considers them to indicate that the outer calcium atmosphere of the K star is not continuous, but consists of irregular condensations or clouds lying high above the photosphere. On the other hand, we realize that as a whole the run of the early intensities, until about April 13, can be well represented by a linear relation. A least-square solution based on the first 11 plates of Table I, which cover this period (plate T664 being excluded), gives :

$$\mathrm{EW} = (t - T)(0{\cdot}042 \pm 0{\cdot}003) + (0{\cdot}178 \pm 0{\cdot}036),$$

where T = March 22·0. The comparison with the observations is to be found in the last column (O – C) of Table I. This equation leads to the date of the first appearance of the K line as March 17·7, and thus to 35 days as the total duration of visibility before the eclipse.

If all 12 plates had been used, with T664, the results would not have differed appreciably, except that then the p.e. become more than double :

$$\mathrm{EW} = (t - T)(0{\cdot}039 \pm 0{\cdot}006) + (0{\cdot}177 \pm 0{\cdot}079).$$

An attempt was made to supplement these measurements by corresponding ones of the chromospheric H line of *Ca*II. The intensities of this line, which is blended with $H\epsilon$, were measured on all plates, but the individual

* W. H. Christie, *Publ. Astr. Soc. Pac.*, **50**, 53, 1938.

scatter of the resulting EW is too great, owing also to the disturbance of the wings of this strong blend by several other lines. It could be seen that already in the early stages of this eclipse, *i.e.* a considerable time before its beginning, a number of absorptions became conspicuous, which did so only considerably later in 1934.* Plate T667, for instance, shows between K and λ 3990, clearly marked, the following lines : 3944·0 *Al*, 3948·7 *Ti – Fe*, 3952·6 *Fe*, 3956·5 *Ti – Fe* and 3958·2 *Zr – Ti*, 3961·5 *Al*, 3968·5 *H*(*Ca*II), 3970·1 *Hε*, 3973·6 *Ni*, 3981·8 *Fe – Ti*. Nevertheless, we may note the 4-day means of the EW of this blend (H + *Hε*) : March 27·8 (6·22 A.), March 31·3 (6·68), April 5·4 (7·29), April 8·3 (7·38), April 12·3 (7·88).

It was fortunate that for the remaining nine days before eclipse, when clouds prevented further observations at Cambridge, the additional material, secured at Sidmouth and Rome, became available. Mr. D. L. Edwards, the Director of the Norman Lockyer Observatory, very kindly put at my disposal the plates obtained with the 12-inch telescope at Sidmouth. Microphotometer tracings gave the following results :—

TABLE II

No.	*t*	*I*	EW	[EW]
5305	1937 April 17·88	984	4·53	1·03
5306	17·96	1128	5·19	1·83
5307	18·86	1301	5·98	2·78

The third column, *I*, gives the total intensities as measured on the tracings in sq. mm. Since the dispersion of the spectra is 23 A./mm. at K, and the magnification on the tracings 50-fold, 1 mm. on the tracing corresponds to 0·46 A., and we have, therefore, for the EW in the next column, expressed in units of 1 mm. width and 100 per cent. depth,

$$\mathrm{EW} = I \,.\, 0{\cdot}46/100.$$

This value refers to the total absorption A_{BK} of the K line in the composite spectrum. If we denote with A_K the total absorption of the line in the normal K5 spectrum, and with A_B that of the chromospheric K line, as produced by the B8 star, we have the relation : †

$$A_B = A_{BK} + \frac{1}{a}(A_{BK} - A_K),$$

where a denotes the ratio of the intensities of the continuous spectrum in the K region of the two components :

$$a = I_{CB}/I_{CK}.$$

A photographic determination by H. Brück ‡ gives $a = 4{\cdot}76$.

The value of A_K adopted by us is 21·3 A., being the mean of three

* W. H. Christie and O. C. Wilson, *Ap. J.*, **81**, 213, 1935, Plate V. On p. 237 these authors, too, decided to discard the measures of the *Hε* line.

† Christie-Wilson, *loc. cit.*, p. 228.

‡ Brück, *Acta Pontif. Acad. Scient.*, Anno II, Vol. II, No. 6, p. 56, Rome, 1938.

determinations, namely, 23·6 A. from measurements on a tracing of the Cambridge plate T671, taken 1937 April 21·9, *i.e.* 3 days after the chromospheric K line had disappeared; 24 A. from Brück's paper, *l.c.*, p. 58; 16·3 A. from Christie-Wilson, *l.c.*, p. 21, Table VII.

Inserting these data in the above formula, we obtain the required values A_B, given as [EW] in the last column of Table II.

The following five additional values can be taken from Brück's paper, p. 58: April 15·85 (1·0 A.), 16·84 (2·2), 17·82 (3·5), 20·81 (3·5), 21·83 (12·1).

The accuracy of the line intensities obtained in the period after April 12 is naturally considerably smaller than for the time before this date, when a slit spectrograph could be used. To smooth out individual differences we combine the last-mentioned figures with those of Table II and with plate T669 of Table I, forming the means of the 2 plates of April 15–16, the 3 plates of April 17, the 3 plates of April 18–20, and add the observation of April 21. We thus obtain

TABLE III

April 16·34,	EW = 1·60 A.
17·89,	2·12
19·84,	2·91
21·83,	12·1

Fig. 1 contains these last-mentioned values, together with those of Table II. The extremely steep increase of the K-line intensity with approaching eclipse is well illustrated. In order to make this figure comparable with the situation in 1934, the latter * has been inserted after adjustment of the time-scale (beginning and end of 1934 eclipse, J.D. 2427674·35 and 2427711·05, respectively). Time has been converted into distance of the B star from the surface of the K star, whose radius R_K corresponds to 19·15 days.† We note that an EW of 1 A. was reached in 1934 only 3 days before eclipse, while in 1937 this was the case already 9 days before; and, furthermore, that the total visibility of this line changed between these two eclipses from 9 to 35 days.

It is of special interest to convert fig. 1 into fig. 2 by changing the ordinates from EW (A) to N, this being the number of atoms in the line of sight. Christie and Wilson ‡ did this after having discussed the validity of their assumed relation:

$$A \propto \sqrt{N}.$$

On the other hand, they have also derived a theoretical expression for N, based on Milne's theory of chromospheric equilibrium:

$$N \propto \frac{R-h_0}{(R+H)^2-(h_0-R)^2} + \frac{2(R+H)^2}{[(R+H)^2-(h_0-R)^2]^{3/2}} \tan^{-1} \frac{\sqrt{(R+H)^2-(h_0-R)^2}}{H+h_0}.$$

The quantities characterising Milne's layer are conveniently taken as

* Beer, *loc. cit.*, 1934, fig. 1, and Christie-Wilson, *loc. cit.*, 1935, fig. 8.

† Christie-Wilson, *loc. cit.*, p. 225.

‡ *Loc. cit.*, pp. 238 and 245.

$R = 1{\cdot}05$ and $h = 0{\cdot}05$, while H denotes the distance of closest approach of the line of sight to the photosphere. We now adjust the values of N by an appropriate factor, in order to be able to compare the run of the theoretical

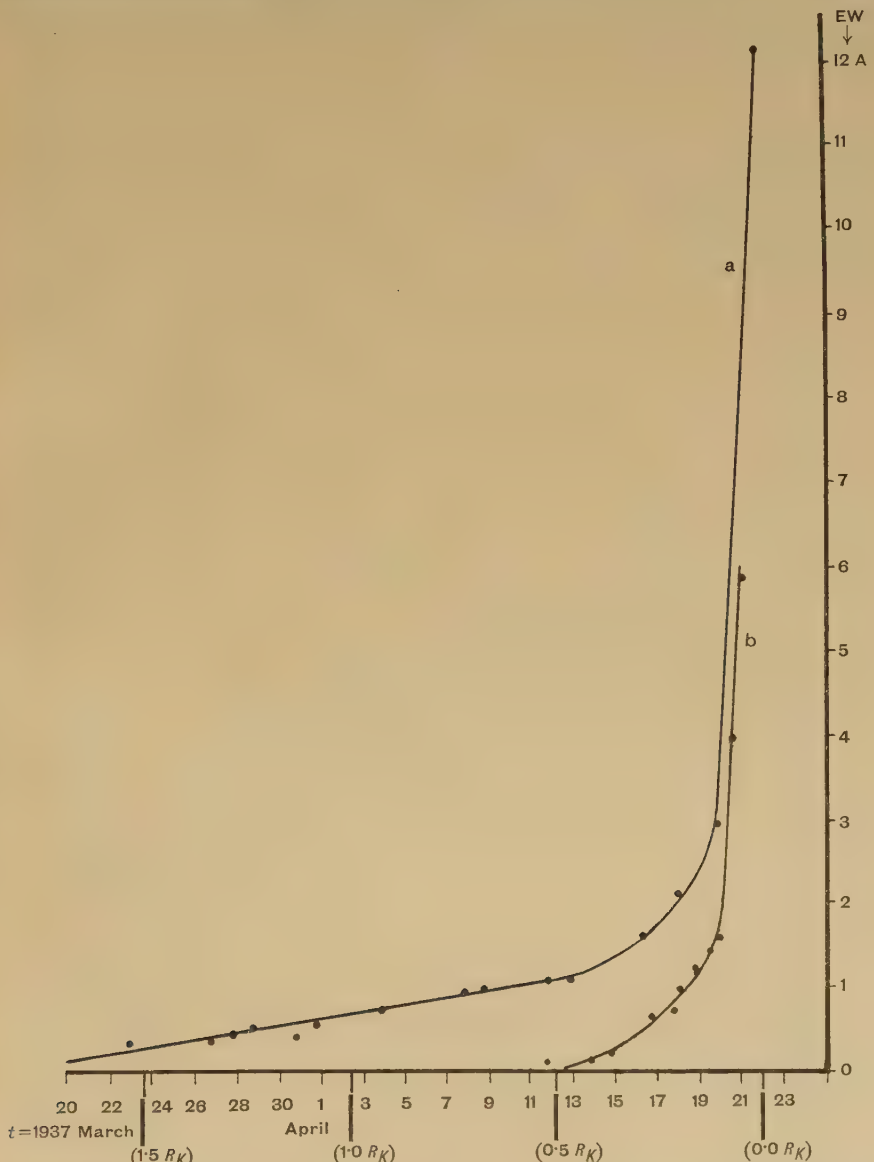

FIG. 1.—*Comparison of the K-line intensities of ζ Aurigæ during its eclipses of* 1937 (*a*) *and* 1934 (*b*).

curve with the observed one. The above formula furnishes us, then, with the following values of log N, for different values of H (expressed in R_K):

$$H = 0{\cdot}00,\ 0{\cdot}05,\ 0{\cdot}1,\ 0{\cdot}2,\ 0{\cdot}3,\ 0{\cdot}5,\ 0{\cdot}7,\ 1{\cdot}0,\ 1{\cdot}5$$
$$\log N = 2{\cdot}39,\ 1{\cdot}94,\ 1{\cdot}70,\ 1{\cdot}39,\ 1{\cdot}20,\ 0{\cdot}94,\ 0{\cdot}79,\ 0{\cdot}61,\ 0{\cdot}44.$$

The diagram, fig. 2, confirms that the theoretical curve certainly does not fit the observations of 1934, a fact which led Christie and Wilson (*l.c.*, p. 245) to the statement: "Accordingly we conclude that the observations of the

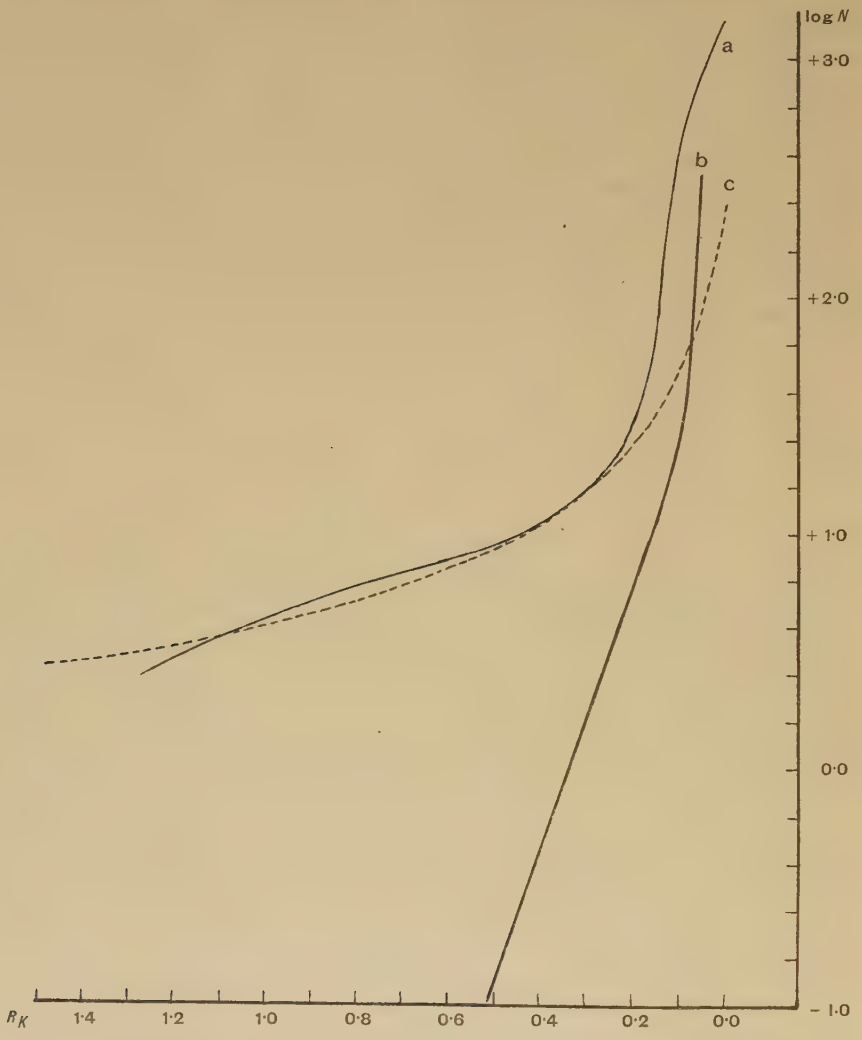

FIG. 2.—*Number of Ca*II *atoms in the line of sight in the chromosphere of ζ Aurigæ.*
——— =1937 (*a*). ——— =1934 (*b*). - - - - - =*Milne's Theory* (*c*).

*Ca*II envelope surrounding ζ Aurigæ are in disagreement with the predictions of Milne's theory."

It is now obvious, however, noticing the agreement with the other curve in fig. 2, that the changing conditions prevailing in the atmosphere of ζ Aurigæ do not allow this conclusion to be extended to the 1937 eclipse.

Summary

Spectrophotometric investigations of the behaviour of the K line of ζ Aurigæ during its 1937 eclipse reveal, when compared with those of 1934, fundamental changes in the conditions of the star's atmosphere and a much improved agreement with Milne's theory.

I am very grateful to Professor F. J. M. Stratton, Director of the Solar Physics Observatory, Cambridge, and to Mr. D. L. Edwards, Director of the Norman Lockyer Observatory, Sidmouth, for kindly arranging my present stay in Cambridge, after the University of London Observatory closed down at the outbreak of war, and for the use of the additional material.

Solar Physics Observatory,
Cambridge :
1940 *May.*

OCCULTATIONS OF STARS BY THE MOON, OBSERVED AT THE NIZAMIAH OBSERVATORY, HYDERABAD, DURING THE YEAR 1939

(Communicated by the Director)

No.	Star	Mag.	Phase	Date 1939	U.T. h m s
1	χ' Orionis	4·6	D	Jan. 4	19 08 30·2
2	B.D. $-19°$ 4357	6·4	R	,, 15	23 54 22·0
3	B.D. $+19°$ 886	6·9	D	,, 31	14 56 02·6
4	B.D. $+19°$ 893	6·2	D	,, 31	16 03 48·1
5	α Virginis	1·2	D	Feb. 8	23 18 10·8
6	α Virginis	1·2	R	,, 9	0 39 07·2
7	β' Scorpii	2·9	D	,, 11	23 48 10·6
8	β' Scorpii	2·9	R	,, 12	0 44 00·7
9	B.D. $-19°$ 4308	5·1	R	,, 12	0 45 09·5
10	A.G. Toulouse $+9°$ 1^h 8^m 31	...	D	,, 23	13 30 28·1
11	B.D. $+9°$ 145	8·8	D	,, 23	13 31 27·2
12	B.D. $+9°$ 144	8·6	D	,, 23	13 51 11·0
13	57 Orionis	5·9	D	,, 28	14 15 07·1
14	B.D. $+19°$ 1128	8·5	D	,, 28	14 23 21·8
15	B.D. $+17°$ 1479	6·2	D	Mar. 1	18 20 04·4
16	1 Cancri	6·0	D	,, 2	13 53 47·6
17	α Cancri	4·3	D	,, 3	14 36 52·3
18	κ Cancri	5·1	D	,, 3	20 42 14·9
19	B.D. $+19°$ 986	8·5	D	,, 27	14 02 58·1
20	Paris $+20°$ 5^h 28^m 935	...	D	,, 27	14 06 34·0
21	B.D. $+19°$ 998	8·0	D	,, 27	15 07 24·5
22	α Virginis	1·2	D	Apr. 4	19 54 02·7
23	α Virginis	1·2	R	,, 4	21 10 43·4
24	B.D. $-14°$ 5781	6·2	R	,, 12	23 24 10·7
25	B.D. $+18°$ 632	7·9	D	,, 22	14 14 11·8
26	B.D. $+18°$ 633	6·0	D	,, 22	14 22 00·1
27	B.D. $+14°$ 1879	7·1	D	,, 26	15 46 11·1
28	B.D. $-15°$ 3948	9·5	D	May 3	14 55 19·4
29	Tacubaya $-15°$ 14^h 44^m 31	...	D	,, 3	14 56 45·2
30	B.D. $-19°$ 4406	5·6	R	,, 5	18 45 57·8
31	B.D. $-19°$ 5047	6·5–7·3	R	,, 7	20 04 28·8
32	B.D. $+13°$ 1940	6·4	R	Oct. 7	22 12 01·6
33	6 Leonis	5·3	R	,, 8	22 20 24·3
34	B.D. $-18°$ 4983	9·5	D	,, 18	14 15 56·6
35	Hyd. $-18°$ 18^h 24^m 54373	...	D	,, 18	14 44 59·6
36	B.D. $-18°$ 4986	7·0	D	,, 18	14 50 41·4
37	Hyd. $-18°$ 18^h 24^m 54376	...	D	,, 18	14 54 24·2
38	B.D. $-18°$ 4994	7·0	D	,, 18	16 15 15·9
39	B.D. $-17°$ 5601	9·1	D	,, 19	14 01 14·2
40	B.D. $-17°$ 5611	6·9	D	,, 19	15 08 27·8
41	ϵ Piscium	4·4	D	,, 26	22 41 13·4
42	65 Leonis	5·7	R	Nov. 6	22 59 33·1

No.	Star	Mag.	Phase	Date	U.T.
				1939	h m s
43	25 Piscium	6·2	D	Nov. 21	18 30 19·2
44	β Capricorni	3·2	R	Dec. 14	12 37 08·9
45	B.D. -14° 5734	7·0	D	,, 14	14 03 32·4
46	ϵ Piscium	4·4	D	,, 20	14 42 47·6
47	σ Arietis	5·5	D	,, 22	20 45 21·0
48	A′ Cancri	5·7	R	,, 28	22 50 48·3
49	6 Leonis	5·3	R	,, 29	17 01 34·4

Notes

No. 5 : disappearance instantaneous.
No. 24 : seen through clouds ; time somewhat uncertain.

Three observations (Nos. 28, 29, and 45) were made by T. P. Bhaskaran and the rest by M. K. Bappu. The instrument used throughout was the 15-inch visual refractor. The clock corrections were determined from observations with the transit instrument.

The reductions were carried out by M. V. V. Sastri, assisted by S. Aravamudan and V. V. Raghaviah. A correction of $0^h{\cdot}0076$ has been added to the observed time to allow for the error of $1''{\cdot}5$ in the mean longitude of the Moon.

No.	$\sigma' - \sigma$	$\cos(\rho - \chi)$	$\sin(\rho - \chi)$	No.	$\sigma' - \sigma$	$\cos(\rho - \chi)$	$\sin(\rho - \chi)$
	"				"		
1	−0·1	+0·66	+0·75	26	+0·8	+0·96	+0·28
2	+0·6	−0·67	−0·74	27	+0·9	+0·87	+0·49
3	−2·2	+0·98	−0·20	28	−0·7	+0·99	+0·11
4	−2·3	+0·98	−0·19	29	+2·3	+0·84	−0·55
5	−0·9	+0·95	+0·31	30	+2·1	−0·99	−0·15
6	0·0	−0·80	+0·60	31	0·0	−0·76	+0·65
7	+2·0	+0·42	−0·91	32	−2·7	−0·89	−0·45
8	+0·6	−0·68	−0·73	33	+1·5	−0·66	+0·75
9	+0·2	−0·70	−0·72	34	−3·5	+0·88	+0·47
10	−0·5	+0·82	−0·57	35	+1·1	+0·92	−0·39
11	[+5·1]	+0·83	−0·55	36	+1·9	+0·79	−0·62
12	+2·3	+0·08	+1·00	37	+1·3	+0·88	−0·48
13	+2·1	+1·00	+0·07	38	−1·2	+0·40	+0·92
14	+2·0	+0·89	−0·45	39	+1·4	+0·99	−0·16
15	+2·2	+0·83	−0·55	40	−0·5	+0·98	−0·20
16	+0·9	+0·98	+0·22	41	0·0	+0·93	−0·36
17	+0·3	+0·99	−0·16	42	+1·5	−0·76	+0·65
18	+0·3	+0·90	−0·43	43	−2·9	+0·97	−0·25
19	+3·4	+0·85	+0·52	44	+1·0	−0·58	−0·81
20	+2·0	+0·93	+0·36	45	−2·2	+0·76	+0·65
21	+1·5	+0·67	+0·74	46	+0·2	+0·38	+0·93
22	−0·4	+0·79	−0·61	47	−0·5	+0·64	+0·77
23	0·0	−0·93	−0·36	48	−0·3	−0·74	−0·67
24	[+7·1]	−0·82	+0·58	49	+1·6	−0·92	−0·40
25	−1·5	+0·97	−0·23				

The mean places for 1939·0 of fourteen stars in the above list are given in the following table. For stars A.G. Leipzig 456, A.G. Berlin 1618 and 1164, proper motions have been applied to the co-ordinates in the Catalogue, in computing the mean places for use in the reductions :—

No.	R.A. (1939·0)	Dec. (1939·0)	Remarks
	h m s	° ′ ″	
10	1 13 45·87	+ 9 33 44·2	Toulouse +9° 1h 8m, No. 31 ; +9° 1h 16m, No. 2.
11	1 13 48·01	+ 9 34 03·8	A.G. Leipzig 456. P.M. μ_α +0s·0070 ; μ_δ −0″·120.
12	1 13 04·75	+ 9 55 50·0	A.G. Leipzig 451.
14	5 51 23·19	+19 35 41·4	A.G. Berlin 1761.
19	5 33 57·93	+19 44 37·6	A.G. Berlin 1606.
20	5 34 08·80	+19 41 44·8	Paris +19° 5h 32m, No. 91 ; +20° 5h 28m, No. 935.
21	5 35 31·55	+19 44 06·2	A.G. Berlin 1618. P.M. μ_α +0s·0007 ; μ_δ +0″·001.
25	4 21 10·06	+18 46 25·5	A.G. Berlin 1164. P.M. μ_α −0s·0002 ; μ_δ −0″·019.
28	14 43 20·24	−15 35 03·9	Tacubaya −15° 14h 44m, No. 39 ; −16° 14h 40m, No. 209.
29	14 43 03·40	−15 44 57·4	Tacubaya −15° 14h 44m, No. 31 ; −16° 14h 40m, No. 204.
34	18 26 51·11	−18 43 41·8	Hyderabad −18° 18h 24m, No. 54245 ; −19° 18h 20m, No. 50752; −19° 18h 28m, No. 51186.
35	18 27 42·55	−18 53 57·2	Hyderabad −18° 18h 24m, No. 54373 ; −19° 18h 28m, No. 51210.
37	18 27 55·28	−18 54 17·7	Hyderabad −18° 18h 24m, No. 54376 ; −19° 18h 28m, No. 51211.
39	19 18 48·54	−17 26 11·0	Hyderabad −17° 19h 16m, No. 58042 ; −18° 19h 20m, No. 58251 ; −18° 19h 12m, No. 57812.

Nizamiah Observatory,
Hyderabad (Deccan), India.

Editorial Note on Dr. Burch's Article: The Williams Interferometer
(*M.N.*, **100**, 488, 1940)

Dr. C. R. Burch has written to say that the above article, though optically sound, is quite misleading regarding priority. He points out that the instrument described is actually the original form of interferometer described in British Patent No. 103832 of 1916 (expiring 1942 January 3) and also in *Ap. J.*, **48**, 256 (1918). In offering his apologies to Messrs. Twyman and Green, for having missed Mr. Twyman's note in *Ap. J.*, he expresses the hope that the article and this note will secure wider publicity for this extremely convenient but relatively unknown form of interferometer.

LIST OF ADDITIONS

TO THE

LIBRARY OF THE SOCIETY

1939 OCTOBER 1–NOVEMBER 30

Unless otherwise indicated, the donor is the author or the Institution concerned.

An asterisk (*) indicates that the work is an excerpt.
A dagger (†) indicates that the work has been purchased.

British Association for the Advancement of Science, Seismology Committee :

Index to the International Seismological Summary (a continuation of Catalogue of Earthquakes 1925–1930) for 1931, 1932.
8vo. Newport, I. of W., 1939

Gutenberg (Beno) :

†Internal Constitution of the Earth. Cr. 8vo. London, 1939

Hartree (D. R.) :

*Note on an Integral occurring in the Cascade Theory of Cosmic Ray Showers. (*Manchester Lit. and Phil. Soc.*) 8vo. Manchester, 1939

Hartree (D. R.) and S. Johnston :

*Note on the function $\chi(x) = \int_0^\infty e^{-(r-w^2)^2} dw$.
(*Manchester Lit. and Phil. Soc.*) 8vo. Manchester, 1939

Inglis (J. Gall) :

An Easy Guide to the Constellations: with a Star Atlas. (Based on the work of the same name by Rev. James Gall.) sm. 4to. Edinburgh, 1939

Jeffreys (Harold) :

Theory of Probability. 8vo. Oxford, 1939

Jones (H. Spencer) :

The Earth as a Clock. (The Halley Lecture, delivered on 5 June 1939.)
8vo. Oxford, 1939

Leonard (F. C.) :

*Some Astronomical Terms. 8vo. San Francisco, 1939

——: *The Goose Lake Siderite: California's Largest Known Meteorite.
8vo. Northfield, Minn., 1939

H.M. Nautical Almanac Office :
Seven-figure Trigonometrical Tables for every Second of Time. Prepared by H.M. Nautical Almanac Office. 8vo. London, 1939

Pledge (H. T.) :
Science since 1500. 8vo. London, 1939
(*Director, Science Museum.*)

Plummer (H. C.) :
Probability and Frequency. 8vo. London, 1939

Reed's Nautical Almanac :
Almanac for 1940. 8vo. Sunderland, 1939
(*Captain O. M. Watts.*)

Rome, Istituto di Studi Romani :
Gli Istituto Scientifici di Roma. VII. G. Stein, La Specola Vaticana. 8vo. Rome, 1939

Rome, Specola Astronomia Vaticana :
Ricerche Astronomiche. Vol. I, no. 1. 8vo. Città del Vaticano, 1939

LIST OF ADDITIONS

TO THE

LIBRARY OF THE SOCIETY

1939 DECEMBER 1–31

Unless otherwise indicated, the donor is the author or the Institution concerned.

An asterisk (*) indicates that the work is an excerpt.

Association for the Study of Snow and Ice :

Vol. I, no. 3. Papers and Discussions (Summaries) at the Meeting held at the Royal Geographical Society, London, on Wednesday, 12th July 1939, at 5.0 p.m. 8vo. (*s.l.*) 1939

Barritt (Maria) :

Barritt's Revised Celestial Album (160 Photographs). 4to. Brooklyn, N.Y., 1939

Raman (B. V.) :

A Manual of Hindu Astrology. 8vo. Bangalore, 1939

Rosseland (Svein) :

*Mechanische Integration von Differentialgleichungen. 4to. Berlin, 1939

Störmer (Carl) :

*Auroral Work in Southern Norway in the Year 1938. 8vo. Baltimore, 1939

LIST OF ADDITIONS

TO THE

LIBRARY OF THE SOCIETY

1940 JANUARY 1 TO FEBRUARY 29

Unless otherwise indicated, the donor is the author or the Institution concerned.

An asterisk (*) indicates that the work is an excerpt.
A dagger (†) indicates that the work has been purchased.

Abetti (G.) :
*Altezza della Cromosfera nel 1938 e Andamento del Ciclo Solare. 8vo. Roma, 1939

Barocas (V.) :
*Prominences and the Sunspot Cycle. 8vo. Chicago, 1939

Chapman (S.) and T. G. Cowling :
†The Mathematical Theory of Non-uniform Gases. Large Royal 8vo. Cambridge, 1940

Hope-Jones (F.) :
†Electrical Timekeeping. Demy 8vo. London, 1940

Indiana University, Kirkwood Observatory :
Publications. Nos. 1, 2. 8vo. Bloomington, Ind., 1939

LIST OF ADDITIONS

TO THE

LIBRARY OF THE SOCIETY

1940 MARCH 1–31

Unless otherwise indicated, the donor is the author or the Institution concerned.

An asterisk (*) indicates that the work is an excerpt.
A dagger (†) indicates that the work has been purchased.

Bramanti (Luigi) :
*La Pioggia in Funzione del Tempo Lunare. 4to. Perugia, 1939

Fourcade (H. G.) :
*A Projection Method of Mapping from Air Photographs. 4to. Cape Town, 1940

Kahn (M. A. R.) :
*The Zodiacal Light. 4to. Hyderabad, 1939

Kwasan Observatory :
Circular, No. 1. 4to. Kyoto, 1940

Licetus (F.) :
†De Regulari Motu minimaque Parallaxi Cometarum Caelestium Disputationes. 4to. Utine (N. Shiratti), 1640

Indian Science Congress :
——: 26th, Lahore, 1939; 27th, Madras, 1940. Presidential Addresses, Section of Mathematics and Physics. 8vo. Calcutta, 1939, 1940

1939. K. R. Ramanathan, The Earth's Magnetism and the Upper Atmosphere.
1940. A. C. Banerji, The Development of Galactic Dynamics and some Allied Problems.

Spencer (L. J.) :
*Tektites and Silica-glass. 8vo. London, 1939

Stockholm, Kungl. Svenska Vetenskaps Akadamien :
Förhistoria, Grundläggning och Första Organisation. 8vo. Stockholm, 1939

Stockholm, Kungl. Svenska Vetenskaps Akadamien :

——: Peter Wilhelm Wargentin, av N. V. E. Nordenmark (avec un résumé français). 8vo. Stockholm, 1939

——: Johan Carl Wilcke, Experimental Fysiker, av C. W. Osen. 8vo. Stockholm, 1939

Washington, Smithsonian Institution :

*Publications, Nos. 3493, 3495. 8vo. Washington, 1938

No. 3493. E. Hubble, The Nature of the Nebulæ.
No. 3495. P. M. S. Blackett, Cosmic Radiation.

LIST OF ADDITIONS

TO THE

LIBRARY OF THE SOCIETY

1940 APRIL 1–30

Unless otherwise indicated, the donor is the author or the Institution concerned.

An asterisk (*) indicates that the work is an excerpt.
A dagger (†) indicates that the work has been purchased.

Abetti (Giorgio) :
*Il R. Osservatorio Astrofisico di Arcetri in Firenze. 8vo. Bologna, 1940

Eagle (Albert) :
——: *Note on Synchronizing "Clocks" in a Moving System by a Connecting Spindle. 8vo. London, 1939
——: *An Alternative Explanation of Relativity Phenomena. 8vo. London, 1939

Eddington (Sir A. S.) :
*Sir Frank Watson Dyson, 1868–1939. 4to. London, 1940

Giovanelli (R. G.) :
*The Relations between Eruptions and Sunspots. 8vo. Chicago, 1939

Giovanelli (R. G.) and A. J. Higgs :
*The Association of Radio Fade-outs with Solar Eruptions. 8vo. Baltimore, 1939

Loreta (E.) :
——: *Notes sur Trois Etoiles Variables de la Classe W Cygni. 4to. Marseille, 1940
——: *Turbolenza di Correnti Stratosferiche rivelate da Scie Persistenti di Bolidi. 4to. Roma, 1940

Miller (J. C. P.) :
†Tables for converting Rectangular to Polar Co-ordinates. 8vo. London, 1939

Netherlands East Indies, Topographical Service, Geodetic Section :
——: Report on the World Longitude Operation 1933, made at the Bosscha Astronomical Observatory at Lembang (Java), by K. Gsöllpointner and E. A. Scharpff. 4to. Weltevreden, 1940
——: Eine grafische Methode zur Bestimmung der Instrumentalfehler des Zenitteleskops aus den Fehlerkurven, von K. Gsöllpointner. 4to. Weltevreden, 1940

Stetson (H. T.) :
——: *Auroras, Radio Field-strengths and Recent Solar Activity. 8vo. Baltimore, 1940
——: *The Sun and the Atmosphere. 8vo. Washington, 1939

LIST OF ADDITIONS

TO THE

LIBRARY OF THE SOCIETY

1940 APRIL 1–30

Unless otherwise indicated, the donor is the author or the Institution concerned.

An asterisk (*) indicates that the work is an excerpt.
A dagger (†) indicates that the work has been purchased.

Giovanelli (R. G.) :
*The Motion of Eruptive Prominences. 8vo. Chicago, 1940

Gregory (Sir Richard) :
Religion in Science and Civilization. 8vo. London, 1940

Russell (Henry Norris) and Charlotte E. Moore :
†The Masses of the Stars, with a General Catalogue of Dynamical Parallaxes (Astrophysical Monograph). 8vo. Chicago, 1940

Walkey (O. R.) and H. Subramania Aiyar :
Concise General Astronomy. 8vo. Trivandrum, 1940

LIST OF ADDITIONS

TO THE

LIBRARY OF THE SOCIETY

1940 MAY 1–AUGUST 31

Unless otherwise indicated, the donor is the author or the Institution concerned.

An asterisk (*) indicates that the work is an excerpt.
A dagger (†) indicates that the work has been purchased.

Chapman (Sydney) and Julius Bartels :
†Geomagnetism. (International Series of Monographs on Physics. General Editors, R. H. Fowler and P. Kapitza.) 2 vols. 4to. Oxford, 1940
Vol. 1. Geomagnetic and Related Phenomena.
Vol. 2. Analysis of the Data, and Physical Theories.

Chiplonkar (M. W.) :
*The Distribution of Temperature in the Lower Stratosphere. 4to. Bangalore, 1940

Hellweg (J. F.) :
*United States Navy Time Service. 8vo. San Francisco, 1940
(*U.S. Naval Observatory.*)

Houga (Gers), Observatoire :
Publications. No. 1. 8vo. Orléans, 1940

Jones (H. Spencer) :
Life on Other Worlds. 8vo. London, 1940
(*English Universities Press, Ltd.*)

Khan (M. A. R.) :
——: Meteoric Astronomy. 8vo. Trichy, 1939
——: *The Zodaical Light (Supplementary Paper). 8vo. Madras, 1940
——: *Meteor Observations in 1939. 8vo. Madras, 1940

H.M. Nautical Almanac Office :
Apparent Places of Fundamental Stars, 1941. Imp. 8vo. London, 1940

Pogson (Norman) :

*Catalogue of 53 Variable Stars.
(*Miss Bellamy.*) (3 copies.) 8vo. Oxford (*s.d.*)

Skellet (A. M.) :

The Coronaviser. (Bell Telephone System Technical Publications, Monograph B.1223.) 8vo. New York, 1940

Wellington (N.Z.), Carter Observatory :

——: Astronomical Bulletin. Nos. 1, 2, 3. 8vo. Dunedin, 1940
——: Reprint No. 1. 8vo. Dunedin, 1940

No. 1. Catalogue of Aurora Australis Displays, 1931–38. By M. Geddes.

Wellington (N.Z.), New Zealand Astronomical Society :

*Observation of Meteors for the years 1935–1938 in New Zealand. Fourth Report of the Meteor Section of the N.Z. Astronomical Society. By R. A. McIntosh. 8vo. Dunedin, 1940

INDEX

PAGE

Adam, M. G., Variation of faint Fraunhofer lines across the solar disc (Second paper) 595
Ali, A., The Corona Borealis cluster 570
Ali, A., W. M. Smart and, The Perseus cluster 560
Allen, C. W., Stark effect and damping factor in the Fraunhofer spectrum 4
—— Photometry of the solar D lines 10
—— The spectrum of bright chromospheric eruptions 635
Alter, George, A photographic survey of galactic clusters. I. Method of work and application to N.G.C. 581 (M 103) 387
Alter, George, D. R. Barber and D. L. Edwards, The fog effect in photographic astro- and spectro-photometry 529
Annual General Meeting, Report of the proceedings of the 213
Archenhold, G. H. A., Some problems concerning the distribution of sunspots over the Sun's disc 645
Armagh Observatory, Report of the proceedings of 277
Atkinson, R. d'E., Accretion and stellar energy 500
Atkinson, R. d'E., A. Hunter and E. G. Martin, The relations between colour indices and gradients 196
Auditors of the Treasurer's accounts for 1939, Appointment of 59
—— Report of the 223

Baldwin, J. M., Occultations of stars by the Moon observed at Melbourne Observatory in 1938 56
—— —— in 1939 417
Barber, D. R., A sensitometric study of some developers and emulsions of astro-physical interest 180
Barber, D. R., G. Alter—and D. L. Edwards, The fog effect in photographic astro- and spectro-photometry 529
Barker, Robert, Report of his observatory (Cheshunt) 298
Bates, D. R., The quantal theory of continuous absorption of radiation by various atoms in their ground states. I. The atoms from boron to neon 25
Beer, Arthur, The variable extent of the atmosphere of ζ Aurigæ 693
Burch, C. R., The Williams Interferometer 488
—— —— Editorial note on Dr. Burch's article 702
Butler, H. E., and A. D. Thackeray, Dispersion in estimates of spectral type 450
Bye-laws, Additional, special to the present emergency, carried at a Special General Meeting 1940 November 10 1

Cambridge Observatory, Report of the proceedings of the 277
Cambridge University, Solar Physics Observatory, Report of the proceedings of the ... 278
Camm, G. L., The Sun's speed of galactic rotation determined from the globular clusters 45
Canberra, Commonwealth Solar Observatory, Report of the proceedings of the ... 294
Candidates proposed 3, 59, 138, 213, 353, 421, 499
Candler, W. E., Some theorems for a star with variable polytropic index 14
Cape of Good Hope, Royal Observatory, Stellar parallaxes determined photographically (Eleventh list) 128
—— Report of the proceedings of the 273
—— Occultations observed in 1939 414
Chaudhuri, P. C., The photographic proper motions of stars belonging to the cluster Præsepe from plates taken with the Radcliffe telescope... 378
—— The 61 Cygni cluster 574
Comets, Council report on, in 1939, Rev. M. Davidson 327
Cosmic Evolution : On the origin of the solar system, R. A. Lyttleton 546
—— Accretion and stellar energy, R. d'E. Atkinson 500

PAGE

Eddington, Sir A. S., The correction of statistics for accidental error 354
—— The physics of white dwarf matter 582
Edinburgh, Royal Observatory, Report of the proceedings of the 272
Edwards, D. L., G. Alter, D. R. Barber and, The fog effect in photographic astro- and spectro-photometry 529
Eros, On the suitability of, for the accurate determination of the solar parallax, H. Spencer Jones 422
Errata 333
Errors, Theory of : The statistical theory of errors (Council Report on the progress of astronomy), H. R. Hulme 303
—— The correction of statistics for accidental error, Sir A. S. Eddington 354
Evans, David S., Photometric observations of *Hα* in the solar spectrum 156
Eversbed, J., Report of his observatory (Ewhurst) 298

Fellows elected 1, 137, 213, 353, 421, 499, 581

Galactic Rotation, The Sun's speed of, determined from the globular clusters, G. L. Camm 45
—— The *K* term and the galactic rotational constants, W. M. Smart 370
Gascoigne, S. C. B., A null test for concave mirrors 462
George Darwin Lecture, 1940, not to be delivered owing to war-time conditions ... 353
Gifts to the general funds and property of the Society 224
Glasgow University Observatory, Report of the proceedings of the 279
Gold Medal of the Society, The, awarded to Dr. E. P. Hubble for his outstanding work on the distances, velocities, distribution and nature of the extra-galactic nebulæ 138, 342
Goodridge Bequest 227
Greenwich, Royal Observatory, Stellar parallaxes 51
—— Relative gradients of 250 stars 189
—— Report of the proceedings of the 266
—— Mean areas and heliographic latitudes of sunspots in the year 1937 495
Grove-Hills Special Fund 225

Hagihara, Yusuke, The electron velocity distribution in the planetary nebulæ ... 631
Haughton, J. L., Report of his observatory (Teddington) 299
Heath, M. B. B., Report of his observatory (Kingsteignton) 300
Helwan Observatory, Egypt, Report of the proceedings of 290
Holborn, F. M., Report of his observatory (Streatham Hill) 300
Hubble, E. P., The Gold Medal of the Society awarded him for his outstanding work on the distances, velocities, distribution and nature of the extra-galactic nebulæ 138, 342
Hulme, H. R., The statistical theory of errors (Council report on the progress of astronomy) 303
Hunter, A., R. d'E. Atkinson—and E. G. Martin, The relations between colour indices and gradients 196
Hunter, A., and E. G. Martin, The effect of absolute magnitude on star colours ... 656
—— Space reddening in the galaxy 669
Hyderabad, Nizamiah Observatory, Report of the proceedings of the 290
—— Occultations of stars by the Moon, observed during the year 1939 700

Instruments bequeathed to the Society by the late A. Stanley Williams 230
Instruments and Appliances, etc. : A null test for concave mirrors, S. C. B. Gascoigne 462
—— Appendix: The Williams Interferometer, C. R. Burch 488
—— Editorial note on Dr. Burch's article 702
Investments 222

Jeffreys, Harold, The variation of latitude 139
Johannesburg, Union Observatory, Report of the proceedings of the 292
Jones, H. Spencer, On the suitability of Eros for the accurate determination of the solar parallax 422

Kodaikanal Observatory, Report of the proceedings of 291

PAGE

Latitude Variation : The variation of latitude, Harold Jeffreys 139
Library, List of donors to the, in 1939 334
—— List of exchanges 335
—— Periodicals purchased 341
—— to be opened once a month during the recess 581
London, University of, Observatory and University College Observatory, Report of the proceedings of 280
Lyttleton, R. A., On the origin of the solar system 546

McIntosh, R. A., Seasonal variation in the height of meteors 510
Martin, E. G., R. d'E. Atkinson, A. Hunter and, The relations between colour indices and gradients 196
Martin, E. G., A. Hunter and, The effect of absolute magnitude on star colours ... 656
—— Space reddening in the galaxy 669
Melbourne Observatory, Report of the proceedings of 295
Meteors (Council report on the progress of astronomy), E. Öpik 315
—— Seasonal variation in the height of, R. A. McIntosh 510
Mirrors, A null test for concave, S. C. B. Gascoigne 462
—— —— Appendix: The Williams Interferometer, C. R. Burch 488
—— —— Editorial note on Dr. Burch's article 702

Nebulæ, Extra-galactic, The orientation of the, A. G. Walker 623
—— Presidential address on presenting the Gold Medal of the Society to Dr. E. P. Hubble, H. C. Plummer 342
—— Planetary, The electron velocity distribution in the, Yusuke Hagihara 631
Newbegin, A. M., Report of his observatory (Worthing) 300

Obituary : List of Fellows deceased 231
Obituary Notices : Fellows :—
Bartrum, Clement Osborn 231
Billing, John Morton 232
Brook, Charles Lewis 233
Crommelin, Andrew Claude de la Cherois 234
Douglas, Henry Percy 236
Durrad, John William 238
Dyson, Frank Watson 238
Feldman, William Moses 246
Fotheringham, David Ross 247
Goff, Park 248
Hedley, Herbert... 249
Hollis, Henry Park 249
Jackson, James Thomas 251
Kennelly, Arthur Edwin 251
Levin, Arthur Everard 253
Long, Arthur William 254
Nielsen, Charles... 255
O'Leary, William 255
Phillips, Montague Austin 257
Robins, Herbert George 258
Sampson, Ralph Allen 258
Sharp, Martin Charles 263
Waters, Henry Hayden... 264
Werner, Jacob 265
Observatories, Work at various : see reports of individual observatories (or observers) under their respective headings.
Occultations of stars by the Moon observed at Melbourne Observatory in 1938, J. M. Baldwin 56
—— Observations of, at Sydney Observatory during 1938 135
—— observed at the Royal Observatory, Cape of Good Hope, in 1939 414
—— of stars by the Moon observed at Melbourne Observatory in 1939, J. M. Baldwin 417
—— of stars by the Moon observed at Birmingham during the year 1939, James Young 419

PAGE

Occultations of stars by the Moon observed at the Nizamiah Observatory, Hyderabad, during the year 1939 700
Officers and Council, 1940–41, List of 351
Öpik, E., Meteors (Council report on the progress of astronomy) 315
Ottawa, Dominion Observatory, Report of the proceedings of the 284
Oxford, University Observatory, Report of the proceedings of the 281

Peek, B. M., Report of his observatory (Solihull) 301
Phillips, Rev. T. E. R., Report of his observatory (Headley) 301
Photography, Astronomical: A sensitometric study of some developers and emulsions of astrophysical interest, D. R. Barber 180
—— The fog effect in photographic astro- and spectro-photometry, G. Alter, D. R. Barber and D. L. Edwards 529
Photography, Celestial: List of reproductions of celestial photographs by the Society 230
Plummer, H. C., Presidential address on presenting the Gold Medal of the Society to Dr. Edwin P. Hubble 342
Potter, Archdeacon Beresford, Fund 226
Presents announced 3, 59, 138, 353, 421, 499, 581
Pretoria, Radcliffe Observatory, Report of the proceedings of the 293
Progress and present state of the Society 215
Publications of the Society 230

Riverview College Observatory, N.S.W., Report of the proceedings of 296
Ryves, P. M., On a change in the period of RW Sagittarii 491

Sampson, Professor R. A., Death of 59
Sellers, F. J., Report of his observatory (Muswell Hill) 301
Sidmouth, Norman Lockyer Observatory, Report of the proceedings of the 282
Smart, W. M., The Scorpio-Centaurus cluster (the southern stream) 60
—— The *K* term and the galactic rotational constants 370
Smart, W. M., and A. Ali, The Perseus cluster 560
Smart, W. M., and T. R. Tannahill, The constants of the star-streams from the Cape photographic proper motions of 18,323 stars 30
—— Star-streaming in relation to spectral type from the Cape photographic proper motions 688
South Kensington, Imperial College Observatory, Report of the 280
Spectroscopy and Spectrophotometry: Stark effect and damping factor in the Fraunhofer spectrum, C. W. Allen 4
—— Photometry of the solar D lines, C. W. Allen 10
—— The quantal theory of continuous absorption of radiation by various atoms in their ground states. I. The atoms from boron to neon, D. R. Bates ... 25
—— Photometric observations of *Hα* in the solar spectrum, David S. Evans 156
—— Relative gradients of 250 stars, Royal Observatory, Greenwich 189
—— The relations between colour indices and gradients, R. d'E. Atkinson, A. Hunter and E. G. Martin 196
—— Dispersion in estimates of spectral type, H. E. Butler and A. D. Thackeray ... 450
—— The fog effect in photographic astro- and spectro-photometry, G. Alter, D. R. Barber and D. L. Edwards 529
Spencer, Herbert, Bequest 225
Spitzer, Lyman, Jr., The stability of isolated clusters 396
Star Clusters: The Sun's speed of galactic rotation determined from the globular clusters, G. L. Camm 45
—— The Scorpio-Centaurus cluster (the southern stream), W. M. Smart 60
—— The photographic proper motions of stars belonging to the cluster Præsepe from plates taken with the Radcliffe telescope, P. C. Chaudhuri 378
—— A photographic survey of galactic clusters. I. Method of work and application to N.G.C. 581 (M 103), George Alter 387
—— The stability of isolated clusters, Lyman Spitzer, Jr. 396
—— The Perseus cluster, W. M. Smart and A. Ali 560

PAGE

Star Clusters (*contd.*): The Corona Borealis cluster, A. Ali 570
—— The 61 Cygni cluster, P. C. Chaudhuri 574
Star Colours: Relative gradients of 250 stars determined at the Royal Observatory, Greenwich 189
—— The relations between colour indices and gradients, R. d'E. Atkinson, A. Hunter and E. G. Martin 196
—— The effect of absolute magnitude on star colours, A. Hunter and E. G. Martin ... 656
—— Space reddening in the galaxy, A. Hunter and E. G. Martin 669
Stark Effect and damping factor in the Fraunhofer spectrum, C. W. Allen 4
Stars, Distribution and Motions of: The constants of the star-streams from the Cape photographic proper motions of 18,323 stars, W. M. Smart and T. R. Tannahill 30
—— The Scorpio-Centaurus cluster (the southern stream), W. M. Smart 60
—— Star-streaming in relation to spectral type from the Cape photographic proper motions, W. M. Smart and T. R. Tannahill 688
Stars, Double and Multiple: Council report on, in 1939, W. H. van den Bos ... 332
Stars, Magnitude of: The effect of absolute magnitude on star colours, A. Hunter and E. G. Martin 656
Stars, New: Nova Herculis 1934, Relative dimensions of shells around, W. S. Tai... 435
Stars, Parallaxes of: Stellar parallaxes determined at the Royal Observatory, Greenwich 51
—— Stellar parallaxes determined photographically at the Royal Observatory, Cape of Good Hope (Eleventh list) 128
Stars, Proper Motions of: The constants of the star-streams from the Cape photographic proper motions of 18,323 stars, W. M. Smart and T. R. Tannahill 30
—— The photographic proper motions of stars belonging to the cluster Præsepe, from plates taken with the Radcliffe telescope, P. C. Chaudhuri 378
—— Star-streaming in relation to spectral type from the Cape photographic proper motions, W. M. Smart and T. R. Tannahill 688
Stars, Spectra of: The variable spectrum of α^2 Canum Venaticorum, W. S. Tai ... 94
—— The variable extent of the atmosphere of ζ Aurigæ, Arthur Beer 693
—— Dispersion in estimates of spectral type, A. D. Thackeray and H. E. Butler ... 450
Stars, Structure of: Some theorems for a star with variable polytropic index, W. E. Candler 14
—— On Trumpler's stars, Jaakko Tuominen 86
—— The evolution of convective stars, J. Wasiutynski 362
—— Accretion and stellar energy, R. d'E. Atkinson 500
—— The physics of white dwarf matter, Sir A. S. Eddington 582
Stars, Variable: α^2 Canum Venaticorum, The variable spectrum of, W. S. Tai ... 94
—— RW Sagittarii, On a change in the period of, P. M. Ryves 491
—— ζ Aurigæ, The variable extent of the atmosphere of, Arthur Beer 693
Steavenson, W. H., Report of his observatory (West Norwood) 302
Stonyhurst College Observatory, Report of the proceedings of 283
Sun, Chromosphere and Prominences: Council report on solar activity in 1939: Prominences, A. L. Narayan 331
—— The spectrum of bright chromospheric eruptions, C. W. Allen 635
Sun, Eclipses of the: The solar corona of 1937 June 8, I. L. Thomsen 554
Sun, Parallax of the: On the suitability of Eros for the accurate determination of the solar parallax, H. Spencer Jones 422
Sun, Spectrum of the: Photometric observations of *Hα* in the solar spectrum, David S. Evans 156
—— Variation of faint Fraunhofer lines across the solar disc (Second paper), M. G. Adam 595
—— Convective equilibrium and solar limb darkening, A. D. Thackeray 614
—— The spectrum of bright chromospheric eruptions, C. W. Allen 635
Sunspots and Faculæ: Council report on solar activity in 1939: Sunspots, H. W. Newton 330
—— Mean areas and heliographic latitudes of sunspots in the year 1937, Royal Observatory, Greenwich 495
—— Some problems concerning the distribution of sunspots over the Sun's disc, G. H. A. Archenhold 645

PAGE

Sydney Observatory, Observations of occultations during 1938 135
—— Report of the proceedings of 296

Tai, W. S., The variable spectrum of α^2 Canum Venaticorum 94
—— Relative dimensions of shells around Nova Herculis 435
Tannahill, T. R., W. M. Smart and, The constants of the star-streams from the Cape photographic proper motions of 18,323 stars 30
—— Star-streaming in relation to spectral type from the Cape photographic proper motions 688
Thackeray, A. D., Convective equilibrium and solar limb darkening 614
Thackeray, A. D., H. E. Butler and, Dispersion in estimates of spectral type 450
Thomsen, I. L., The solar corona of 1937 June 8 554
Toronto University, David Dunlap Observatory, Report of the proceedings of the ... 286
Treasurer's accounts for 1939 216
Trust Funds 227
Tuominen, Jaakko, On Trumpler's stars 86

Victoria, B.C., Dominion Astrophysical Observatory, Report of the proceedings of the 287

Walker, A. G., The orientation of the extra-galactic nebulæ 623
Wasiutynski, J., The evolution of convective stars 362
Wellington, N.Z., Carter Observatory, Report of the proceedings of the 297
Wellington, N.Z., Dominion Observatory, Report of the proceedings of the 298
Williams, the late A. Stanley, Instruments bequeathed by, to the Society 230
Wolsingham Observatory, Report of the proceedings of 302

Young, James, Occultations of stars by the Moon observed at Birmingham during the year 1939 419

University of London
Library.

P.R. [illegible]

MONTHLY NOTICES

OF THE

ROYAL ASTRONOMICAL SOCIETY

Vol. 100 No. 1 1939 November

Published and Sold by the
ROYAL ASTRONOMICAL SOCIETY
BURLINGTON HOUSE
LONDON, W. 1

Price Four Shillings

NOTICE TO AUTHORS

1. Authors are notified that papers should be received by one of the Secretaries or by the Assistant Secretary not later than the Saturday previous to each Meeting.

2. Papers should, when practicable, contain a summary to be printed at the end of the paper.

3. Diagrams should be drawn on a scale from two to three times the intended final size, and should be in a state suitable for direct photographic reproduction. *All lettering should be inserted in pencil.* In the event of diagrams being unsuitably drawn the Secretaries are empowered to request authors to have them re-drawn, at their own expense, by a professional artist.

4. Manuscripts must be clearly written or typewritten, and tabular matter arranged so that it can be printed upright on the page. Authors should conform as closely as possible to the recommendations of the International Astronomical Union. In particular, the abbreviation U.T. should be used to denote Mean Time commencing at Greenwich midnight.

The attention of authors is particularly directed to the rule of the Council that when the cost of alterations to proofs exceeds 5 per cent. of the cost of setting up the type of a paper, the excess must be borne by the author.

The Council has decided to destroy all MSS. of papers presented to the Society which remain in their possession after the expiration of twelve months from the dates of publication. Authors who desire to recover their MSS. after that interval may do so if previous notice is given.

Epidiascope.—Readers of papers are requested to note that diagrams, tabular matter, etc. to be exhibited on the screen with the epidiascope should not exceed six inches square.

ANNOUNCEMENT OF PROGRAMMES OF MEETINGS

Post-cards, giving as far as is practicable the programme of each Meeting, will be sent to those Fellows who inform the Assistant Secretary of their wish to receive them.

CONTENTS

Special General Meeting for passing additional Bye-laws 1

Fellows Elected ... ... *ib.*

Candidates proposed 3

Presents announced ... ... *ib.*

C. W. Allen, Stark Effect and Damping Factor in the Fraunhofer Spectrum 4

C. W. Allen, Photometry of the Solar D Lines 10

W. E. Candler, Some Theorems for a Star with Variable Polytropic Index 14

D. R. Bates, The Quantal Theory of Continuous Absorption of Radiation by Various Atoms in their Ground States. I. The Atoms from Boron to Neon 25

W. M. Smart and T. R. Tannahill, The Constants of the Star-Streams from the Cape Photographic Proper Motions of 18,323 Stars 30

G. L. Camm, The Sun's Speed of Galactic Rotation determined from the Globular Clusters 45

Royal Observatory, Greenwich, Stellar Parallaxes determined at the Royal Observatory, Greenwich 51

J. M. Baldwin, Occultations of Stars by the Moon observed at Melbourne Observatory in 1938 56

Printed in Edinburgh by Neill & Co., Ltd., 1939 December